



Universiteit  
Leiden  
The Netherlands

## Applications of AdS/CFT in Quark Gluon Plasma

Atmaja, A.N.

### Citation

Atmaja, A. N. (2010, October 26). *Applications of AdS/CFT in Quark Gluon Plasma*. *Casimir PhD Series*. Retrieved from <https://hdl.handle.net/1887/16078>

Version: Corrected Publisher's Version

License: [Licence agreement concerning inclusion of doctoral thesis in the Institutional Repository of the University of Leiden](#)

Downloaded from: <https://hdl.handle.net/1887/16078>

**Note:** To cite this publication please use the final published version (if applicable).

# **Applications of AdS/CFT in Quark Gluon Plasma**

Ardian Nata Atmaja



# Applications of AdS/CFT in Quark Gluon Plasma

P R O E F S C H R I F T

ter verkrijging van  
de graad van Doctor aan de Universiteit Leiden,  
op gezag van Rector Magnificus prof. mr. P. F. van der Heijden,  
volgens besluit van het College voor Promoties  
te verdedigen op dinsdag 26 oktober 2010  
klokke 13.45 uur

door

Ardian Nata Atmaja

geboren te Medan, Indonesië  
in 1979

**Promotiecommissie:**

Promotor: prof. dr. J. de Boer (Universiteit Amsterdam)  
Co-Promotor: dr. K. Schalm  
Overige leden: prof. dr. A. Achúcarro  
prof. dr. J. Zaanen  
prof. dr. E.P. Verlinde (Universiteit Amsterdam)  
prof. dr. J.M. van Ruitenbeek

ISBN: 978-908593088-4  
Casimir PhD Series, Delft-Leiden 2010-28

*Untuk almarhum papa, mama, dan nenekku tersayang  
yang cinta dan kasih sayangnya melewati batas ruang dan waktu.*



*Bismillah Hir-Rahman Nir-Rahim.*





---

# CONTENTS

---

<b>1</b>	<b>Introduction</b>	<b>1</b>
1.1	Quark Gluon Plasma . . . . .	3
1.2	<i>D</i> -branes . . . . .	5
1.2.1	Non-abelian gauge theory on D3-branes . . . . .	6
1.3	<i>p</i> -Branes . . . . .	7
1.4	AdS/CFT correspondence . . . . .	8
1.4.1	GKPW procedure and holographic renormalization . . . . .	9
1.4.2	Top-down approach . . . . .	10
1.4.3	Bottom-up approach . . . . .	11
1.5	Holographic models of Hadrons . . . . .	11
1.5.1	Hard-wall model . . . . .	11
1.5.2	Soft-wall model . . . . .	13
1.6	Thermal field theory . . . . .	14
1.7	Holographic real-time propagator . . . . .	17
1.7.1	Minkowski prescription I . . . . .	18
1.7.2	Minkowski prescription II . . . . .	20
1.8	Outline . . . . .	21
<b>2</b>	<b>Photon Production in Soft Wall Model</b>	<b>23</b>
2.1	Introduction . . . . .	23
2.2	Photon and dilepton production . . . . .	24
2.2.1	Photon and dilepton rates at strong coupling . . . . .	25
2.3	Solving the system . . . . .	28
2.3.1	Lightlike momenta . . . . .	28
2.3.2	Timelike and spacelike momenta . . . . .	35
2.3.3	Electrical conductivity . . . . .	36
2.4	Conclusion: Soft wall cut-offs as an IR mass-gap. . . . .	37
2.A	Spectral function low frequency limit for lightlike momenta . . . . .	41
2.B	The susceptibility and the diffusion constant . . . . .	42

<b>3</b>	<b>Holographic Brownian Motion and Time Scales in Strongly Coupled Plasmas</b>	<b>45</b>
3.1	Introduction . . . . .	45
3.2	Brownian motion in AdS/CFT . . . . .	47
3.2.1	Boundary Brownian motion . . . . .	47
3.2.2	Bulk Brownian motion . . . . .	49
3.2.3	Generalizations . . . . .	54
3.3	Time scales . . . . .	57
3.3.1	Physics of time scales . . . . .	57
3.3.2	A simple model . . . . .	58
3.3.3	Non-Gaussian random force and Langevin equation . . . . .	62
3.4	Holographic computation of the $R$ -correlator . . . . .	62
3.4.1	Thermal field theory on the worldsheet . . . . .	63
3.4.2	Holographic approach . . . . .	67
3.4.3	General polarizations . . . . .	68
3.5	The IR divergence . . . . .	69
3.6	Generalizations . . . . .	72
3.6.1	Mean-free-path time for the general case . . . . .	72
3.6.2	Application: STU black hole . . . . .	75
3.7	Discussion . . . . .	81
3.A	Normalizing solutions to the wave equation . . . . .	83
3.B	Low energy solutions to the wave equation . . . . .	84
3.C	Various propagators and their low frequency limit . . . . .	87
3.D	Holographic renormalization and Lorentzian AdS/CFT . . . . .	90
3.D.1	Holographic renormalization . . . . .	90
3.D.2	Propagators and correlators . . . . .	93
3.D.3	Lorentzian AdS/CFT . . . . .	98
3.D.4	Low frequency correlators . . . . .	100
3.D.5	Retarded 4-point function . . . . .	101
3.E	Computation of $\eta$ for the STU black hole . . . . .	102
<b>4</b>	<b>Drag Force in 4D Kerr-AdS Black Hole</b>	<b>105</b>
4.1	Introduction . . . . .	105
4.2	Drag force on a string in a global 4D AdS black hole . . . . .	106
4.2.1	Great circle at $\theta = \pi/2$ . . . . .	108
4.2.2	General solution of the great circle . . . . .	110
4.3	Anisotropic drag on a string in 4D Kerr-AdS black hole . . . . .	113
4.3.1	Static solution . . . . .	116
4.3.2	Drag force . . . . .	118
4.4	Discussion and conclusion . . . . .	120
	<b>Bibliography</b>	<b>123</b>
	<b>Summary</b>	<b>133</b>

<b>Samenvatting</b>	<b>136</b>
<b>Acknowledgement</b>	<b>140</b>
<b>Curriculum Vitae</b>	<b>142</b>
<b>List of Publications</b>	<b>144</b>



# CHAPTER 1

---

## INTRODUCTION

---

For many years, people have attempted to develop an ultimate theory that would explain the fundamental structure of matter and the very basic mechanisms of nature. One promising candidate is string theory. Born in the late 1960s as a theory that was expected to describe the strong interaction in hadrons, string theory had to accept the fact that another theory, known as QCD (Quantum Chromodynamics), correctly describes the strong nuclear force and the properties of hadrons. A new face of string theory arose in 1974 when John Schwarz and Joel Scherk proposed an interpretation of the spin-two massless particle in the spectrum of string theory to describe the quantum of gravity, namely graviton. Ever since string theory has received great attention of many scientists, not only from high-energy physicists, but also from various other fields of study and so a journey to the ultimate theory has taken a new direction.

String theory today is a forefront in the world of scientific research. It does not only requires knowledge of other fields and sophisticated tools in mathematics but at some level it also tries to solve some puzzles in physics by providing a new approach to the problems. Nevertheless, string theory still lacks of experimental evidences. The natural length scale of the theory is thought to be at the order of Plank scale  $\sim 10^{19} \text{ GeV}$ , out of reach of any current or future machines built for experiment. The energy scale at which string theoretic effects become relevant is very large compared to the energy scale of well established theory of particle physics namely the Standard Model (electroweak scale  $\sim 246 \text{ GeV}$  and QCD scale  $\sim 300 \text{ MeV}$ ).

In string theory the fundamental objects are one-dimensional objects called strings instead of points-like as in the usual quantum field theory.

String theory is characterized by one parameter  $\alpha'$ , the string tension, which is also related to the length of strings  $l_s = \sqrt{\alpha'}$ . These strings have to be embedded into 26-dimensional space-time (without supersymmetry) or 10-dimensional space-time (with supersymmetry) in order to be consistent. The 26-dimensional strings is called bosonic string theory and 10-dimensional strings is called superstring theory [1].

There are two types of strings one can consider. First is closed strings where the two ends of the string meet and form a loop. The second is open strings where the end points of string are confined to subsurfaces in space time (hypersurfaces) called branes. The spectrum of those type of strings are quite different, for example the open string has a massless spin-one gauge field while the closed string has a massless spin-two graviton.

One of the most important developments in string theory is the AdS/CFT correspondence. It is based on holographic principle which states that the description of a volume of space can be thought of as encoded on a boundary of that region. This correspondence encodes a way of using string theory to perform non-perturbative calculation in gauge theory which is still a complicated problem.

The best known example of the correspondence is between weakly coupled gravity theory with AdS (Anti de Sitter) as space-time background and strongly coupled gauge theory with conformal symmetry in one lower dimension. Subsequently people have tried to extend this correspondence to non-conformal gauge theory since the Standard Model itself is not a conformal theory. This extension affects the space-time background where the gravity theory lives in. With this attempt now the correspondence is widely known as gauge/gravity correspondence<sup>1</sup>. Unfortunately there is still no version of the correspondence which realizes Standard Model or even pure QCD.

Nevertheless, the last several years we have seen a considerable success in the application of the AdS/CFT correspondence [2–4] to the study of real world strongly coupled systems, in particular the QGP (Quark Gluon Plasma). The (successful) application hinges on the belief that the QGP of QCD is thought to be qualitatively very similar to the plasma of  $\mathcal{N} = 4$  super Yang–Mills theory at finite temperature, which is dual to string theory in an AdS black hole spacetime. The analysis of scattering amplitudes in the AdS black hole background led to the universal viscosity bound [34], which played an important role in understanding the physics of the elliptic flow observed at RHIC. On the other hand, the study of the physics of trailing strings in the AdS spacetime explained the dissipative and diffusive physics of a quark moving through a field theory plasma, such as the diffusion coefficient and transverse momentum broadening [35, 38–41, 53–55]. The relation between the hydrodynamics of the field theory plasma and the bulk black hole dynamics was first revealed

---

<sup>1</sup>It is from the massless spectrum of open and closed strings that AdS/CFT correspondence gets another name gauge/gravity correspondence.

in [56, 97] (see also [63]).

This thesis is based on works in [19, 20] and ongoing work in [21]. The works describe some applications of AdS/CFT correspondence in QGP. In the following sections we give a brief introduction to string theory; an inside view of QGP; the basic and technical tools of AdS/CFT correspondence; and the outline of this thesis.

## 1.1 Quark Gluon Plasma

The low-energy properties of the strong interactions are governed by a chiral symmetry. The QCD Lagrangian possesses an  $SU(3)_L \times SU(3)_R \times U(1)_V$  symmetry in chiral limit ( $m_u, m_d, m_s \rightarrow 0$ ). At the current status, we do not know how to solve QCD in low-energy as the standard perturbation theory can not be applied for energy below QCD scale  $\sim 300 \text{ MeV}$ . Below this scale quarks are in a confined phase and bound to form what is called hadron. In this state quarks can not be separated from each others since the QCD coupling constants are large. Therefore perturbation theory can not be used and we need to work with non-perturbative calculation. As we increase the energy above QCD scale, the QCD coupling constants decrease and the quarks are slowly separated from the hadron. At some point there will be a phase transition to a deconfined phase where the quarks are deconfined from the hadron form and can be identified individually. In this phase the perturbation theory works very well especially at infinite energy where quarks do not interact with each others and it is known as asymptotically freedom.

Perturbative aspects of QCD have been tested to a few percents. In contrast, non-perturbative aspects of QCD have barely been tested. Recent development in gravity/gauge correspondence has revived the hope that the strongly coupled regime of QCD can be reformulated as a solvable string theory.

QGP is a phase of QCD which exists at extremely high temperature and/or density. The QGP contains quarks and gluons, just as normal matter(hadron) does. Unlike hadrons where quarks are confined, in the QGP these mesons and baryons lose their identities and dissolve into a fluid of quarks and gluons. Quarks in QGP are deconfined and make a much larger total mass compared to the corresponding hadron mass. The QGP is believed to have existed during the first 20 or 30 microseconds after the universe came into existence in the Big Bang.

A plasma is matter in which electric charges are screened due to the presence of other mobile charges. Likewise, the colour charge of the quarks and gluons in QGP are screened. There are also dissimilarities due to the fact that the colour charge is non-abelian, whereas the electric charge in a normal plasma is abelian.

The QGP can be created by heating high density matter up to a temperature of  $190 \text{ MeV}$  per particle. To produce such high energy, two heavy particles



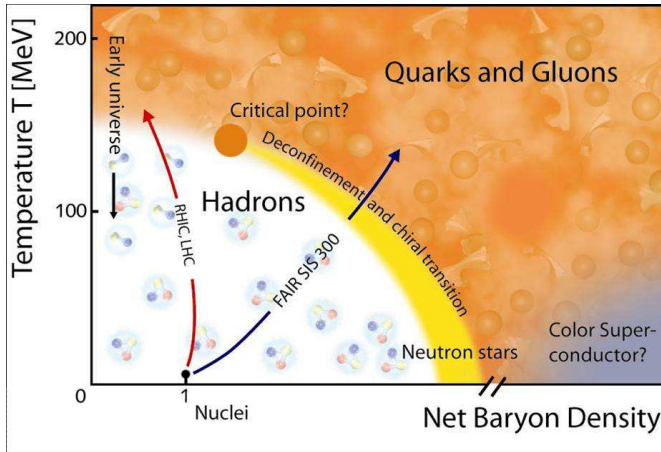


Figure 1.1: QCD phase diagram [17].

are accelerated to ultrarelativistic speeds and slammed into each other. They largely pass through each other, but a significant fraction collides, melts, and “explodes” into a hot fireball. Once created, this fireball expands under its own pressure, and cool while expanding. By carefully studying this flow, experimentalists hope to test the theory.

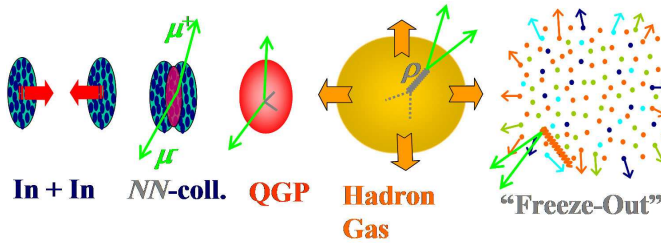


Figure 1.2: Creation process of QGP [18].

As conventional thermodynamic characteristics, the resulting QGP is largely controlled by the equation of state relating the  $P$  (pressure) and  $T$  (temperature). The equation of state is an important input for the flow equations. The mean free path of quarks and gluons can be computed using perturbation theory as well as string theory. There are indications that the mean free time of quarks and gluons in the QGP may be comparable to the average interparticle spacing: hence the QGP is a liquid as far as its flow properties go. It has been found recently that some mesons built from heavy quarks (such as the charm

quark) do not dissolve until the temperature reaches about  $350 \text{ MeV}$ . This has led to speculation that many other kinds of bound states may exist in the plasma. Some static properties of the plasma (similar to the Debye screening length) constrain the excitation spectrum.

Unfortunately, the aspects or properties of QGP which are easiest to compute are not always the ones which are the easiest to probe in experiments. Hence, it is still a difficult task to declare the existence of QGP in the experiments such as in RHIC or LHC. The important classes of experimental observations are:

- Single particle spectra
- Strangeness production
- Photon and muon rates
- Elliptic flow
- Jet quenching
- Fluctuations
- Hanbury-Brown and Twiss effect
- Bose-Einstein correlations.

In general QGP can be weakly or strongly coupled. However, there are a couple of indications that strongly coupled QGP has been created in heavy ion collision experiments at RHIC (and expected stronger signals from the ongoing LHC) with the energy around  $200 \text{ GeV}$  per nucleon [103]. So far the main theoretical tools to explore the theory of the QGP is lattice gauge theory. One of the properties of QGP computed by lattice gauge theory is the transition temperature in which the latest simulation yields approximately  $190 \text{ MeV}$  [8]. Surprisingly, with a few steps and an input from the lightest  $\rho$ -meson, an AdS/CFT computation shows that the transition temperature is around [16]  $191 \text{ MeV}$  which is close to the lattice result. In this thesis, we will use AdS/CFT correspondence to work on photon production [19], fluctuation [20], and elliptic flow [21] of the corresponding strongly coupled QGP.

## 1.2 *D*-branes

In addition to strings, string theory contains soliton-like “membranes” of various internal dimension called Dirichlet branes (*D*-branes) which are defined in a very simple way in string perturbation theory [43]. In ten dimensional string theory, a  $Dp$ -brane is a  $p+1$  dimensional hyperplane living in  $9+1$  dimensional

space-time to which the ends of open strings are confined. It is charged under a  $p+1$ -form gauge potential which is part of the massless closed string modes.

The world-volume action of  $Dp$ -brane is the so-called DBI (Dirac-Born-Infeld) action. In a flat background it consists of a gauge field  $A_\alpha$  and  $9-p$  scalars  $\Phi^i$  and some fermionic fields, with  $\alpha = 0, \dots, p$  and  $i = p+1, \dots, 9$ . In static gauge the bosonic part of DBI action is given by

$$S_{DBI} = -T_{Dp} \int d^{p+1} \sigma \sqrt{-\det(\eta_{\alpha\beta} + 4\pi^2 \alpha'^2 \partial_\alpha \Phi^i \partial_\beta \Phi^i + 2\pi \alpha' F_{\alpha\beta})}, \quad (1.1)$$

where we have rewritten the coordinates that are orthogonal to  $Dp$ -brane as scalar fields  $\Phi^i$  and with  $\eta_{\alpha\beta}$  is the flat metric in  $Dp$ -brane world-volume and

$$T_{Dp} = \frac{1}{g_s (2\pi)^p (\alpha')^{(p+1)/2}} \quad (1.2)$$

is the tension of  $Dp$ -brane. Including background fields (graviton  $g_{\mu\nu}$ , dilaton  $\phi$ , and the two-form field  $B_{\mu\nu}$ ) takes the following form<sup>2</sup>

$$S_{DBI} = -T_{Dp} \int d^{p+1} \sigma e^{-\phi} \sqrt{-\det(g_{\alpha\beta} + B_{\alpha\beta} + 4\pi^2 \alpha'^2 \partial_\alpha \Phi^i \partial_\beta \Phi^i + 2\pi \alpha' F_{\alpha\beta})}, \quad (1.3)$$

where  $g_{\alpha\beta}$  and  $B_{\alpha\beta}$  are the pullbacks of  $g_{\mu\nu}$  and  $B_{\mu\nu}$ , with  $\mu, \nu = 0, \dots, 9$ . E.g.

$$g_{\alpha\beta} = g_{\mu\nu} \frac{\partial X^\mu}{\partial \sigma^\alpha} \frac{\partial X^\nu}{\partial \sigma^\beta}. \quad (1.4)$$

### 1.2.1 Non-abelian gauge theory on D3-branes

The previous DBI action has an abelian  $U(1)$  gauge symmetry. For non-abelian case, the symmetry is enhanced non-abelian gauge symmetry for example with  $U(N)$  gauge group by considering  $N$  parallel  $Dp$ -branes sitting at one point. The fields content are now represented by hermitian  $N \times N$  matrices

$$A_\alpha = \sum_n A_\alpha^n T_n, \quad \Phi^i = \sum_n \Phi^{i,n} T_n, \quad (1.5)$$

with  $n = 1, \dots, N^2$  and  $T_n$  are hermitian  $N \times N$  matrices satisfying  $\text{Tr}(T_n T_m) = N \delta_{mn}$ . We also define

$$F_{\alpha\beta} = \partial_\alpha A_\beta - \partial_\beta A_\alpha + i[A_\alpha, A_\beta], \quad D_\alpha \Phi^i = \partial_\alpha \Phi^i + i[A_\alpha, \Phi^i]. \quad (1.6)$$

---

<sup>2</sup>The presence of  $\Phi^i$  terms must be read carefully since it overlaps with the transverse components of  $g_{\alpha\beta}$ . We add this terms just to show the explicit dependent of scalar fields  $\Phi^i$ .

The generalization of DBI action with  $U(N)$  gauge symmetry is rather complicated but the leading order action of the non-abelian DBI action reduces to Yang-Mills theory

$$S = -\frac{T_{Dp}(2\pi\alpha')^2}{4} \int d^{p+1} \sigma e^{-\phi} \text{Tr} [F_{\alpha\beta} F^{\alpha\beta} + 2D_\alpha \Phi^i D_\alpha \Phi^i + [\Phi^i, \Phi^j]^2]. \quad (1.7)$$

The analysis of loop diagrams in the Yang-Mills theory shows that perturbative calculation is valid when

$$g_{YM}^2 N \sim g_s N \ll 1. \quad (1.8)$$

In the case of  $N$  parallel  $D3$ -branes, the low energy effective action at leading order is  $\mathcal{N} = 4 U(N)$  supersymmetric Yang-Mills theory.

### 1.3 $p$ -Branes

The  $p$ -branes are defined to be classical solutions to supergravity field equations. They also carry a charge under an antisymmetric tensor field  $A_{\mu_1 \dots \mu_{p+1}}$  since the low energy effective action of type  $IIA/B$  superstring theory is supergravity action. The  $p$ -brane solutions are also solutions of the full closed string theory. In string theory  $p$ -brane corresponds to  $Dp$ -brane and they are believed to be two different descriptions of the same object, and we shall from here on call them by the same name.

One of the example of  $p$ -branes is the  $D3$ -branes solution in type  $IIB$  supergravity with the following action [44]:

$$S = \frac{1}{(2\pi)^7 l_s^8} \int d^{10} x \sqrt{-g} \left( e^{-2\phi} (R + 4(\nabla\phi)^2) - \frac{2}{5!} F_{(5)}^2 \right), \quad (1.9)$$

where  $F_{(5)}$  is a self-dual five-form field strength. Here we set the other supergravity fields to zero. The  $D3$ -branes solution is given by

$$\begin{aligned} ds^2 &= \frac{1}{\sqrt{H}} (-dt^2 + dx_1^2 + dx_2^2 + dx_3^2) + \sqrt{H} (dr^2 + r^2 d\Omega_5), \\ F_{(5)} &= (1 + *) dt dx_1 dx_2 dx_3 dH^{-1}, \quad e^{-2\phi} = g_s^{-2}, \\ H &= 1 + \frac{L^4}{r^4}, \quad L^4 \equiv 4\pi g_s \alpha'^2 N, \end{aligned} \quad (1.10)$$

with  $*$  is the Hodge dual operator and parameter  $N$  is the flux of five-form Ramond-Ramond field strength on  $S^5$ ,

$$N = \int_{S^5} *F_{(5)}. \quad (1.11)$$

This solution corresponds to  $N$  parallel  $D3$ -branes at the center  $r = 0$ . This solution is called extremal solution which saturates the BPS bound (inequality between the mass  $M$  and the charge  $Q$  of the black hole). One can also check that this solution has zero Hawking temperature.

This supergravity approximation is valid if the curvature of the geometry is small compared to the string scale,  $L \gg l_s$ . In order to suppress the string loop corrections, the effective string coupling  $e^\phi$  needs to be small and in the case of  $D3$ -branes the string coupling is constant with  $g_s < 1$ . So, the  $D3$ -branes solution is valid when  $1 \ll g_s N < N$ .

## 1.4 AdS/CFT correspondence

A long time ago 't Hooft proposed a generalization of the  $SU(3)$  gauge group of QCD to  $SU(N)$  and computed the Feynman graph [7]. In the limit where  $N$  is large while keeping  $g_{YM}^2 N$  fixed, each graph is weighted by a topological factor  $N^\lambda$  where  $\lambda$  is the Euler characteristic of the graph. These factors also appear in calculation of closed string partition function, if we identify  $1/N$  as the string coupling constant, with  $N^2$  for spheres (tree level diagrams),  $N^0$  for tori (one-loop diagrams), etc. Another interesting point is that since the closed string coupling constant is of order  $N^{-1}$ , in the large  $N$  limit, the string theory is weakly coupled.

From the viewpoint of string theory in the background of  $N$  parallel  $D3$ -branes sitting together, the relevant parts of low energy effective action are the brane action and the bulk action. The low energy effective action of the brane action is just the pure four-dimensional  $\mathcal{N} = 4 U(N)$  gauge theory and it is known to be conformal field theory while the bulk action is described by supergravity action moves freely at long distance.

On the other hand the low energy limit of the background solution (1.10) has two kinds of low energy excitations. The first excitations are massless particles propagating in the bulk region and the other is any kind of excitations that close to  $r = 0$ . These two types of excitations decouple from each other because of the present of large gravitational potential. Therefore, there are two low energy theories that live in different region, one is a free bulk supergravity and the other one is living near horizon of the geometry which is  $AdS_5 \times S^5$ ,

$$ds^2 = \frac{r^2}{L^2}(-dt^2 + dx_1^2 + dx_2^2 + dx_3^2) + \frac{L^2}{r^2}dr^2 + L^2 d\Omega_5^2. \quad (1.12)$$

This metric can be obtained physically by taking low energy limit  $\alpha' \rightarrow 0$  but at the same time we keep the energies to be fixed in string units. It then requires that  $r/\alpha'$  is fixed or another way is taking  $r \rightarrow 0$  besides the supergravity approximation limit that we had before,  $g_s N \gg 1$ .

These two different observations of strings under  $D3$ -branes background lead Maldacena to conjecture that  $\mathcal{N} = 4 U(N)$  supersymmetric-Yang-Mills

theory in four-dimensional space-time is dual to type *IIB* superstring theory on  $AdS_5 \times S^5$  [2].

The solution (1.10) is not the only solution of the type *IIB* supergravity action (1.9). There is natural generalization to a non-extremal called Black 3-branes solution with non-zero Hawking temperature. This solution is non-extremal because it does not saturate the BPS bound. Taking the same decoupling limit as we did for the extremal *D3*-brane solution, the near-extremal of Black 3-branes solution is given by

$$ds^2 = L^4 \left[ u^2 (-h dt^2 + dx_1^2 + dx_2^2 + dx_3^2) + \frac{1}{hu^2} du^2 + d\Omega_5^2 \right]$$

$$h = 1 - \frac{(\pi T_H)^4}{u^4}, \quad u^2 = \frac{r^2}{L^4}, \quad (1.13)$$

with  $T_H$  is the Hawking temperature. The dual gauge theory interpretation of this solution is a field theory at finite temperature. The Hawking temperature is interpreted as temperature on the gauge theory side.

### 1.4.1 GKPW procedure and holographic renormalization

Having correspondence between two different theories, we still need to know how they are connected precisely. Gubser, Klebanov, Polyakov, and Witten proposed that the string partition function is equal to generating function of correlation functions in the field theory [3, 4]<sup>3</sup>,

$$\left\langle e^{\int d^4x \phi_0(\vec{x}) \mathcal{O}(\vec{x})} \right\rangle_{CFT} = \mathcal{Z}_{string} [\phi(\vec{x}, z=0) = \phi_0(\vec{x})], \quad (1.14)$$

where  $\phi(\vec{x}, z)$  is any fields of string theory with boundary condition at the boundary of AdS,  $z = 0$ , is  $\phi(\vec{x}, z = 0) = \phi_0(\vec{x})$  interpreted as the source for operator  $\mathcal{O}(\vec{x})$  in conformal field theory. The correlators in gauge theory can be computed by taking derivatives of (1.14) with respect to the source  $\phi_0(\vec{x})$  where each derivative will bring down an operator  $\mathcal{O}(\vec{x})$  in the conformal field theory.

The correspondence in (1.14) is strictly speaking only valid for massless scalar field  $\phi$ . For massive case, there is relation between the mass  $m$  of the field  $\phi$  and the scaling dimension  $\Delta$  of the operator  $\mathcal{O}$ . In  $AdS_{d+1}$ , the Klein-Gordon equation for a massive field  $\phi$  in Euclidean signature has two independent solutions that behave as  $z^{d-\Delta}$  and  $z^\Delta$  near the boundary  $z = 0$ , with

$$\Delta = \frac{d}{2} + \sqrt{\frac{d^2}{4} + L^4 m^2} \quad (1.15)$$

---

<sup>3</sup>Here we use coordinate  $z \propto \frac{1}{u}$ .

which is the largest root of  $\Delta(\Delta - d) = L^4 m^2$ . In that case, the boundary condition should be changed to  $\phi(\vec{x}, \epsilon) = \epsilon^{d-\Delta} \phi_0(\vec{x})$  with  $\epsilon \rightarrow 0$ . A detailed study reveals that one has to regulate the theory by introducing an IR cutoff.

Generically correlators in quantum field theory can contain divergences. Therefore, we need to renormalize the theory in order to have meaningful observables. These divergences must also appear in string theory as the feature of gauge/gravity correspondence. Indeed, there is a relation of divergences between two side of these theories called as UV/IR connection [10]. It connects the ultraviolet effects or UV-divergences in quantum field theory with the infrared effects or IR-divergences in string theory. Eliminating the IR-divergences in string theory should effect on removing the UV-divergences in quantum field theory. The procedure to remove this IR-divergences in string theory is known as holographic renormalization [22, 72].

The background metrics considered in gauge/gravity correspondence are mostly asymptotically AdS. The on-shell action of a bulk field on these metrics near the boundary contains terms that are divergent depending on the scale dimension of the dual operator. In order to remove these divergent terms, we first regulate the on-shell action by cutting the space near the boundary at a point that is very close to the boundary at  $z = \epsilon$  where  $\epsilon$  is a small positive number. The regulated action contain two terms which are divergent and convergent as we take a limit  $\epsilon \rightarrow 0$ ,

$$S_{reg}[\epsilon] = S_{reg}^{div}[\epsilon] + S_{reg}^{con}[\epsilon]. \quad (1.16)$$

The divergent part of the regulated action can be removed by a counterterm action<sup>4</sup>

$$S_{ct}[\phi; \epsilon] = -S_{reg}^{div}[\phi_0; \epsilon]. \quad (1.17)$$

Now we obtain a renormalized on-shell action without IR-divergencies which is given by

$$S_{ren}^{on-shell}[\phi] = \lim_{\epsilon \rightarrow 0} (S_{reg}[\phi; \epsilon] + S_{ct}[\phi; \epsilon]). \quad (1.18)$$

A detail application of this holographic renormalization will be discussed in section 3.D.1.

### 1.4.2 Top-down approach

AdS/CFT gives a tool to study the strongly coupled regime of quantum field theories. In the original proposal of AdS/CFT by Maldacena [2], the  $\mathcal{N} = 4$   $U(N)$  supersymmetric Yang-Mills is clearly far from the expected theory

<sup>4</sup>There is a subtlety in writing the counterterm action. The counterterm action must be covariant and be written in terms of the bulk field  $\phi$  instead of the boundary source  $\phi_0$ . The details of how to write the covariant counter term action can be found in [22, 72].

namely QCD. Beside the finite large gauge symmetry group, it has maximum supersymmetry and does not have flavor symmetry. One proposal to break supersymmetry is to consider  $D4$ -brane system and to compactify one of the spatial direction in  $D4$ -branes with anti-periodic boundary conditions on fermions breaking the supersymmetry [9]. The flavor symmetry can also be added to the system within the frame work of probe  $D$ -branes [36].

One can consider various  $D$ -branes configurations and try to get as close as possible to the more realistic models. All these setups have a clear gravity picture where one can write down the low energy effective action on the gravity side. These  $D$ -branes constructions are known as “top-down” approach. Many examples of the “top-down” approach can be found in [37] and the references therein.

### 1.4.3 Bottom-up approach

In “top-down” approach most of the theories which can be solved using AdS/CFT techniques differ substantially from QCD in particular regarding the lack of asymptotically freedom and the strong coupling in the UV regime. Inspired by holography and using the tools that were reviewed in section 1.4.1, another approach is to start from the known phenomenological models in gauge theory and try to construct the background metric and field content of the gravity side. In this approach, we don’t have a complete picture of the gravity theory but nevertheless we can loosely apply the correspondence between some of the fields in gravity theory, with a background metric and usually non-interacting action, and operators in gauge theory. This type of construction is called “bottom-up” approach. Examples of this “bottom-up” approach will be discussed in the next section.

## 1.5 Holographic models of Hadrons

### 1.5.1 Hard-wall model

A theory has been built starting from QCD and constructing its 5-dimensional holographic dual which differs from other theories, by means of “top-down” approach, which are basically trying to deform supersymmetric Yang-Mills theory in order to obtain QCD. This theory from its approach is in the class of Holographic model of Hadrons and in particular known as AdS/QCD model [12, 15].

This model has 4 free parameters which can be fixed by the number of colors  $N_c$ ,  $\rho$  meson mass,  $\pi$  mass, and pion decay constant  $F_\pi$ . Fixing these parameters, the model can predict other low energy hadronics observables within 10% – 15% accuracy [12]. Furthermore, the properties such as vector



meson dominance and QCD sum rules show up naturally in this AdS/QCD model.

The field content of 5D-theory consists of one scalar and two gauge fields. It was engineered to reproduce holographically the dynamics of chiral symmetry breaking in QCD. On the 4D-theory, the relevant operators are one quark condensate operator and two current operators which are the left- and right-handed currents corresponding to the  $SU(N_f)_L \times SU(N_f)_R$  chiral flavor symmetry. The global chiral flavor symmetry will correspond to gauge symmetry in the 5D-theory. These operators are important in the chiral dynamics and the relation of their parameters with 5-dimensional fields are described in table 1.1

4D: $\mathcal{O}(x)$	5D: $\phi(x, z)$	$p$	$\Delta$	$(m_5)^2$
$\bar{q}_L \gamma^\mu t^a q_L$	$A_{L\mu}^a$	1	3	0
$\bar{q}_R \gamma^\mu t^a q_R$	$A_{R\mu}^a$	1	3	0
$\bar{q}_R^\alpha q_L^\beta$	$\frac{2}{z} X^{\alpha\beta}$	0	3	-3

Table 1.1: 4D-Operators/5D-fields of the holographic model

The 5D masses  $m_5$  are determined via the relation [4]

$$(m_5)^2 = (\Delta - p)(\Delta + p - 4), \quad (1.19)$$

where  $\Delta$  is the dimension of the corresponding  $p$ -form operator. The factor  $1/z$  in table 1.1 is to give the correct dimension to the operator  $\bar{q}q$  with  $z$  corresponds to the energy scale of QCD.

The simplest possible metric for this AdS/QCD model is a slice of the AdS metric

$$ds^2 = \frac{1}{z^2}(-dz^2 + dx^\mu dx_\mu), \quad 0 < z \leq z_m. \quad (1.20)$$

As we mentioned before, the fifth coordinate  $z$  corresponds to the energy scale [13] with momentum transfer  $Q \sim 1/z$ . With this metric, we neglect the running of the QCD gauge coupling in a window of scales until an IR(infrared) scale  $Q_m \sim 1/z_m$  where the 4-dimensional theory is confining and at this scale the AdS space is cut-off by introducing an IR cutoff or "infrared brane"(IR-brane) in the metric at  $z = z_m$  and imposing certain boundary conditions on the fields at  $z = z_m$ . Therefore this model is called hard-wall model. In addition, an UV cutoff can be provided to  $z = \epsilon$  with  $\epsilon \ll 1$ .

## 5D action

The action of the 5D-theory is given by [12]

$$S = \int d^5x \sqrt{g} Tr \left\{ |DX|^2 + 3|X|^2 - \frac{1}{4g_5^2}(F_L^2 + F_R^2) \right\}, \quad (1.21)$$

where

$$D_\mu X = \partial_\mu X - iA_{L\mu}X + iXA_{R\mu}, \quad X = X_0 e^{2i\pi^a t^a} \quad (1.22)$$

$$F_{\mu\nu} = \partial_\mu A_\nu - \partial_\nu A_\mu - i[A_\mu, A_\nu], \quad A_{L,R} = A_{L,R}^a t^a, \quad (1.23)$$

where  $X_0$  is the background field and  $\pi^a$  are the  $N_f^2 - 1$  pion fields.

At the IR-brane, we must impose some gauge invariant boundary conditions and the simplest choice is  $(F_L)_{z\mu} = (F_R)_{z\mu} = 0$ . We also fix the gauge  $A_z = 0$  in which the boundary conditions now become Neumann. The classical solution to  $X$  is determined in such it satisfies the UV boundary condition  $(2/\epsilon)X(\epsilon) = M$  and the IR boundary condition where the quarks condensate:

$$X_0(z) = \frac{1}{2}Mz + \frac{1}{2}\Sigma z^3, \quad (1.24)$$

where matrix  $M$  and  $\Sigma$  are the quark mass and the quark condensate respectively act as input parameters. Assume the mass and quark condensate matrixes to be the following;  $M = m \cdot \mathbb{I}$  and  $\Sigma = \sigma \cdot \mathbb{I}$ , with  $m$  and  $\sigma$  are constants.

As we can see this hard-wall model has four free parameters:  $m, \sigma, z_m$ , and  $g_5$ . The gauge coupling  $g_5$  can be fixed by comparing the holographic computation with the QCD OPE(Operator Product Expansion) [14] for the product of two currents, where the current corresponds to vector defined as  $V = (A_L + A_R)/2$ , which gives us

$$g_5^2 = \frac{12\pi^2}{N_c}, \quad (1.25)$$

with  $N_c$  is the number of gauge fields.

## 1.5.2 Soft-wall model

The hard-wall model successfully describes the spectrum of the lowest energy hadrons, however it is unable to explain the linear spectrum of excited hadrons,  $m_n^2 \sim n$ . Instead, it shows that the masses of excited hadron grow as  $m_n \sim n^2$ . An improvement was made to the hard-wall model by considering a smooth rather than a hard cutoff in the 5D-theory of AdS/QCD model. This model is called soft-wall model specifically the IR-brane is now replaced by a smooth dilaton profile up to  $z = +\infty$ .

### 5D action

The 5D-action, is that of the hard-wall model plus a non-dynamical dilaton, with  $U(1)$  gauge symmetry is [15]

$$S = \int d^5x e^{-\Phi} \sqrt{g} \left\{ -|DX|^2 + 3|X|^2 - \frac{1}{4g_5^2} (F_L^2 + F_R^2) \right\}, \quad (1.26)$$

where  $g_5^2$  is given by (1.25) and the background fields for metric and dilaton are

$$ds^2 = e^{2A(z)} (dz^2 + dx^\mu dx_\mu), \quad (1.27)$$

$$\Phi = \Phi(z). \quad (1.28)$$

Solutions to these background fields are obtained by considering the spectrum of radial  $\rho$  excitations in such a way  $\Phi(z) - A(z) \sim z^2$  for large  $z$ . Another consideration should be taken into account is the conformal symmetry in the UV near the boundary which is  $\Phi(z) - A(z) \sim \ln z$  for small  $z$ . The simplest example solution for the background fields (1.27) and (1.28) is  $\Phi(z) - A(z) = z^2 + \ln z$ . Indeed this solution gives a nice formula for the mass spectrum of  $\rho$  mesons in the units of the lowest  $\rho$  spectrum [15]:

$$m_n^2 = 4(n + 1). \quad (1.29)$$

## 1.6 Thermal field theory

QGP is considered as a finite temperature system. Therefore we need AdS/CFT correspondence in which the gravity theory possesses the characteristic features of finite temperature system of the corresponding gauge theory. First, let's briefly review the characteristic features of a finite temperature system from field theory perspective.

In finite temperature system of field theory, time is a complex variable with imaginary part is periodic. The period of the imaginary part is  $\beta = 1/T$  which is the inverse of temperature. Physics can be studied using imaginary or real time-formalisms. In this thesis we will only discuss the real-time formalism which is more interesting in particular if we want to study the system that slightly deviates from the equilibrium.

In real-time formalism, time  $t$  is allowed to be a complex variable with aforementioned periodicity in its imaginary part. The path  $\mathcal{C}$  in complex  $t$ -plane is taken such that the imaginary part of  $t$  is decreasing, as we increase the parameter of the path  $\vartheta$ , in order to have a well defined propagator. The time-ordering  $\mathcal{T}_{\mathcal{C}}$  is generalized to the complex  $t$ -plane along this path  $\mathcal{C}$ ,  $t = t(\vartheta)$  (with large value of  $\vartheta$  is later than small value of  $\vartheta$ ). We also generalize  $\delta$ - and  $\theta$ -functions in terms of the path  $\mathcal{C}$ .

Thermal Green's functions  $G_\beta(x_1, \dots, x_n)$  of an operator  $O$  are defined by [25]

$$G_\beta(x_1, \dots, x_n) = \frac{1}{\text{Tr} e^{-\beta H}} \text{Tr} [e^{-\beta H} \mathcal{T}_{\mathcal{C}} (O(x_1) \cdots O(x_n))], \quad (1.30)$$

where  $H$  is the Hamiltonian operator. In terms of the generating functional  $Z[j]$ , the thermal Green's function can be written as

$$G_\beta(x_1, \dots, x_n) = \frac{1}{i^n Z_{\mathcal{C}}[\beta, j]} \frac{\delta^n Z_{\mathcal{C}}[\beta, j]}{\delta j(x_1) \cdots \delta j(x_n)} \Big|_{j=0}, \quad (1.31)$$

with

$$Z_C[\beta, j] = \text{Tr} \left[ e^{-\beta H} \mathcal{T}_C \exp \left( i \int_C d^4x j(x) O(x) \right) \right]. \quad (1.32)$$

In the form of a path integral, the generating functional is given by

$$Z_C[\beta, j] = \int \mathcal{D}O \exp \left( i \int_C d^4x (\mathcal{L}(x) + j(x) O(x)) \right), \quad (1.33)$$

where  $\mathcal{L}(x)$  is the Lagrangian density and  $j(x)$  is the source for field  $O(x)$ . Note that we have a boundary condition<sup>5</sup>  $O(t, \vec{x}) = O(t - i\beta, \vec{x})$ .

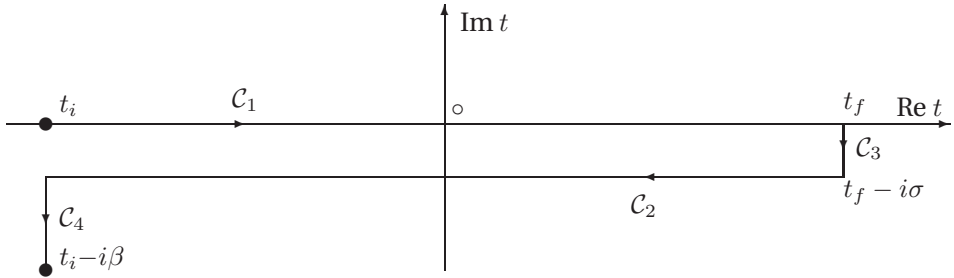


Figure 1.3: The modified Schwinger-Keldysh time contour

The path  $\mathcal{C}$  can be taken in various ways. One common version is drawn in Figure 1.3 where the path  $\mathcal{C}$  (also the fields and operators) is divided into four segments  $\mathcal{C}_1, \mathcal{C}_2, \mathcal{C}_3$ , and  $\mathcal{C}_4$ . The first path  $\mathcal{C}_1$  starts from  $t_i$  and ends at  $t_f$ . This is where the physical field  $O_1$  that we observe lives. It is continued by  $\mathcal{C}_3$  which makes a vertical turn from  $t_f$  to  $t_f - i\sigma$ , with  $\sigma$  is arbitrary between 0 to  $\beta$ . The next path is  $\mathcal{C}_2$  which is parallel to path  $\mathcal{C}_1$  but takes the opposite direction from  $t_f - i\sigma$  to  $t_i - i\sigma$ . The field  $O_2$  lives in  $\mathcal{C}_2$  acts as a “ghost” field which contribute only to the internal line of the thermal Green’s function. Lastly, the path  $\mathcal{C}_4$  takes another vertical turn starts from  $t_i - i\sigma$  and ends at  $t_i - i\beta$ . With this division of the path  $\mathcal{C}$ , the generating functional consists of four Lagrangian densities correspond to different segments.

In general, parameter  $\sigma$  can be chosen arbitrarily. One of the example is  $\sigma = \beta/2$  which was studied in [45]. If  $(t_i = -t_f) \rightarrow +\infty$ , the generating functional can be factorized in to two parts

$$Z_C = Z_{\mathcal{C}_{12}} Z_{\mathcal{C}_{34}}, \quad (1.34)$$

<sup>5</sup>Here we assume field  $O(x)$  to be bosonic. For fermionic case, the boundary condition is anti-periodic in the direction of imaginary component of  $t$ .

where  $C_{ij} = C_i \cup C_j$ . Therefore, we can effectively work with just generating functional  $Z_{C_{12}}$ . The action for  $Z_{C_{12}}$  is the sum of contributions from the two parts of the path,

$$S = \int_{t_i}^{t_f} dt L(t) - \int_{t_i}^{t_f} dt L\left(t - i\frac{\beta}{2}\right), \quad (1.35)$$

where

$$L(t) = \int d\vec{x} \mathcal{L}[O(t, \vec{x})]. \quad (1.36)$$

So, the generating functional  $Z_{C_{12}}$  is

$$Z_{C_{12}}[j_1, j_2] = \int \mathcal{D}\phi \exp\left(iS + i \int_{t_i}^{t_f} dt \int d\vec{x} j_1(x) O_1(x) - i \int_{t_i}^{t_f} dt \int d\vec{x} j_2(x) O_2(x)\right), \quad (1.37)$$

where  $j_1(j_2)$  is the physical(“ghost”) source living in  $C_1(C_2)$  and for the fields living in path  $C_2$  the time is understood to be  $t \equiv t - i\beta/2$ . From now on the parameter  $\beta$  will be implicit.

Now we can take second variations of  $Z_{C_{12}}$  with respect to the source  $j_1$  or  $j_2$  and obtain the Schwinger-Keldysh propagators from the free action,

$$iD_{ab}(x-y) = \frac{1}{i^2} \frac{\delta^2 \ln Z_{C_{12}}[j_1, j_2]}{\delta j_a(x) \delta j_b(y)} \Big|_{j_a=j_b=0} = i \begin{pmatrix} D_{11} & -D_{12} \\ -D_{21} & D_{22} \end{pmatrix}, \quad (1.38)$$

with  $a, b = 1, 2$  and

$$\begin{aligned} iD_{11}(t, \vec{x}) &= \langle T O_1(t, \vec{x}) O_1(0) \rangle, & iD_{12}(t, \vec{x}) &= \langle O_2(0) O_1(t, \vec{x}) \rangle, \\ iD_{21}(t, \vec{x}) &= \langle O_2(t, \vec{x}) O_1(0) \rangle, & iD_{22}(t, \vec{x}) &= \langle \overline{T} O_2(t, \vec{x}) O_2(0) \rangle. \end{aligned} \quad (1.39)$$

where  $\overline{T}$  denotes reversed time ordering in path  $C_2$ , and

$$O_1(t, \vec{x}) = e^{iHt - i\vec{P}\cdot\vec{x}} O(0) e^{-iHt + i\vec{P}\cdot\vec{x}}, \quad (1.40a)$$

$$O_2(t, \vec{x}) = e^{iH(t-i\beta/2) - i\vec{P}\cdot\vec{x}} O(0) e^{-iH(t-i\beta/2) + i\vec{P}\cdot\vec{x}}. \quad (1.40b)$$

These Schwinger-Keldysh propagators are related to the retarded and advanced Green's functions, which are defined as

$$iG^{\text{Ret}}(x-y) = \theta(x^0 - y^0) \langle [O(x), O(y)] \rangle, \quad (1.41a)$$

$$iG^{\text{Adv}}(x-y) = \theta(y^0 - x^0) \langle [O(y), O(x)] \rangle. \quad (1.41b)$$

In momentum space, defined by

$$G(k) = \int dx e^{-ik\cdot x} G(x), \quad (1.42)$$

we can show that

$$G^{Adv}(k) = G^{\text{Ret}*}(k). \quad (1.43)$$

Furthermore, we can rewrite the Schwinger-Keldysh propagators in terms of retarded Green's function as below (for bosons):

$$\begin{aligned} D_{11}(k) &= \text{Re } G^{\text{Ret}}(k) + i \coth \frac{\omega}{2T} \text{Im } G^{\text{Ret}}(k), \\ D_{22}(k) &= -\text{Re } G^{\text{Ret}}(k) + i \coth \frac{\omega}{2T} \text{Im } G^{\text{Ret}}(k), \\ D_{12}(k) &= D_{21}(k) = \frac{2ie^{-\frac{\beta}{2}\omega}}{1 - e^{-\beta\omega}} \text{Im } G^{\text{Ret}}(k). \end{aligned} \quad (1.44)$$

with  $\omega \equiv k^0$ .

## 1.7 Holographic real-time propagator

The gauge/gravity correspondence was originally formulated with Euclidean signature. For some cases, we need to perform computation of Green's functions of gauge theory with Lorentzian signature. While there are subtleties working with Lorentzian signature AdS/CFT correspondence [46–48], one could try to avoid Minkowski formulation of AdS/CFT by working with the Euclidean version. The resulting correlators can be analytically continued to Minkowski space using Wick rotation. Unfortunately this does not always work, in particular for finite temperature gauge theory. Analytic continuation to Minkowski space is possible only when we know the Euclidean correlators for all Matsubara frequencies which are beyond reach.

To see how the problem arises, consider as an example a scalar field  $\phi$  in the  $AdS_5$  black hole background with metric

$$\begin{aligned} ds^2 &= \frac{L^2}{z^2} \left( -h(z)dt^2 + dx^i dx^i + \frac{1}{h(z)} dz^2 \right) = g_{\mu\nu} dx^\mu dx^\nu + g_{zz} dz^2, \\ h(z) &= 1 - \frac{z^4}{z_H^4}, \end{aligned} \quad (1.45)$$

where  $i = 1, 2, 3$  and  $z$  in the range  $z_B \leq z \leq z_H$ , with the following action

$$S = \int d^4x \int_{z_B}^{z_H} \sqrt{-g} (g^{zz} (\partial_z \phi)^2 + g^{\mu\nu} \partial_\mu \phi \partial_\nu \phi + m^2 \phi^2). \quad (1.46)$$

The integration is taken between the boundary  $z_B$  and the horizon  $z_H$ .

The equation of motion for  $\phi$  is given by

$$\frac{1}{\sqrt{-g}} \partial_z (\sqrt{-g} g^{zz} \partial_z \phi) + g^{\mu\nu} \partial_\mu \partial_\nu \phi - m^2 \phi = 0. \quad (1.47)$$

The equation has to be solved with a fixed value at  $z_B$  for the solution of the form

$$\phi(z, x) = \int \frac{d^4 k}{(2\pi)^4} e^{ik_\mu x^\mu} f_k(z) \phi_0(k), \quad (1.48)$$

with  $f_k(z_B) = 1$  and  $\phi_0(k)$  is identified as the Fourier transform of a source field in the gauge theory. The effective equation of motion for the radial profile  $f(z)$  is

$$\frac{1}{\sqrt{-g}} \partial_z (\sqrt{-g} g^{zz} \partial_z f_k) - (g^{\mu\nu} k_\mu k_\nu + m^2) f_k = 0. \quad (1.49)$$

In order to have a unique solution for  $f_k(z)$ , we need to impose a condition at the horizon  $z_H$ . In the Euclidean signature, this can be done by imposing a regularity condition at the horizon  $z_H$ . But this is not the case for Lorentzian signature since near the horizon  $f_k(z)$  oscillates wildly and has two modes (incoming and outgoing modes). Physical reasoning implies that the incoming modes correspond to the retarded Green's function while the outgoing modes correspond to the advanced Green's function.

Knowing the choices for boundary condition at the horizon does not immediately solve the problem. Suppose we want to compute the retarded Green's function by taking the incoming-wave boundary condition. The on-shell action of (1.46) reduces to

$$S = \int \frac{d^4 k}{(2\pi)^4} \phi_0(-k) \mathcal{F}(z, k) \phi_0(k) \Big|_{z_B}^{z_H},$$

$$\mathcal{F}(z, k) = \sqrt{-g} g^{zz} f_{-k}(z) \partial_z f_k(z). \quad (1.50)$$

The retarded Green's function is computed by taking two functional derivatives over  $\phi_0$  of the on-shell action which give us

$$G^{\text{ret}}(k) = -\mathcal{F}(z, k) - \mathcal{F}(z, -k) \Big|_{z_B}^{z_H}. \quad (1.51)$$

Using  $f_k^*(z) = f_{-k}(z)$ , which is also a solution, we can show that the imaginary part of  $\mathcal{F}$  is proportional to a conserved flux and such it is independent of  $z$ . This means that the retarded Green's function  $G^{\text{ret}}(k)$  is a real function which is not a satisfying result since the retarded Green's function in general is a complex function.

### 1.7.1 Minkowski prescription I

Son and Starinets gave an ad hoc resolution to this problem of how to compute the Green's function in Minkowski AdS/CFT correspondence consistently [26]. They provided a prescription and various checks on the validity of the formula. The prescription goes as follows:

1. Solve the mode equation (1.48) with two boundary conditions at the boundary  $z_B$  and the horizon  $z_H$ . First, at the boundary  $z = z_B$ ,  $f_k(z_B) = 1$ . Second, the asymptotic solution is incoming(outgoing) wave at the horizon for retarded(advanced) Green's function. If we have space-like momenta then the second boundary condition is similar to the Euclidean version which is regular at the horizon.
2. Evaluating at the boundary  $z = z_B$ , the retarded(advanced) Green's function is given by

$$G(k) = -2\mathcal{F}(z_B, k), \quad (1.52)$$

where  $\mathcal{F}$  is computed from the surface terms of the on-shell action as shown in (1.50).

Despite the success of the prescription, it can only be applied to two point-functions. Extension of the prescription to more than two-point functions was not known. Besides, the lack on the details of how the prescription works left some questions to be answered.

The real-time formulation in finite temperature field theory involves doubling the degree of freedom. At the same time, the full Penrose diagram of asymptotically AdS metric containing a black hole has two boundaries and it was conjectured that there are doubler fields living on the second boundary of the AdS dual. These features were indeed realized by Herzog and Son's formulation of a more rigorous way to compute the Green's function in Minkowski AdS/CFT [42]. Their results originate in studies on black holes thermal radiation by Hawking and Hartle [49], Unruh [50], and Israel [51].

The upshot of their observation is that the gravity action must be modified by adding contribution from region  $L$ , where the doubler fields live, as shown in Figure 1.4; time in the region  $L$  reverses its direction. The bulk fields in both regions  $R$  and  $L$  are written in terms of physical and "ghost" sources of the finite temperature field theory, as defined previously, with boundary conditions that at the boundary of  $R$  the bulk fields in  $R$  becomes the physical sources and at the boundary of  $L$  the bulk fields in  $L$  becomes the "ghost" sources. At the horizon, the natural boundary conditions are defined so that positive frequency modes are incoming and negative frequency modes are outgoing in region  $R$  of the Penrose diagram. With the definition of retarded and advanced Green's functions in [26], as given in (1.52), second functional derivatives of the boundary action on gravity side over the sources yields Schwinger-Keldysh propagators (1.44).

There are a few interesting points in Herzog and Son's formula. It looks natural from gravity side to take the path  $\mathcal{C}$  for complex time plane as shown in Figure 1.3 with  $\sigma = \beta/2$ . Since the Green's functions are obtained by functional derivatives on the gravity action, in principal we can extend the formula to more than two-point functions. A detailed discussion on thermal three-point functions from Minkowski AdS/CFT using this formula can be found in [52].



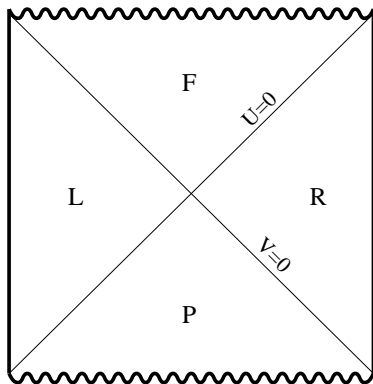


Figure 1.4: The full Penrose diagram for asymptotically AdS metric with a black hole solution.  $U$  and  $V$  are the Kruskal coordinates.

### 1.7.2 Minkowski prescription II

Although Herzog and Son's formula gives the correct Schwinger-Keldysh propagators of the finite temperature system, there are still some unsatisfactory issues in the procedure. The computation they did in [42] did not include the boundary contribution from timelike infinity to the on-shell action which is non vanishing in general. Furthermore, it depends entirely on the retarded and advanced Green's function that are still conjectured in Minkowski AdS/CFT.

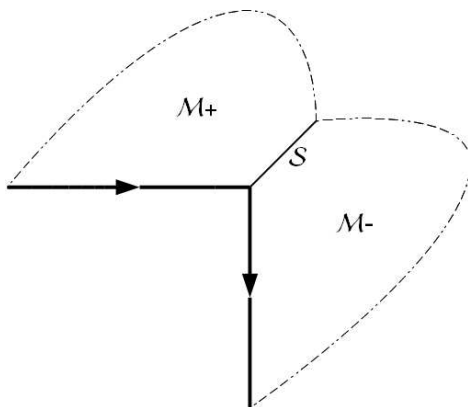


Figure 1.5: Holographic path. The bold lines with arrow are the segments of complex time path of the field theory at the boundary.

Skenderis and van Rees subsequently showed how to overcome these is-

sues and developed a fully holographic prescription [73, 74]. The idea is try to construct a bulk manifold  $\mathcal{M}_{\mathcal{C}}$  from a given complex time path  $\mathcal{C}$  in finite temperature field theory at the boundary. It involves gluing different manifolds for each segments of the path  $\mathcal{C}$ . The paths that live in the real part of time correspond to Lorentzian solutions and ones live in the imaginary part of time correspond to Euclidean solutions.

When two segments of the complex time path  $\mathcal{C}$  intersect at a point, the point is extended to a hypersurface  $\mathcal{S}$  in the bulk. The time signature of the metric changes at this hypersurface corresponds to this intersection point. In this hypersurface  $\mathcal{S}$ , we need to impose two matching conditions:

1. Continuity of the field  $\phi$  across  $\mathcal{S}$ :

$$\phi_{-}(\mathcal{S}) = \phi_{+}(\mathcal{S}). \quad (1.53)$$

2. If the two bulk manifolds  $\mathcal{M}_{-}$  and  $\mathcal{M}_{+}$  (correspond to two segments of the path) intersect at a boundary  $\mathcal{S}$  (corresponds to the intersection point between two segments of the path) then we also impose continuity of the momentum conjugate  $\pi^{\phi}$  across  $\mathcal{S}$ :

$$\pi_{-}^{\phi}(\mathcal{S}) = \eta \pi_{+}^{\phi}(\mathcal{S}), \quad (1.54)$$

where  $\pi_{\pm}^{\phi}$  is the conjugate momentum in  $\mathcal{M}_{\pm}$ . We set  $\eta = -i$  if  $\mathcal{M}_{-}$  is Euclidean and  $\mathcal{M}_{+}$  is Lorentzian; and  $\eta = 1$  if both  $\mathcal{M}_{-}$  and  $\mathcal{M}_{+}$  are Lorentzian (this is the case with  $\sigma = 0$  in Figure 1.3).

A more detailed application of Skenderis and Van Rees's holographic prescription can be found in section 3.D.3.

## 1.8 Outline

In chapter 2, we will apply gauge/gravity correspondence on photon and dilepton production in QGP. We start with definition of spectral density function in momentum space  $\chi(K)$  which is proportional to the photon and dilepton production rates. Having determined the observables in gauge theory or QGP, We write down the relevant  $5D$ -action in gravity theory with AdS black hole background metric. In particular we consider the AdS/QCD soft-wall model, as discussed in 1.5.2, with non-trivial dilaton background. Using holographic real-time prescription 1.7.1, we compute the spectral density function by means of solving the equations of motion of the dual fields numerically and also analytically for low- and high-frequency.

Using a semiclassical approach to gauge/gravity duality, we describe in chapter 3 Brownian motion of a quark in strongly coupled plasma, for example QGP, from string theory perspective. We first define properties of Brownian motion given by a generalized Langevin equation. In this case, the random

force  $R$  is assumed to be Gaussian and the Langevin equation is linear in momentum. The gravity description is given by the motion of a string under some black hole background metric where the ends of the string are stretching from boundary to horizon. The end of the string at the boundary is interpreted as an external quark behaves as Brownian particle moving in a heat bath, which are represented by the black hole background metric. Explicitly, we consider the background metrics which are non-rotating BTZ black hole for neutral plasma and STU black holes for charged plasma.

The two- and four-point functions of the random force  $R$  can be computed by taking derivatives of the dual coordinate in the expansion of the Nambu-Goto action. In computing the correlation functions, we use the holographic real-time prescription 1.7.2 together with holographic renormalization 1.4.1 to removed the UV divergences while the IR divergences are removed by introducing a cutoff near the horizon. Most of the calculations are done in low frequency limit,  $\omega \rightarrow 0$ . This way we can find the impedance  $\mu(\omega)$  from the two-point functions which eventually gives us the friction coefficient in non-relativistic limit. With a simple model of random force profile, a time scale can be extracted from the two- and four-point functions which is defined as mean-free path time  $t_{mfp}$ .

The last chapter 4 is an attempt to study anisotropic effects in QGP from semiclassical string point of view as we already used in chapter 3. Here, we argue that the anisotropic in QGP can be encoded in rotating black hole solutions. This chapter mainly discusses about how to compute the drag force with a given background metric. We first consider a  $4D$  AdS-Schwarzschild black hole and compute the drag force of the great circle solution at the equatorial plane with linear ansatz and then generalize the drag force computation for non-equatorial case.

As one example of rotating black hole solutions, we look at  $4D$  Kerr-AdS black hole in Boyer-Lindquist coordinates. A simple drag force computation will be the equatorial great circle solution with linear ansatz. The non-equatorial solutions in general are very difficult. For a simple case, we consider drag forces at the leading order for small angular momentum  $a$  and velocity  $\omega$  of the Kerr-AdS black hole. We use a map of coordinates transformation from Kerr-AdS coordinates to Boyer-Lindquist coordinates to derive an ansatz for “static” string solution in Boyer-Lindquist coordinates. The solution is written in terms of the static thermal rest mass quark  $m_{rest}$  and the temperature of plasma  $T$ . We also plot the drag forces for different values of angular momentum  $a$  and parameter  $M_T$ .

# CHAPTER 2

---

## PHOTON PRODUCTION IN SOFT WALL MODEL

---

### 2.1 Introduction

One of the current challenges in theoretical particle physics is to compute properties of the strongly coupled QGP(sQGP) discovered at RHIC. AdS/CFT tools have given us some insight into the strongly coupled thermodynamics of gauge theories [2, 4, 9, 11]. However, it remains a mystery why these, mostly  $\mathcal{N} = 4$  supersymmetric, YM calculations work well for QCD. Part of the challenge is to either understand why this is so, or to find AdS duals of theories resembling QCD closer than  $\mathcal{N} = 4$  SYM. In this latter context a phenomenological AdS dual to Chiral perturbation theory or AdS/QCD constructed by Erlich et.al. is perhaps a good candidate [12].

Introducing the IR-cutoff is the essential new ingredient in AdS/QCD compared to AdS/CFT. Here we shall investigate the effects of this cutoff on photon and dilepton production rates at strongly coupling. Remarkably the  $\mathcal{N} = 4$  SYM CFT computation of these production rates suggested they are not affected by a hard IR-cutoff even for temperatures infinitesimally above the cutoff [5]. Intuitively this seems rather strange. At energies and temperatures close the QCD scale IR effects should start to affect the production rate. We shall find that for smoothly IR-cutoff AdS/QCD this is indeed the case. The robustness of our phenomenological result of how photon production rates are effected by changing the IR-cutoff is confirmed by a calculation by Mateos and Patiño [23] of the photon production rate in AdS dual of a  $\mathcal{N} = 2$  theory with

massive flavor. Here the flavor sector acts as the effective IR-cutoff, and we will be able to show this by relating the mass-parameter to the soft-wall cutoff scale. Soft-wall AdS/QCD is more crude than massive flavor models, of course, and this is evident in the lack of spectral peaks that we shall find.

Photon production in a medium such as QGP was discussed in detail both from strong and weak coupling point view in [5]. We briefly review this in section 2.2 and show there how the strong coupling calculation is modified by considering AdS/QCD instead of pure  $\mathcal{N} = 4$  SYM. In section 2.3, we present our solution and discuss its results in section 2.4 with a comparison to photon production in AdS duals of  $\mathcal{N} = 2$  massive flavor theories.

## 2.2 Photon and dilepton production

One of the observational phenomena in RHIC is the spontaneous production of photons from the sQGP of hot charged particles. This direct photon spectrum ought to be a good probe of the strongly coupled quark-gluon soup, as the weakly interacting photons should escape nearly unaffected from the small finite size collision area [24].

As is described in [5], we can therefore regard the dynamically formed sQGP to first approximation as a field theory at finite temperature. For a standard perturbative electromagnetic current coupling  $eJ_\mu^{\text{EM}}A^\mu$ , the first order photon production rate is then given by [5, 25]

$$d\Gamma_\gamma = \frac{d^3k}{(2\pi)^3 2k^0} e^2 n_B(k^0) \eta^{\mu\nu} \chi_{\mu\nu}(K)|_{k^0=|\vec{k}|}. \quad (2.1)$$

Here  $K \equiv (k^0, \vec{k})$  is a momentum 4-vector,  $n_B(k^0) = 1/(e^{\beta k^0} - 1)$  the Bose-Einstein distribution function, and the spectral density  $\chi_{\mu\nu}(K)$  is proportional to the imaginary part of the (finite temperature) retarded current-current correlation function

$$\begin{aligned} \chi_{\mu\nu}(K) &= -2 \text{Im}(G_{\mu\nu}^{R,\beta}(K)), \\ G_{\mu\nu}^{R,\beta}(K) &= \int d^4X e^{-iK \cdot X} \langle J_\mu^{\text{EM}}(0) J_\nu^{\text{EM}}(X) \rangle_\beta \theta(-x^0). \end{aligned} \quad (2.2)$$

At finite temperature, Lorentz invariance is broken by the heat bath. We can use the remaining rotational symmetry plus gauge invariance to simplify the retarded correlator to

$$G_{\mu\nu}^{R,\beta \neq 0}(K) = P_{\mu\nu}^T(K) \Pi^T(K) + P_{\mu\nu}^L(K) \Pi^L(K), \quad (2.3)$$

Here the transverse and longitudinal projectors are  $P_{00}^T(K) = 0$ ,  $P_{0i}^T(K) = 0$ ,  $P_{ij}^T(K) = \delta_{ij} - k_i k_j / |\vec{k}|^2$ , and  $P_{\mu\nu}^L(K) = P_{\mu\nu}(K) - P_{\mu\nu}^T(K)$ , with  $i, j = x, y, z$ . We

can trivially consider charged lepton production as well by considering non-lightlike momenta for off-shell photons: The leptons then result from virtual photon decay. Lepton pair production for each lepton species in the leading order of the electromagnetic couplings  $e$  and  $e_l$ , is given by [5, 25]

$$d\Gamma_{\bar{l}l} = \frac{d^4K}{(2\pi)^4} \frac{e^2 e_l^2}{6\pi|K|^5} [-K^2 - 4m^2]^{1/2} (-K^2 + 2m^2) n_b(k^0) \chi_{\mu}^{\mu}(K) \theta(k^0) \theta(-K^2 - 4m^2), \quad (2.4)$$

with  $e_l$  the electric charge of the lepton,  $m$  the lepton mass,  $\theta(x)$  a unit step function, and the spectral density  $\chi_{\mu\nu}(K)$  is evaluated at the timelike momentum of the emitted particle pair. Note that both  $\Pi^T$  and  $\Pi^L$  contribute to the dilepton rate, but only  $\Pi^T$  contributes to the photon emission rate, because the longitudinal part must vanish for lightlike momenta, i.e. the unphysical longitudinal mode is not a propagating degree of freedom.

Finally, fluctuation-dissipation relates the zero-frequency limit of the spectral density to the electrical conductivity  $\sigma$ :

$$\sigma = \lim_{k^0 \rightarrow 0} \frac{e^2}{6T} n_B(k_0) \eta^{\mu\nu} \chi_{\mu\nu}(k^0, \vec{k} = 0), \quad (2.5)$$

or, if  $k_{\mu}$  is lightlike

$$\sigma = \lim_{k^0 \rightarrow 0} \frac{e^2}{4T} n_B(k_0) \eta^{\mu\nu} \chi_{\mu\nu}(K) \Big|_{|\vec{k}|=k^0}. \quad (2.6)$$

### 2.2.1 Photon and dilepton rates at strong coupling

The AdS/CFT dictionary gives that the large  $N_c$  limit of strongly coupled  $d = 4$   $\mathcal{N} = 4$  SYM theory at finite temperature  $T$  has a dual description in terms of five dimensional AdS-supergravity in the background of a black hole [9]

$$ds^2 = \frac{(\pi T R)^2}{u} [-f(u) dt^2 + dx^2 + dy^2 + dz^2] + \frac{R^2}{4u^2 f(u)} du^2. \quad (2.7)$$

Here  $f(u) = 1 - u^2$ , with  $u \in [0, 1]$  a dimensionless radial AdS coordinate related through  $u = (\pi T z)^2$  to standard AdS coordinates, and  $R$  is the curvature radius of the AdS space.<sup>1</sup> The metric (2.7) has a horizon at  $u = 1$  with Hawking temperature  $T$  and a boundary at  $u = 0$ .

Qualitatively the same is expected hold for other 4-dim field theories. As a model for low energy QCD we shall take the AdS dual of chiral perturbation theory. This AdS/QCD consists of the fields  $A_{L\mu}^a, A_{R\mu}^a$ , dual to the  $SU(N_f)_L \times SU(N_f)_R$  currents and a scalar  $X$  dual to the quark condensate in

<sup>1</sup> We will keep to Lorentzian signature throughout since we seek information regarding the response of the thermal ensemble to small perturbations. This requires the use of real-time Green's functions [26].

an AdS background which is cutoff at some finite distance  $u = u_0$  [12]. To this we add an extra  $U(1)$  field,  $V_\mu$  dual to the electromagnetic current  $J_\mu^{EM}$ . Recall that  $u_0$  corresponds to the introduction of the QCD-scale in the field theory: it enforces the mass-gap by hand by explicitly cutting-off any dynamics in the IR. For the reasons we explained in the introduction, here we are going to use a soft wall cut-off [15, 16]. Formally we can introduce this cut-off by modifying the AdS bulk action to (we give only the term relevant for calculating the photon production rate)

$$S \sim \int d^5x \sqrt{g} \left( -\frac{1}{4} F_{AB} F^{AB} + \dots \right) \Rightarrow S \sim -\frac{1}{4} \int d^5x \sqrt{g} e^{-\Phi} F_{AB} F^{AB} + \dots \quad (2.8)$$

Here  $A, B = t, x, y, z, u$  and the ‘‘dilaton’’ takes the fixed form  $\Phi = cu$  where  $c = \frac{\Lambda_{IR}^2}{(\pi T)^2}$ , with  $\Lambda_{IR}$  the IR scale below which physics is cut-off. This introduction into the action is formal in the sense that (1) we shall not consider  $\Phi$  a dynamical field and (2) we assume that the presence of the cut-off does not affect the geometric AdS background, see also [16]. We thus still work with the metric (2.7) for the finite temperature version of AdS/QCD, but with the equation of motion for the fluctuations derived from action (2.8). We will discuss the validity of this approach in detail in section 2.4.

For photon production, we need only the  $U(1)$  gauge field equation of motion  $\partial_A (\sqrt{g} e^{-cu} g^{AB} g^{CD} F_{BD}) = 0$  with  $F_{AB} = \partial_A V_B - \partial_B V_A$  the Maxwell field strength. The 4d electric fields are  $E_i \equiv F_{ti}$  with  $i = x, y, z$ . Note that we use  $A$  as a vector index and  $V_B$  for the AdS gauge field. To compute the AdS boundary 2-point correlation function from which to extract the spectral density  $\chi_{\mu\nu}$ , we follow [5] and split the equation of motion into parts perpendicular ( $V_x, V_y \equiv V_\perp$ ) and parallel ( $V_z \equiv V_\parallel$ ) to a predefined spatial three-momentum  $\vec{k} = (0, 0, k)$ , the Gauss constraint ( $V_0$  e.o.m.) and the radial AdS ( $V_u$ ) equation of motion. After a Fourier transformation along  $t, x, y, z$ , and defining  $\omega = \frac{k^0}{2\pi T}$ ,  $q = \frac{k}{2\pi T}$ , we find respectively

$$\partial_u^2 V_\perp + \left( \frac{\partial_u f}{f} - c \right) \partial_u V_\perp + \frac{\omega^2 - q^2 f}{u f^2} V_\perp = 0, \quad (2.9)$$

$$\frac{q}{u f} (q V_t + \omega V_\parallel) - (\partial_u^2 V_t + i(2\pi T)\omega \partial_u V_u) + c(\partial_u V_t + i(2\pi T)\omega V_u) = 0, \quad (2.10)$$

$$\frac{\omega}{u f^2} (q V_t + \omega V_\parallel) + \left[ \left( \frac{\partial_u f}{f} - c \right) \partial_u V_\parallel + \partial_u^2 V_\parallel \right] - i(2\pi T)q \left[ \left( \frac{\partial_u f}{f} - c \right) V_u + \partial_u V_u \right] = 0. \quad (2.11)$$

The equation of motion for  $V_u$ ,

$$\sqrt{g} e^{-cu} g^{uu} \left( g^{tt} \partial_t F_{tu} + g^{\parallel\parallel} \partial_\parallel F_{\parallel u} \right) = 0, \quad (2.12)$$

can be simplified to

$$V_u = \frac{i}{2\pi T} \frac{(\omega \partial_u V_t + qf \partial_u V_{\parallel})}{(\omega^2 - q^2 f)}. \quad (2.13)$$

Let us define  $E_{\perp} = \omega V_{\perp}$  and  $E_{\parallel} = qV_t + \omega V_{\parallel}$ . From Eq. (2.9) and combining eq. (2.11) with eq. (2.10) and eq. (2.13) in the gauge  $V_u = 0$  we obtain the two decoupled equations

$$\partial_u^2 E_{\perp} + \left( \frac{\partial_u f}{f} - c \right) \partial_u E_{\perp} + \frac{\omega^2 - q^2 f}{u f^2} E_{\perp} = 0, \quad (2.14)$$

$$\partial_u^2 E_{\parallel} + \left[ \frac{\omega^2 \partial_u f}{f(\omega^2 - q^2 f)} - c \right] \partial_u E_{\parallel} + \frac{\omega^2 - q^2 f}{u f^2} E_{\parallel} = 0. \quad (2.15)$$

We shall need to solve these two equations to obtain the spectral density  $\chi_{\mu\nu}$ . These differential equations (2.14) and (2.15) have three regular singular points at  $u = \pm 1, 0$ , and one irregular singular point at  $\infty$ .<sup>2</sup>

Formal solutions for such equations are difficult to construct. Note that the irregular nature of the point at infinity becomes regular when we remove the IR-cutoff  $c$ . The irregular point, however, is outside the physical region of interest  $u \in (0, 1)$  and we can, for instance, solve the equations (2.9) and (2.15) near the boundary  $u \rightarrow 0$  using Frobenius expansion  $E = u^{\lambda} \sum_{n=0}^{\infty} a_n u^n$  where the indicial equation has solutions for  $\lambda = 0, 1$ .

To solve the equations (2.14), (2.15) explicitly shall be the main part of this note. The solutions to these 5-d AdS equations of motion then give the 4-d field theory two point correlation as the functional derivative with respect to the boundary values of the on-shell AdS action

$$S = -\frac{1}{4g_B^2} \int d^4 x du \sqrt{g} e^{-cu} F_{AB} F^{AB} \Big|_{\text{on-shell}}, \quad (2.16)$$

with  $g_B^2 = 16\pi^2 R/N_c^2$ . Considering  $V_u = 0$  gauge, we can write this as

$$\begin{aligned} S_{\text{on-shell}} &= -\frac{N_c^2}{32\pi^2 R} \int_{-\infty}^{\infty} d^4 x (\sqrt{g} e^{-cu} V_{\mu} F^{u\mu}) \Big|_{u=0}^{u=1} \\ &= \frac{N_c^2 T^2}{16} \int_{-\infty}^{\infty} d^4 x e^{-cu} (V_t \partial_u V_t - f V_i \partial_u V_i) \Big|_{u=0}^{u=1}. \end{aligned} \quad (2.17)$$

Fourier transforming to momentum space and selecting the particular direction chosen previously, we can rewrite the action using Minkowskian prescription formulated by Son and Starinets [26]. Together with the boundary condi-

<sup>2</sup>Recall that an irregular singular point for a differential equation  $y'' + P(x)y' + Q(x)y = 0$  is a point  $x_0$  for which either  $\lim_{x \rightarrow x_0} (x - x_0)P(x)$  or  $\lim_{x \rightarrow x_0} (x - x_0)^2 Q(x)$  diverges. The point at infinity is irregular if  $\lim_{x \rightarrow \infty} (2 - xP(x))$  or  $\lim_{x \rightarrow \infty} x^2 Q(x)$  diverges. Using that  $f = (1 - u^2)$  one clearly sees how the introduction of  $c$  introduces a divergence in  $\lim_{u \rightarrow \infty} 2 - u(\partial_u \ln f - c) = \lim_{u \rightarrow \infty} 2 + 2u^2/(1 - u^2) + uc$ .



tion that the solution of equations (2.9) and (2.15) must satisfy the incoming-wave boundary condition at the horizon  $u = 1$ , the resulting on-shell action becomes

$$S_{\text{on-shell}} = \frac{N_c^2 T^2}{16} \lim_{u \rightarrow 0} \int \frac{d\omega dq}{(2\pi)^2} e^{-cu} \left[ \frac{f}{q^2 f - \omega^2} \partial_u E_{\parallel}(u, K) E_{\parallel}(u, -K) - \frac{f}{\omega^2} \partial_u E_{\perp}(u, K) E_{\perp}(u, -K) \right]. \quad (2.18)$$

From Eq. (2.18) and the condition described above, we can now compute the retarded current-current correlation function in term of two independent scalar functions<sup>3</sup>

$$\Pi^L(K) = -\frac{N_c^2 T^2}{8} \lim_{u \rightarrow 0} \frac{\partial_u E_{\parallel}(u, K)}{E_{\parallel}(u, K)}, \quad (2.19)$$

$$\Pi^T(K) = -\frac{N_c^2 T^2}{8} \lim_{u \rightarrow 0} \frac{\partial_u E_{\perp}(u, K)}{E_{\perp}(u, K)}. \quad (2.20)$$

These functions in turn give us the photon and dilepton production at strong coupling via eq. (2.3) and eqs. (2.1) and (2.4).

## 2.3 Solving the system

In this section we will solve the equations (2.14) and (2.15) in order to compute the two scalar functions (2.19) and (2.20). Furthermore, we will take the imaginary part of those scalar functions and obtain the spectral density function (2.2) for finite temperature system.

The solutions which satisfy the incoming-wave boundary condition can be written in general as a Frobenius expansion near  $u \rightarrow 1$

$$E_i(u) = (1 - u)^{-i\omega/2} y_i(u), \quad (2.21)$$

with  $y_i(u)$  regular at  $u = 1$ . We will solve and discuss these equations extensively for lightlike momenta relevant for photon-production, both semi-analytically for asymptotically small and large frequency and numerically for various values of the cut-off  $c$  for the full range of momenta. For timelike and spacelike momenta we only present the numerical solution.

### 2.3.1 Lightlike momenta

As has been explained in section 2.2, the longitudinal part of the scalar functions vanishes for lightlike momenta and we just need to compute the transverse part.

---

<sup>3</sup>For a more detailed derivation of these functions see [28].

### Analytic solutions for lightlike momenta at low and high frequency

We are mainly interested in the effect of the IR-cut-off on photon production as compared to the previous AdS photon production calculation for scale-invariant  $\mathcal{N} = 4$  SYM [5]. In the low-frequency limit where its effect should be largest, we can solve (2.9) perturbatively using  $\omega \ll 1$  as a small parameter. As noted in [5], there is a shortcut to do so. Given the two independent solutions  $\phi_1 \pm i\phi_2$  to the differential equation  $\phi'' + A(x)\phi' + B(x)\phi = 0$ , the Wronskian times  $\exp(\int^x A(x'))$  is strictly conserved

$$\partial_x \left( e^{\int^x A(x')} [\bar{\phi} \partial_x \phi - \phi \partial_x \bar{\phi}] \right) = 0. \quad (2.22)$$

The transverse scalar can be rewritten as

$$\begin{aligned} \Pi^T(K) &= \lim_{u \rightarrow 0} \Pi^T(u, K), \\ \Pi^T(u, K) &\equiv -\frac{N_c^2 T^2}{8} \left[ e^{-cu} (1-u^2) \frac{\bar{E}_\perp(u, K)}{\bar{E}_\perp(0, K)} \partial_u \frac{E_\perp(u, K)}{E_\perp(0, K)} \right]. \end{aligned} \quad (2.23)$$

The imaginary part of the transverse scalar  $\Pi^T(u, K)$  is then proportional to the conserved Wronskian and therefore independent of the radial coordinate  $u$ :

$$\partial_u \text{Im}[\Pi^T(u, K)] = 0. \quad (2.24)$$

With this fact, we can evaluate the imaginary part of (2.23) at any given value of  $u$  which is convenient to our calculation. Let us choose  $u = 1$ . Because the transverse scalar (2.23) contains an explicit factor of  $(1-u)$ , only the pole in  $\bar{E}_\perp \partial_u E_\perp$  will contribute. Recalling that for any finite frequency  $\omega$  the boundary conditions determine  $E_\perp(u)$  to be of the form (2.21), we immediately see that the undetermined regular part  $y$  contains no pole by definition. Therefore without needing to solve the equation motion we see that

$$\Pi^T(1, K) = \frac{-N_c^2 T^2}{8} \left( \frac{-i\omega}{2} \right) \left[ 2e^{-c} \left| \frac{y(1)}{y(0)} \right|^2 \right]. \quad (2.25)$$

The leading term in the limit  $\omega \ll 1$  is the  $\omega$ -independent contribution to  $|y(1)/y(0)|$ . The determining equation (2.14) simplifies in that limit to effectively the first order equation (recall that  $\omega = q$  for lightlike momenta)

$$\partial_u \partial_u E_\perp + (\partial_u (\ln f - cu)) \partial_u E = 0 + \mathcal{O}(\omega^2). \quad (2.26)$$

The incoming wave boundary condition demands that the  $\omega = 0$  solution be regular at  $u = 1$ . Since  $f = (1-u)(1+u)$ , this solution is the trivial constant one. Therefore

$$\Pi^T(1, K) = \frac{i\omega N_c^2 T^2}{8} e^{-c} + \mathcal{O}(\omega^2). \quad (2.27)$$

In Appendix 2.A we compute the same answer directly by solving the differential equation perturbatively in  $\omega$ , which shows explicitly that  $E_{\perp}(u) = \text{constant} + \mathcal{O}(\omega)$  is indeed the correct solution to the boundary conditions.

Given  $\Pi(1, K)$ , the trace of spectral density function at low-frequency limit for lightlike momenta in photon production is proportional to its  $u$ -independent imaginary part

$$\begin{aligned}\chi_{\mu}^{\mu}(\omega = q) &= -4 \text{Im}(\Pi^T(\omega = q)) \\ &= \frac{\omega N_c^2 T^2}{2} e^{-c} + \mathcal{O}(\omega^2).\end{aligned}\quad (2.28)$$

For  $c = 0$ , we reproduce back the result from [5] at the first order. The vanishing of  $c$  corresponds to either the limit  $T \rightarrow \infty$  or to removing the IR scale  $\Lambda_{IR}$ . We see explicitly our intuition confirmed that the trace of spectral density at low-frequency depends on the cutoff parameter  $c$ , while simultaneously reproducing the  $\mathcal{N} = 4$  result at high  $T$ .

At high-frequencies we do not expect the IR-cut-off to have a major effect. Let us show that to leading order the spectral function is in fact independent of the value of  $c$  as one would expect. In this limit  $\omega \gg 1$ , the argument leading up to eq. (2.25) does not hold<sup>4</sup> and one cannot obtain the answer without solving the equation of motion (2.14). Following [5], we will use the Langer-Olver method [29] to find the solution. The first step is to redefine

$$E_{\perp}(u) = \frac{e^{cu/2}}{\sqrt{-f(u)}} y(u) \quad (2.29)$$

for equation (2.14) and rewrite it as

$$y''(x) = [\omega^2 H(x) + G(x)] y(x), \quad (2.30)$$

where  $H(x) = \frac{x}{f(x)^2}$  and  $G(x) = \frac{c^2}{4} - \frac{cx}{f(x)} - \frac{1}{f(x)^2}$  with  $x = -u \in [-1, 0]$ . For large  $\omega$  the first term on the RHS dominates. Since it has a simple zero at  $x = 0$ , we can transform Eq. (2.30) to Airy's equation plus terms subleading in  $\omega$ . To do so, we introduce a new independent variable  $\zeta$  and change variables to

$$\zeta \left( \frac{d\zeta}{dx} \right)^2 = H(x) = \frac{x}{(1-x^2)^2}. \quad (2.31)$$

Choosing conditions  $\zeta(0) = 0$  and  $\zeta'(0) > 0$  determines  $\zeta$  to be

$$\zeta = \left[ \frac{3}{2} \int_0^x \sqrt{H(t)} dt \right]^{2/3}. \quad (2.32)$$

---

<sup>4</sup>Note e.g. that in the singular term  $(1-u)^{-i\omega/2}$  the order of limits  $u \rightarrow 1$  and  $\omega \rightarrow \infty$  do not commute.

Rescaling  $y(x)$  to

$$y = \left( \frac{d\zeta}{dx} \right)^{-1/2} W, \quad (2.33)$$

eq. (2.30) becomes

$$\frac{d^2 W}{d\zeta^2} = [\omega^2 \zeta + \psi(\zeta)] W, \quad (2.34)$$

with

$$\psi(\zeta) = \frac{5}{16\zeta^2} + \frac{[4H(x)H''(x) - 5H'^2(x)]}{16H^3(x)} \zeta + \frac{\zeta G(x)}{H(x)} \quad (2.35)$$

For large  $\omega$  we may ignore  $\psi(\zeta)$  and the equation reduces to Airy's equation. To leading order the solution is thus

$$W(\zeta) = A_0 \text{Ai}(\omega^{2/3} \zeta) + B_0 \text{Bi}(\omega^{2/3} \zeta) + \dots, \quad (2.36)$$

The incoming-wave boundary conditions at the horizon imply that  $B_0$  should vanish. Thus the solution for  $E_\perp(u)$  in asymptotic expansion for large  $\omega$  is

$$E_\perp(u) = \frac{A_0 e^{cu/2}}{\sqrt{-f(u)}} \left[ \frac{-u}{f(u)^2 \zeta(-u)} \right]^{-1/4} \text{Ai}(\omega^{2/3} \zeta(-u)) + \dots, \quad (2.37)$$

and the transverse scalar at high-frequency limit equals

$$\Pi^T = -\frac{N_c^2 T^2}{8} \lim_{u \rightarrow 0} \left( \frac{c}{2} + \frac{1}{4} \partial_u \ln \left( \frac{-\zeta(-u)}{u} \right) + \frac{\partial_u \text{Ai}(\omega^{2/3} \zeta(-u))}{\text{Ai}(\omega^{2/3} \zeta(-u))} \right) + \dots \quad (2.38)$$

Before we move on, it is helpful to expand  $\zeta(-u)$  around  $u = 0$

$$\zeta(-u) = -(-1)^{2/3} u - \frac{2}{7} (-1)^{2/3} u^3 + \mathcal{O}(u^5). \quad (2.39)$$

Therefore the middle term in (2.38),

$$\partial_u \ln \left( \frac{-\zeta(-u)}{u} \right) = \frac{1}{(-1)^{2/3} + \dots} \left( \frac{6}{7} (-1)^{2/3} u + \dots \right), \quad (2.40)$$

vanishes as  $u \rightarrow 0$ . Knowing the asymptotics of the Airy function the last term of (2.38) can be written as

$$\begin{aligned} \lim_{u \rightarrow 0} \frac{\text{Ai}'(\omega^{2/3} \zeta(-u))}{\text{Ai}(\omega^{2/3} \zeta(-u))} &= -(-\omega)^{2/3} \frac{\text{Ai}'(0)}{\text{Ai}(0)} \\ &= (-\omega)^{2/3} \frac{3^{1/3} \Gamma(2/3)}{\Gamma(1/3)}, \end{aligned} \quad (2.41)$$

and thus we obtain

$$\Pi^T = -\frac{N_c^2 T^2}{8} \left( \frac{c}{2} + \frac{e^{2\pi i/3} \omega^{2/3} 3^{1/3} \Gamma(2/3)}{\Gamma(1/3)} \right). \quad (2.42)$$

Note that this transverse scalar therefore depends on  $c$ . However, only the real part does. The trace of the spectral density function in high-frequency limit for lightlike momenta

$$\begin{aligned} \chi_\mu^\mu &= -4 \operatorname{Im}(\Pi^T) \\ &\sim \frac{N_c^2 T^2}{4} \frac{\omega^{2/3} 3^{5/6} \Gamma(2/3)}{\Gamma(1/3)}. \end{aligned} \quad (2.43)$$

does not depend on the cutoff parameter  $c$  at least up to first order and yields the same result as the calculation in  $\mathcal{N} = 4$  SYM. The fact that  $c$  does appear in the real part of the transverse scalar indicates that at first subleading order the spectral density function will likely differ from the  $\mathcal{N} = 4$  result. The numerical results in the next section bear this out.

### Numerical solution for lightlike momenta

The analytic asymptotic solutions are a guidance to the full spectral function. The full solutions of equation (2.9) for non-zero  $c$  are very difficult to find, as we remarked earlier. This is due to the irregular singular point at  $u = \infty$  for  $c \neq 0$  where analytic solutions are not known. In this subsection we are going to look for numerical solutions for non-zero  $c$ .

We start from the general solution (2.21) which satisfies the incoming wave boundary condition. To set a parametrization of the initial conditions for the  $u = 1$  regular function  $y_i(u) = E_i(1-u)^{i\omega/2}$  of Eq. (2.21), we write the general solution as a polynomial expansion around  $u = 1$ ,  $y(u) = \sum_{n=0}^{\infty} a_n (1-u)^n$ . Substituting (2.21) into equation (2.14) for lightlike momenta, we obtain the equation

$$\begin{aligned} &\sum_{n=0}^{\infty} \left[ a_n \left( n - i\frac{\omega}{2} \right)^2 (1-u)^{n-2} + c a_n \left( n - i\frac{\omega}{2} \right) (1-u)^{n-1} \right. \\ &\left. - \sum_{m=0}^{\infty} \left[ \frac{a_m}{2^{m+1}} \left( n - i\frac{\omega}{2} + \frac{\omega^2(m+1)}{4} \right) (1-u)^{n+m-1} - \frac{a_m \omega^2}{2^{m+2}} (1-u)^{n+m-2} \right] \right] = 0. \end{aligned} \quad (2.44)$$

The second sum (over  $m$ ) arises from expanding  $\frac{1}{1+u} = \sum_{n=0}^{\infty} \frac{1}{2^{n+1}} (1-u)^n$  and  $\frac{1}{(1+u)^2} = \sum_{n=0}^{\infty} \frac{(n+1)}{2^{n+2}} (1-u)^n$ . In order to find the coefficients  $a_n$ , we have to

solve this equation for each power of  $(1 - u)$  and obtain

$$\begin{aligned}
 (1 - u)^{-2} &: a_0 \text{ (arbitrary)}, \\
 (1 - u)^{-1} &: a_1 = \frac{i\omega(c - 1/2)}{2(1 - i\omega)} a_0, \\
 &\vdots \\
 (1 - u)^{k-2} &: a_k = f_k(\omega, c) a_0,
 \end{aligned} \tag{2.45}$$

with  $f_k$  are functions of  $\omega$  and  $c$  which vanish at  $\omega = 0$ . This gives us  $y(u)$  and  $y'(u)$  at  $u = 1$  in terms of the above coefficients

$$\begin{aligned}
 y(1) &= a_0, \\
 y'(1) &= -a_1 = -a_0 \frac{i\omega(c - 1/2)}{2(1 - i\omega)}.
 \end{aligned} \tag{2.46}$$

These will be the two initial conditions for the differential equation for  $y(u)$ . The explicit differential equation it must satisfy is

$$\begin{aligned}
 y'' + \left( \frac{i\omega}{1 - u} - \frac{2u}{1 - u^2} - c \right) y' \\
 + \left[ \frac{\omega^2 u}{(1 - u^2)^2} + \frac{2i\omega - \omega^2}{4(1 - u)^2} - \frac{i\omega}{2(1 - u)} \left( \frac{2u}{1 - u^2} + c \right) \right] y = 0.
 \end{aligned} \tag{2.47}$$

Notice that the initial conditions for  $y(u)$  still depend on an arbitrary constant  $a_0$ . Physical quantities, such as the spectral density function, depend on ratios of  $y(u)$  and its derivatives and are independent of this constant. We are therefore free to set it to any value; we will choose  $a_0 = 1$ .

Let us express the trace of spectral density function in terms of  $y(u)$ :

$$\chi_\mu^\mu = \frac{N_c^2 T^2}{2} \left( \frac{\omega}{2} + \text{Im} \left( \frac{y'(0)}{y(0)} \right) \right). \tag{2.48}$$

Alternately we could use the modified Wronskian formulation for  $\Pi^T(K)$ , eq. (2.23) and evaluate it at  $u = 1$ . An equivalent expression for the trace of spectral density function in this limit becomes

$$\chi_\mu^\mu = \frac{\omega N_c^2 T^2}{2} e^{-c} \frac{|y(1)|^2}{|y(0)|^2}. \tag{2.49}$$

### The spectral density for lightlike momenta

Solving eq. (2.47) numerically with initial conditions (2.46), we find the spectral density function  $\chi_\mu^\mu$  for lightlike momenta for various values of the IR-cut-off  $c$ .<sup>5</sup> The results are shown in Fig. 2.1 and we clearly see the dependency

<sup>5</sup>Numerical solutions were obtained using the NDSolve routine in Mathematica.

at low frequencies on the IR-cut-off. The behaviour at high-frequency on the other hand appears less and less sensitive. What is remarkable is the similar-

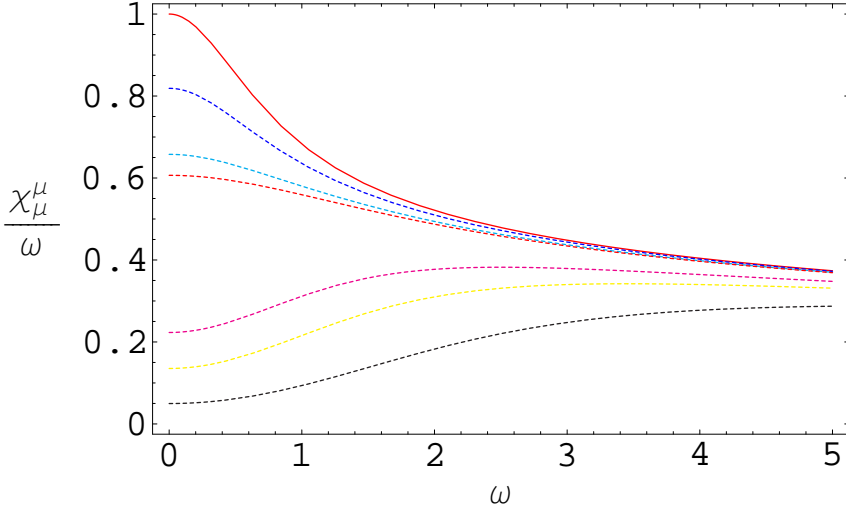


Figure 2.1: Trace of the spectral function for lightlike momenta in units of  $\frac{1}{2}N_c^2T^2$ , plotted as a function of frequency with  $\omega \equiv k^0/(2\pi T)$ . The solid line (red) shows the exact result for  $c = 0$  and the dashed lines downward show numerical analysis for  $c = 0.2, 0.419035, 0.5, 0.6, 1.5, 2, 3$ .

ity between this soft-wall AdS/QCD result, Fig 2.1, for the trace of the spectral function for light-like momenta and of Mateos and Patiño for massive flavor deformations of the AdS dual of  $\mathcal{N} = 2$  theories, Fig. 3 in [23]. As we will discuss in section 2.4, this similarity can be explained by relating the two computations. Inherently this then partially validates the soft-wall AdS/QCD model.

There is, however, one fundamental difference between the result here and the massive  $\mathcal{N} = 2$  computation. Both models are thermodynamically unstable for large IR-cut-off, signalling the transition back to the confining regime. In the  $\mathcal{N} = 2$  model this is clearly illustrated by the appearance of thermal resonances in the spectral function when formally evaluated beyond the critical cut-off. Fig1. shows that in AdS/QCD these resonances remain absent beyond the critical value  $c > 0.419035$  [16]. The absence of thermal resonances was presaged by Huot et al. [5]. Realizing that their results for photon production in the AdS dual of pure  $\mathcal{N} = 4$  SYM are unaffected by a hard-wall IR-cut-off, they speculated that this would be generic. It was premised on the fact that in the hard-wall case, the IR-cut-off is always inside the horizon. Rough dimensional analysis illustrates that the soft-wall case is similar: at the transition the cut-off scale  $c^{-1} \simeq 2.5$  is beyond the horizon  $u = 1$ . However, a similar argu-

ment holds for the massive  $\mathcal{N} = 2$  AdS dual. As we discuss in section 4, the real reason for the absence of thermal resonances is probably simply that an blunt soft- or hard- IR-cut-off is too crude to capture this information.

### 2.3.2 Timelike and spacelike momenta

For time and space-like momenta, both  $\Pi^T$  and  $\Pi^L$  can contribute to spectral density function  $\chi_\mu^\mu(K)$ . Also for these cases, the mode equations (2.9) and (2.15) cannot be solved analytically for arbitrary frequency( $\omega$ ) and wave vector( $q$ ), and we determine the spectral function numerically.

#### Numerical solution for transverse scalar function

Following the same procedure in numerical analysis for lightlike momenta above, we substitute the general solution (2.21) for transverse direction into (2.9) and obtain an equation for  $y(u)$

$$y_\perp'' + \left( \frac{i\omega}{1-u} - \frac{2u}{1-u^2} - c \right) y_\perp' + \left[ \frac{\omega^2 - q^2(1-u^2)}{u(1-u^2)^2} + \frac{2i\omega - \omega^2}{4(1-u)^2} - \frac{i\omega}{2(1-u)} \left( \frac{2u}{1-u^2} + c \right) \right] y_\perp = 0. \quad (2.50)$$

As in the lightlike case, to determine the initial conditions we expand  $y(u) = \sum_{n=0}^{\infty} a_n(1-u)^n$  around  $u = 1$ , with

$$a_0 \text{ (arbitrary)}, \quad a_1 = \frac{\omega^2 - q^2 + i\omega(1/2 - c)}{2(i\omega - 1)} a_0, \quad a_k = f_k(\omega, q, c) a_0, \quad (2.51)$$

where again  $f_k$  are functions of  $\omega, q$  and  $c$  which vanish at  $\omega = q = 0$ . Using the modified Wronskian extension the imaginary part of transverse scalar function is therefore given by

$$\text{Im}(\Pi^T(K)) = -\frac{\omega N_c^2 T^2}{8} e^{-c} \frac{|y_\perp(1)|^2}{|y_\perp(0)|^2}, \quad (2.52)$$

with  $y(u)$  a solution to eq. (2.50) with initial conditions determined from Eq. (2.51).

#### Numerical solution for longitudinal scalar function

Substitute (2.21) into the equation of motion for the longitudinal direction (2.15), we obtain

$$y_\parallel'' + \left( \frac{i\omega}{1-u} - \frac{2u\omega^2}{(1-u^2)(\omega^2 - q^2(1-u^2))} - c \right) y_\parallel' + \left[ \frac{\omega^2 - q^2(1-u^2)}{u(1-u^2)^2} + \frac{2i\omega - \omega^2}{4(1-u)^2} - \frac{i\omega}{2(1-u)} \left( \frac{2u\omega^2}{(1-u^2)(\omega^2 - q^2(1-u^2))} + c \right) \right] y_\parallel = 0. \quad (2.53)$$



Expanding  $y_{\parallel}(u) = \sum_{n=0}^{\infty} a_n(1-u)^n$  around  $u = 1$  gives us

$$a_0 \text{ (arbitrary)}, \quad a_1 = \frac{\omega^2 - q^2 + i\omega \left( \frac{1}{2} - c - \frac{2q^2}{\omega^2} \right)}{2(i\omega - 1)} a_0, \quad a_k = f_k(\omega, q, c) a_0, \quad (2.54)$$

where again  $f_k$  are functions of  $\omega, q$  and  $c$  which vanish at  $\omega = q = 0$ . The imaginary part of the longitudinal scalar function is

$$\text{Im}(\Pi^L(K)) = -\frac{\omega N_c^2 T^2}{8} \left( \frac{1}{2} + \text{Im} \left( \frac{y'_{\parallel}(0)}{\omega y_{\parallel}(0)} \right) \right), \quad (2.55)$$

with  $y_{\parallel}(u)$  the solution to (2.53) with initial conditions determined from Eq. (2.54).

### The spectral density for time- and space-like momenta

Following formula (2.3), we can now write the trace of spectral function for time- and space-like momenta as

$$\chi_{\mu}^{\mu}(K) = \frac{\omega N_c^2 T^2}{2} \left[ e^{-c} \frac{|y_{\perp}(1)|^2}{|y_{\perp}(0)|^2} + \frac{1}{4} + \frac{1}{2\omega} \text{Im} \left( \frac{y'_{\parallel}(0)}{y_{\parallel}(0)} \right) \right]. \quad (2.56)$$

The complete results for  $\chi_{\mu}^{\mu}$  are plotted in Fig.2.2 and Fig.2.3 as a function of frequency for several values of the spatial momentum. As we increase the value for  $c$ , one clearly sees that at low momenta the function decreases compared to  $c = 0$ .

### 2.3.3 Electrical conductivity

With the spectral density in hand, it is now straightforward to compute the electrical conductivity  $\sigma$ . Here, we will use Eq. (2.6) as we have an analytic expression of the spectral density for lightlike momenta. Substituting (2.28) into (2.6) yields

$$\begin{aligned} \sigma &= \lim_{k^0 \rightarrow 0} \frac{e^2}{4T} \frac{\chi_{\mu}^{\mu}(\omega = q)}{e^{k^0/T} - 1} \\ &= \lim_{k^0 \rightarrow 0} \frac{e^2}{8\pi} \frac{N_c^2 \exp(-c) k^0 (1 + O(k^0))}{k^0/T (1 + O(k^0))} \\ &= e^2 \frac{N_c^2 T}{16\pi} \exp(-c), \end{aligned} \quad (2.57)$$

with  $e$  the electric charge. We again note the presence of the scaling factor  $e^{-c}$  which dampens the IR-properties, including charge diffusion, of the system.

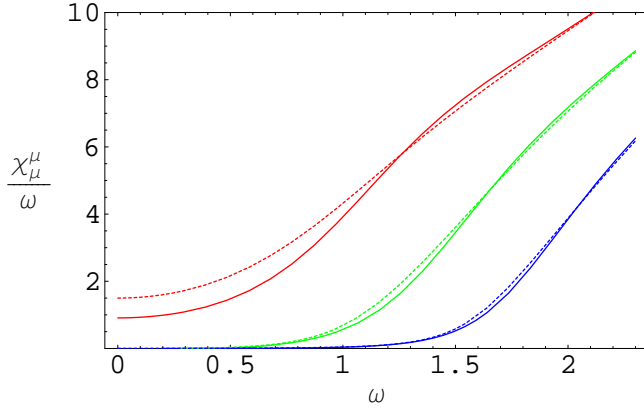


Figure 2.2: Spectral function trace  $\chi_\mu^\mu/\omega$ , in units of  $N_c^2 T^2/2$ , plotted as a function of  $\omega$ . The solid lines describe  $c = 0.5$  and the dashed lines for  $c = 0$  while different colors represent  $q = 0$  (red),  $q = 1$  (green), and  $q = 1.5$  (blue).

Note in particular that this IR-suppression is also present in the charge susceptibility  $\Xi = N_c^2 T^2 c/8(e^c - 1)$  and the more “universal” diffusion constant  $D \equiv \sigma/e^2 \Xi = (1 - e^{-c})/2\pi T c$  (see Appendix 2.B). Physically this makes sense, as a mass-gap should dampen any hydrodynamic behaviour and the general AdS/CFT computation for scale-dependent currents

$$S_{AdS} \sim \int d^4x du \sqrt{-g} \frac{1}{g_{eff}^2(u)} F_{AB} F^{AB}, \quad (2.58)$$

demonstrates this explicitly [30]<sup>6</sup>

$$D \sim \frac{1}{g_{eff}^2(u=1)} \int_0^1 du g_{eff}^2(u) \dots \quad (2.59)$$

## 2.4 Conclusion: Soft wall cut-offs as an IR mass-gap.

The essential new ingredient in Soft-wall AdS/QCD is the ad-hoc cut-off of the radial AdS-direction. It is intended to capture the dominant effects of the scale dependence of QCD [12, 16]. However, its ad-hoc introduction opens it to criticism; especially when interpreted as a dilaton-profile without taking into account back-reaction effects or the dilaton equation of motion (see the

<sup>6</sup>This suggests a trivial violation of the PSS shear-viscosity-bound by IR-suppressing hydrodynamic behaviour. As the derivation of the viscosity in [30] suggests, however, and the explicit computation in massive  $\mathcal{N} = 2$  models shows [31], this is not case.

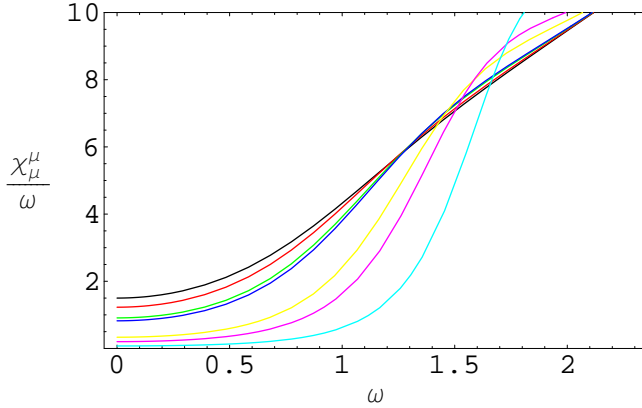


Figure 2.3: Spectral function trace  $\chi_\mu^\mu/\omega$ , in units of  $N_c^2 T^2/2$ , plotted as a function of  $\omega$  for  $q = 0$  and various values of  $c = 0$  (black),  $c = 0.2$  (red),  $c = 0.5$  (green),  $c = 0.6$  (blue),  $c = 1.5$  (yellow),  $c = 2$  (magenta), and  $c = 3$  (cyan).

footnote in the introduction). On the other hand the successful results of the model [15, 16], suggest that it does capture the essential IR behaviour correctly.

The result for AdS/QCD photon production supports this further. As previously emphasized it closely resembles photon production due to quarks for  $\mathcal{N} = 2$  theories with massive flavor in the probe approximation  $N_f \ll N_c$  [23]. These theories descend from brane-constructions in string theory, and therefore have no ad hoc component to criticise. Recall that in these theories, the probe approximation means that one may consider the flavor group as a global symmetry. The  $U(1)$  theory with respect to which photons are defined is a subgroup of this group and the tunable quark mass — a free parameter in the brane construction — functions as the scale in these theories. On the other hand, because the matter and symmetry content is different from QCD, one could question how relevant massive  $\mathcal{N} = 2$  SQCD results are to reality. The observation we make now is that the resemblance between the trace of the spectral function  $\chi_\mu^\mu$  in these  $\mathcal{N} = 2$  SQCD theories as a function of the quark mass  $m$  and the AdS/QCD spectral function as a function of the IR-cut-off  $c$  can be mathematically explained. Both therefore demonstrate again that AdS/CFT results are remarkable universal and robust across fundamentally different theories. This is therefore strong support for soft-wall AdS/QCD, despite its ad-hoc IR-cut-off, as well as massive  $\mathcal{N} = 2$  SQCD, despite its unrealistic matter content, as descriptions of QCD.

To relate the massive  $\mathcal{N} = 2$  SQCD result to AdS/QCD, we note that Mateos and Patiño showed that in  $\mathcal{N} = 2$  SQCD the defining equation relevant for the trace of the spectral function for lightlike momenta can be deduced from an

action<sup>7</sup>

$$S \sim \int du dx_0 dx_1 [-P(u)(\partial_0 V_\perp)^2 + fP(u)(\partial_1 V_\perp)^2 + Q(u)(\partial_u V_\perp)^2], \quad (2.60)$$

where

$$\begin{aligned} P(u) &= \frac{u^3 \sqrt{g(\psi_{m,0}(u), u)}}{uf}, \\ Q(u) &= f \frac{(1 - \psi_{m,0}^2(u))^3}{u^3 \sqrt{g(\psi_{m,0}(u), u)}} \\ &= \frac{1}{u} \frac{u^3 f \sqrt{g(\psi_{m,0}(u), u)}}{uf} \frac{u^2 f^2 (1 - \psi_{m,0}^2(u))^3}{u^6 g(\psi_{m,0}(u), u)}. \end{aligned} \quad (2.61)$$

Here  $f = f(u) = (1 - u^2)$  is the non-extremality function in the D3-brane metric (2.7). The function  $\psi_{m,0}(u)$  is the solution to the embedding equation of motion for the D7-flavor brane derived from the DBI-action

$$S \sim \int du \sqrt{g(\psi_m(u), u)} = \int du \frac{1}{u^3} (1 - \psi_m^2) \sqrt{1 - \psi^2 + 4u^2 f \psi'^2}, \quad (2.62)$$

i.e.  $g(\psi(u), u)$  is the induced metric on the flavor brane. The  $u = 0$  boundary behavior of the solution  $\psi_{m,0} = \frac{m}{\sqrt{2}} u^{1/2} + \Lambda u^{3/2} + \dots$  is determined by the masses  $m$  and condensate expectation value  $\langle qq \rangle \sim \Lambda$  of the quarks. For the massless theory  $\psi_{m=0,0} = 0$  and  $\sqrt{g} = u^{-3}$ . Thus to find the spectral function, one must first solve the differential equation for  $\psi_m(u)$  with the appropriate boundary conditions and then solve the differential equation for  $V_\perp$  [23]. The first step correctly incorporates the backreaction of the modified IR-physics as opposed to the AdS/QCD ad-hoc cut-off.

The massive case  $\psi_{m,0}(u) \neq 0$  is therefore a step more involved than the massless case, unlike AdS/QCD where the scale is a mild modification  $c \neq 0$  of the defining differential equation (2.14). However, searching for a closer match, one quickly realizes that the massless equation (for lightlike momenta  $\omega = \vec{k}$ ),

$$\begin{aligned} \partial_u^2 V_\perp + \partial_u(\ln Q) \partial_u V_\perp + \vec{k}^2 (1 - f) \frac{P}{Q} V_\perp &= 0 \\ \Rightarrow \partial_u^2 V_\perp + \partial_u(\ln(f)) \partial_u V_\perp + \vec{k}^2 (1 - f) \frac{(uf)^{-1}}{f} V_\perp &= 0, \end{aligned} \quad (2.63)$$

is exactly the AdS/QCD equation (2.14) for  $c = 0$  and we are therefore lead to consider a change of variables for the massive case that resembles that of the

<sup>7</sup>We only consider the D3/D7 brane set-up of [23]. The gauge/gravity duality for the D4/D6 brane set-up they also consider is not yet fully understood.

massless case. Thus we define a new variable  $\tilde{u}$  such that

$$du \frac{u^3 \sqrt{g(\psi_{m,0}(u), u)}}{uf} = d\tilde{u} \frac{1}{\tilde{u}\tilde{f}} \quad (2.64)$$

with  $\tilde{f} \equiv f(\tilde{u})$ . By construction the parameter  $P$  in the new variable is identical to the massless case and  $Q$  is seen to be a mild modification

$$\begin{aligned} P(\tilde{u}) &= \frac{1}{\tilde{u}\tilde{f}(\tilde{u})}, \\ Q(\tilde{u}) &= f(\tilde{u}) \frac{\tilde{u}(1 - \psi_{m,0}^2)^3}{u(\tilde{u})}. \end{aligned} \quad (2.65)$$

Note that the solution to the massive embedding equation of motion,  $\psi_{m,0} \neq 0$ , is implicit in the transformation (2.64). In this new variable, however, we see, that its specific form only mildly modifies the massless differential equation

$$\partial_{\tilde{u}}^2 V_{\perp} + \partial_{\tilde{u}} \left[ \ln(\tilde{f}) + \ln\left((1 - \psi_{m,0}^2)^3 \frac{\tilde{u}}{u(\tilde{u})}\right) \right] \partial_{\tilde{u}} V_{\perp} + \tilde{k}^2 (1 - \tilde{f}) \frac{(\tilde{u}\tilde{f})^{-1}}{f(1 - \psi^2)^3} V_{\perp} = 0. \quad (2.66)$$

and the close relation to AdS/QCD is now apparent. The resemblance of the spectral functions is especially explained, if we recall that it is primarily determined by the  $u = 0$  behaviour of the solution (2.20).<sup>8</sup> As we know what the  $u = 0$  behaviour of the solution  $\psi_{m,0} = \frac{m}{\sqrt{2}} u^{1/2} + \dots$  must be, Eq. (2.64) shows that asymptotically  $\tilde{u} = u + \frac{m^2}{4} u^2 + \dots$  and we can putatively identify the mass  $m$  with the IR-cut-off  $c$ :

$$\begin{aligned} -c\tilde{u} &\simeq \ln(1 - \psi_{m,0}^2)^3 \frac{\tilde{u}}{u} = \ln\left(1 - \frac{m^2}{2}\tilde{u} + \dots\right)^3 - \ln\left(1 - \frac{m^2}{4}\tilde{u} + \dots\right) \\ &\simeq -\frac{5}{4}m^2\tilde{u} + \dots \end{aligned} \quad (2.67)$$

The map between AdS/QCD and  $\mathcal{N} = 2$  SQCD is not exact; clearly we should not have expected it to be. The latter shows thermal resonances in the spectral function for masses  $m > 1.3092$  which is the value beyond which the AdS black-hole solution becomes thermodynamically unstable [23]. The AdS/QCD description is much cruder as is no resonances show up even beyond the unstable regime  $c > 0.419035$ . These thermal resonances are encoded in the subtleties of the embedding function  $\psi_{m,0}(u)$  which carries more information than just the mass as an IR-cut-off. Precisely, the embedding function determines whether the flavor D7-brane is in ‘‘Minkowski embedding’’ or ‘‘black hole embedding’’ corresponding to the low  $T$  confining or high  $T$  deconfining

<sup>8</sup>One should be careful in that the change of coordinates (2.64) in principle will also change the boundary conditions one must impose.

phase [23]. Clearly, the  $\mathcal{N} = 2$  SQCD theory has a more detailed description at the physics. On the other hand, the results here do show that in the stable phase the simple AdS/QCD model describes the IR-consequences of a mass-gap remarkably well and the above derivation explains mathematically why. This in itself lends support to continue to study AdS/QCD as a good toy model for real-world physics.

## 2.A Spectral function low frequency limit for lightlike momenta

Here we find an analytic expression for the low-frequency limit of the transverse scalar and spectral density for lightlike momenta by solving the differential equation for the  $E_{\perp}(u)$  perturbatively, rather than using the Wronskian shortcut, explained above eq. (2.22).

We first extract the other regular singularity at  $u = -1$ , writing

$$E_{\perp}(u) = (1-u)^{-i\omega/2}(1+u)^{-\omega/2}Y(u), \quad (2.68)$$

with  $Y(u)$  regular at  $u = 1$  and substitute this into (2.9). Changing variables to  $v = 1/2(1-u)$ , we obtain the differential equation

$$v(1-v)Y'' + [(1-i\omega) - (2-i\omega-\omega-2c)v - 2cv^2]Y' - \left\{ \frac{1}{2}[-\omega-i\omega+i\omega^2] - c[\omega v-i\omega+i\omega v] \right\} Y = 0. \quad (2.69)$$

In the absence of the IR-cutoff,  $c = 0$ , we recognize a hypergeometric equation with solution [5]

$$Y(u) = {}_2F_1 \left( 1 - \frac{1}{2}(1+i)\omega, -\frac{1}{2}(1+i)\omega; 1-i\omega; \frac{1}{2}(1-u) \right). \quad (2.70)$$

As we noted earlier, the presence of  $c$  changes the nature of the equation and no formal solution is known. On physical grounds we expect the effects of  $c$  to dominate the low frequency part of the spectral function. Expanding  $Y(u)$  as

$$Y = Y_0 + \omega Y_1 + \omega^2 Y_2 + \omega^3 Y_3 + \dots, \quad (2.71)$$

we find to first order in  $\omega$ ,

$$\omega^0 \quad : \quad v(1-v)Y_0'' + [1-2v+2cv(1-v)]Y_0' = 0, \quad (2.72)$$

$$\begin{aligned} \omega^1 \quad : \quad & v(1-v)Y_1'' + [v-i(1-v)]Y_1' + [1-2v+2cv(1-v)]Y_1' \\ & + \left\{ \frac{1}{2}(1+i) + c[v-i(1-v)] \right\} Y_0 = 0. \end{aligned} \quad (2.73)$$

These two equations have solutions

$$Y_0(v) = A + B [e^{-2c}\text{Ei}(2c - 2cv) - \text{Ei}(-2cv)], \quad (2.74)$$

$$Y_1(v) = C + \frac{A}{2} [\ln(v - 1) + i \ln v] + [e^{-2c}\text{Ei}(2c - 2cv) - \text{Ei}(-2cv)] \left[ D + \frac{B}{2} [\ln(v - 1) + i \ln v] \right], \quad (2.75)$$

with  $A, B, C, D$  constants of integration and  $\text{Ei}(x) = -\int_{-x}^{\infty} \frac{e^{-t}}{t} dt$  the exponential integral function. To determine the integration constants, recall that by construction the solutions must be regular as  $v \rightarrow 0$  ( $u \rightarrow 1$ ). Since the exponential integral  $\text{Ei}(v)$  diverges at  $v = 0$ , we must set  $B = 0$ . To determine regularity of  $Y_1(v)$ , recall that  $\text{Ei}(x)$  can be written as

$$\text{Ei}(-x) = \gamma + \ln x + \sum_{n=1}^{\infty} \frac{(-1)^n x^n}{n!n}, \quad \text{for } x > 0, \quad (2.76)$$

with  $\gamma$  the Euler-Mascheroni constant. Since the variable  $v \in [0, 1/2]$ , and  $c > 0$ , regularity at  $v = 0$  demands  $D = iA/2$ . For convenience, let us also redefine the constant  $C = i\tilde{C}A/2$ . Substituting those constants into  $Y_1$ , we obtain the solution for  $E_{\perp}$  in the low frequency limit

$$E_{\perp}(u) = A(1 - u)^{-i\omega/2}(1 + u)^{-\omega/2} \left\{ 1 + i\frac{\omega}{2} \left[ \tilde{C} + e^{-2c}\text{Ei}(c(1 + u)) - \text{Ei}(c(u - 1)) - i \ln \left( \frac{u + 1}{2} \right) + \ln \left( \frac{1 - u}{2} \right) \right] + \mathcal{O}(\omega^2) \right\}. \quad (2.77)$$

Using the definition of the exponential integral function, we straightforwardly obtain the leading low-frequency contribution to transverse scalar function

$$\begin{aligned} \Pi^T(\omega = q) &= -\frac{N_c^2 T^2}{8} \left[ -i\frac{\omega}{2} - \frac{\omega}{2} + \frac{i\omega}{2} (ce^{-2c}\text{Ei}'(c) - c\text{Ei}'(-c) - i - 1) + \mathcal{O}(\omega^2) \right] \\ &= \frac{i\omega N_c^2 T^2}{16} [-2i - (e^{-c} + e^{-c}) + \mathcal{O}(\omega^2)]. \end{aligned} \quad (2.78)$$

This is the exact answer. The imaginary part computed via the conserved Wronskian shortcut (2.27) clearly agrees.

## 2.B The susceptibility and the diffusion constant

We follow the procedure to compute the diffusion constant described in [11]. Using the gauge  $V_u = 0$ , we can rewrite equation (2.10) as

$$V_{\parallel} = \frac{uf}{q\omega} V_t'' - c \frac{uf}{q\omega} V_t' - \frac{q}{\omega} V_t. \quad (2.79)$$

Substituting into equation (2.13) we obtain a second order differential equation for  $E = V_t'$

$$E'' + \left[ \frac{(uf)'}{uf} - c \right] E' + \left[ \frac{\omega^2 - q^2 f}{uf^2} - c \frac{(uf)'}{uf} \right] E = 0. \quad (2.80)$$

Imposing the same incoming-wave boundary condition as before and extracting the singularity at the horizon  $u = 1$ , we rewrite  $E = (1 - u)^{-i\omega/2} y$ , where  $y$  is a regular function at the horizon. The function  $y$  must obey the equation

$$y'' + \left[ \frac{i\omega}{1-u} + \frac{(uf)'}{uf} - c \right] y' + \left[ \frac{i\omega(i\omega + 2)}{4(1-u)^2} + \frac{i\omega((uf)') - cuf}{2uf(1-u)} + \frac{\omega^2 - q^2 f}{uf^2} - c \frac{(uf)'}{uf} \right] y = 0. \quad (2.81)$$

For low frequency and momentum, we again solve the equation perturbatively in  $\omega$  and  $q$

$$y(u) = y_{00} + \omega y_{10} + q^2 y_{02} + \dots \quad (2.82)$$

Up to first order in  $\omega$  and  $q^2$ , we find the system of equations

$$\begin{aligned} \omega^0 q^0 &: y''_{00} + \left[ \frac{(uf)'}{uf} - c \right] y'_{00} - c \frac{(uf)'}{uf} y_{00} = 0, \\ \omega^1 q^0 &: y''_{10} + \frac{i}{1-u} y'_{00} + \left[ \frac{(uf)'}{uf} - c \right] y'_{10} + \left[ \frac{i}{2(1-u)^2} + \frac{i((uf)' - cuf)}{2uf(1-u)} \right] y_{00} \\ &\quad - c \frac{(uf)'}{uf} y_{10} = 0, \\ \omega^0 q^2 &: y''_{02} + \left[ \frac{(uf)'}{uf} - c \right] y'_{02} - c \frac{(uf)'}{uf} y_{02} - \frac{f}{uf^2} y_{00} = 0. \end{aligned} \quad (2.83)$$

Using the same analysis for the low frequency of spectral function as described in the previous Appendix, the solutions regular at  $u = 1$  are found to be

$$\begin{aligned} y_{00} &= Ae^{cu} \\ y_{10} &= \frac{iA}{2} e^{cu+c} [C_{10} + 2\text{Ei}(-cu) - e^c \text{Ei}(-c(1+u)) \\ &\quad - e^{-c} (\text{Ei}(c(1-u)) - \ln(u-1))] \\ y_{02} &= \frac{A}{2c} e^{cu+c} [C_{02} - 2\text{Ei}(-cu) + e^c \text{Ei}(-c(1+u)) \\ &\quad + e^{-c} (\text{Ei}(c(1-u)) + 2 \ln u - \ln(u^2 - 1))], \end{aligned} \quad (2.84)$$

where  $A$  and  $C_{10}, C_{02}$  are constants independent of  $u$ . We can determine  $A$  in terms of the boundary values of  $V_t$  and  $V_{\parallel}$  at  $u \rightarrow 0$  defined as

$$\begin{aligned} \lim_{u \rightarrow 0} V_t(u) &= V_t^0, \\ \lim_{u \rightarrow 0} V_{\parallel}(u) &= V_{\parallel}^0. \end{aligned} \quad (2.85)$$



Substituting the solution for  $E = V'_t$  into equation (2.79) and taking limit  $u \rightarrow 0$ , the integration constants  $C_{10}, C_{02}$  drop out and we can determine  $A$  to be

$$A = \frac{q^2 V_t^0 + \omega q V_{\parallel}^0}{i\omega e^c - \frac{e^c}{c} (1 - e^{-c}) q^2 + O(\omega^2, \omega q^2, q^4)}. \quad (2.86)$$

We recognize the hydrodynamic pole and as explained in [11] we can now compute the time-time component of the retarded thermal Green's function of two currents

$$G_{tt} = \frac{N_c^2 T^2 q^2 e^{-c}}{8(i\omega - \frac{(1-e^{-c})}{c} q^2)} + \dots, \quad (2.87)$$

Thus the time-time component of the spectral density function at low frequency and momentum equals

$$\chi_{tt}(k^0, \vec{k}) = -2 \text{Im}[G_{tt}] = \frac{N_c^2 T k^0 |\vec{k}|^2 e^{-c}}{8\pi((k^0)^2 + D|\vec{k}|^2)} + \dots, \quad (2.88)$$

with  $D = \frac{(1-e^{-c})}{2\pi T c}$  the diffusion constant. Comparing the result with the universal hydrodynamic behaviour

$$\chi_{tt}(k^0, \vec{k}) = \frac{2\omega D |\vec{k}|^2}{(k^0)^2 + (D|\vec{k}|^2)^2} \Xi + \dots, \quad (2.89)$$

the charge susceptibility  $\Xi$  is seen to equal  $\Xi = \frac{N_c^2 T^2 c}{8(e^c - 1)}$  and naturally satisfies the Einstein relation  $\Xi = \sigma/e^2 D$ .

# CHAPTER 3

---

## HOLOGRAPHIC BROWNIAN MOTION AND TIME SCALES IN STRONGLY COUPLED PLASMAS

---

### 3.1 Introduction

Brownian motion [6, 32, 33] is a window into the microscopic world of nature. The random motion exhibited by a small particle suspended on a fluid tells us that the fluid is not a continuum but is actually made of constituents of finite size. A mathematical description of Brownian motion is given by the Langevin equation, which phenomenologically describes the force acting on the Brownian particle as a sum of dissipative and random forces. Both of these forces originate from the incessant collisions with the fluid constituents and we can learn about the microscopic interaction between the Brownian particle and the fluid constituents if we measure these forces very precisely. Brownian motion is a universal phenomenon in finite temperature systems and any particle immersed in a fluid at finite temperature undergoes Brownian motion; for example, a heavy quark in the quark-gluon plasma also exhibits such motion.

A quark immersed in a quark-gluon plasma exhibits Brownian motion. Therefore, it is a natural next step to study Brownian motion using the AdS/CFT correspondence. An external quark immersed in a field theory plasma corresponds to a bulk fundamental string stretching between the boundary at infinity and the event horizon of the AdS black hole. In the finite temperature black hole background, the string undergoes a random motion

because of the Hawking radiation of the transverse fluctuation modes [64–66]. This is the bulk dual of Brownian motion, as was clarified in [67, 68]. By studying the random motion of the bulk “Brownian string”, Refs. [67, 68] derived the Langevin equation describing the random motion of the external quark in the boundary field theory and determined the parameters appearing in the Langevin equation. Other recent work on Brownian motion in AdS/CFT includes [69–71].

As mentioned above, by closely examining the random force felt by the Brownian particle, we can learn about the interaction between the Brownian particle and plasma constituents. The main purpose of the current chapter is to use the AdS/CFT dictionary to compute the correlation functions of the random force felt by the boundary Brownian particle by studying the bulk Brownian string. From the random force correlators, we can read off time scales characterizing the interaction between the Brownian particle and plasma constituents, such as the mean-free-path time  $t_{\text{mfp}}$ . The computation of  $t_{\text{mfp}}$  has already been discussed in [67] but there it was partly based on dimensional analysis and the current chapter attempts to complete the computation.

More specifically, we will compute the 2- and 4-point functions of the random force from the bulk and, based on a simple microscopic model, relate them to the mean-free-path time  $t_{\text{mfp}}$ . More precisely, the time scale  $t_{\text{mfp}}$  is related to the non-Gaussianity of the random force statistics. The computation of the 4-point function can be done using the usual GKPW rule and holographic renormalization, see section 1.4.1, with the Lorentzian AdS/CFT prescription of section 1.7.2. In the computation, however, we encounter an IR divergence. This is because we are expanding the Nambu–Goto action in the transverse fluctuation around a static configuration and the expansion breaks down very near the horizon where the local temperature becomes of the string scale. We regularize this IR divergence by cutting off the geometry near the horizon at the point where the expansion breaks down. For the case of a neutral plasma, the resulting mean-free-path time is

$$t_{\text{mfp}} \sim \frac{1}{T \log \lambda}, \quad \lambda \equiv \frac{l^4}{\alpha'^2}, \quad (3.1)$$

where  $T$  is the temperature and  $l$  is the AdS radius. Because the time elapsed in a single event of collision is  $t_{\text{coll}} \sim 1/T$ , this implies that the Brownian particle is undergoing  $\sim \log \lambda$  collisions simultaneously. (So, the term mean-free-path time is probably a misnomer; it might be more appropriate to call  $t_{\text{mfp}}^{-1}$  the collision frequency instead.) We write down a formula for  $t_{\text{mfp}}$  for more general cases with background charges. We apply it to the STU black hole which corresponds to a plasma that carries three  $U(1)$   $R$ -charges. This is more relevant to the actual quark-gluon plasma produced in RHIC and the LHC.

## 3.2 Brownian motion in AdS/CFT

In this section we will briefly review how Brownian motion is realized in the AdS/CFT setup [67, 68], mostly following [67]. If we put an external quark in a CFT plasma at finite temperature, the quark undergoes Brownian motion as it is kicked around by the constituents of the plasma. On the bulk side, this external quark corresponds to a fundamental string stretching between the boundary and the horizon. This string exhibits random motion due to Hawking radiation of its transverse modes, which is the dual of the boundary Brownian motion.

We will explain the central ideas of Brownian motion in AdS/CFT using the simple case where the background plasma is neutral. In explicit computations, we consider the AdS<sub>3</sub>/CFT<sub>2</sub> example for which exact results are available. Then we will move on to discuss more general cases of charged plasmas.

### 3.2.1 Boundary Brownian motion

Let us begin our discussion of Brownian motion from the boundary side, where an external quark immersed in the CFT plasma undergoes random Brownian motion. A general formulation of non-relativistic Brownian motion is based on the generalized Langevin equation [75, 76], which takes the following form in one spatial dimension:

$$\dot{p}(t) = - \int_{-\infty}^t dt' \gamma(t-t') p(t') + R(t) + K(t), \quad (3.2)$$

where  $p = m\dot{x}$  is the (non-relativistic) momentum of the Brownian particle at position  $x$ , and  $\dot{\phantom{x}} \equiv d/dt$ . The first term on the right hand side of (3.2) represents (delayed) friction, which depends linearly on the past trajectory of the particle via the memory kernel  $\gamma(t)$ . The second term corresponds to the random force which we assume to have the following average:

$$\langle R(t) \rangle = 0, \quad \langle R(t)R(t') \rangle = \kappa(t-t'), \quad (3.3)$$

where  $\kappa(t)$  is some function. The random force is assumed to be Gaussian; namely, all higher cumulants of  $R$  vanish.  $K(t)$  is an external force that can be added to the system. The separation of the force into frictional and random parts on the right hand side of (3.2) is merely a phenomenological simplification; microscopically, the two forces have the same origin (collision with the fluid constituents). As a result of the two competing forces, the Brownian particle exhibits thermal random motion. The two functions  $\gamma(t)$  and  $\kappa(t)$  completely characterize the Langevin equation (3.2). Actually,  $\gamma(t)$  and  $\kappa(t)$  are related to each other by the fluctuation-dissipation theorem [77].

The time evolution of the displacement squared of a Brownian particle obeying (3.2) has the following asymptotic behavior [33]:

$$\langle s(t)^2 \rangle \equiv \langle [x(t) - x(0)]^2 \rangle \approx \begin{cases} \frac{T}{m} t^2 & (t \ll t_{relax}) : \text{ballistic regime} \\ 2Dt & (t \gg t_{relax}) : \text{diffusive regime} \end{cases} \quad (3.4)$$

The crossover time scale  $t_{relax}$  between two regimes is given by

$$t_{relax} = \frac{1}{\gamma_0}, \quad \gamma_0 \equiv \int_0^\infty dt \gamma(t), \quad (3.5)$$

while the diffusion constant  $D$  is given by

$$D = \frac{T}{\gamma_0 m}. \quad (3.6)$$

In the ballistic regime,  $t \ll t_{relax}$ , the particle moves inertially ( $s \sim t$ ) with the velocity determined by equipartition,  $|\dot{x}| \sim \sqrt{T/m}$ , while in the diffusive regime,  $t \gg t_{relax}$ , the particle undergoes a random walk ( $s \sim \sqrt{t}$ ). This is because the Brownian particle must be hit by a certain number of fluid particles to lose the memory of its initial velocity. The time  $t_{relax}$  between the two regimes is called the relaxation time which characterizes the time scale for the Brownian particle to thermalize.

By Fourier transforming the Langevin equation (3.2), we obtain

$$p(\omega) = \mu(\omega)[R(\omega) + K(\omega)], \quad \mu(\omega) = \frac{1}{\gamma[\omega] - i\omega}. \quad (3.7)$$

The quantity  $\mu(\omega)$  is called the admittance which describes the response of the Brownian particle to perturbations.  $p(\omega)$ ,  $R(\omega)$ ,  $K(\omega)$  are Fourier transforms, e.g.,

$$p(\omega) = \int_{-\infty}^\infty dt p(t) e^{i\omega t}, \quad (3.8)$$

while  $\gamma[\omega]$  is the Fourier–Laplace transform:

$$\gamma[\omega] = \int_0^\infty dt \gamma(t) e^{i\omega t}. \quad (3.9)$$

In particular, if there is no external force,  $K = 0$ , (3.7) gives

$$p(\omega) = -im\omega x(\omega) = \mu(\omega)R(\omega) \quad (3.10)$$

and, with the knowledge of  $\mu$ , we can determine the correlation functions of the random force  $R$  from those of  $p$  or those of the position  $x$ .

In the above, we discussed the Langevin equation in one spatial dimension, but generalization to  $n = d - 2$  spatial dimensions is straightforward.<sup>1</sup>

---

<sup>1</sup>We assume that  $d \geq 3$  and thus  $n \geq 1$ .

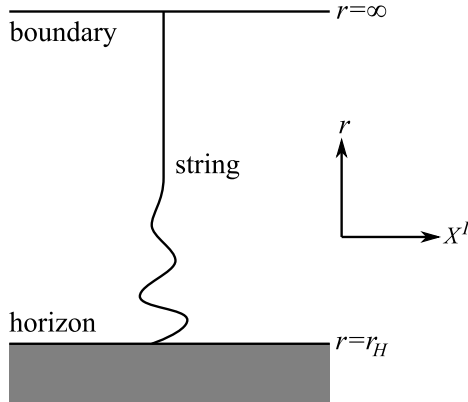


Figure 3.1: The bulk dual of a Brownian particle: a fundamental string attached to the boundary of the AdS space and dipping into the horizon. Because of the Hawking radiation of the transverse fluctuation modes on the string, the string endpoint at infinity moves randomly, corresponding to the Brownian motion on the boundary.

### 3.2.2 Bulk Brownian motion

The AdS/CFT correspondence states that string theory in  $\text{AdS}_d$  is dual to a CFT in  $(d - 1)$  dimensions. In particular, the neutral planar AdS-Schwarzschild black hole with metric

$$ds_d^2 = \frac{r^2}{l^2} [-f(r)dt^2 + (dX^I)^2] + \frac{l^2}{r^2 f(r)} dr^2, \quad f(r) = 1 - \left(\frac{r_H}{r}\right)^{d-1} \quad (3.11)$$

is dual to a neutral CFT plasma at a temperature equal to the Hawking temperature of the black hole,

$$T = \frac{1}{\beta} = \frac{(d-1)r_H}{4\pi l^2}. \quad (3.12)$$

In the above,  $l$  is the AdS radius,  $t \in \mathbb{R}$  is time, and  $X^I = (X^1, \dots, X^{d-2}) \in \mathbb{R}^{d-2}$  are the spatial coordinates on the boundary. We will set  $l = 1$  henceforth.

The external quark in CFT corresponds in the bulk to a fundamental string in the black hole geometry (3.11) which is attached to the boundary at  $r = \infty$  and dips into the black hole horizon at  $r = r_H$ ; see Figure 3.1. The  $X^I$  coordinates of the string at  $r = \infty$  in the bulk define the boundary position of the external quark. As we discussed above, such an external particle at finite temperature  $T$  undergoes Brownian motion. The bulk dual statement is that the black hole environment in the bulk excites the modes on the string and,

as the result, the endpoint of the string at  $r = \infty$  exhibits a Brownian motion which can be modeled by a Langevin equation.

The string in the bulk does not just describe an external point-like quark in the CFT with its position given by the position of the string endpoint at  $r = \infty$ . The transverse fluctuation modes of the bulk string correspond on the CFT side to the degrees of freedom that were induced by the injection of the external quark into the plasma. In other words, the quark immersed in the plasma is dressed with a “cloud” of excitations of the plasma and the transverse fluctuation modes on the bulk string correspond to the excitation of this cloud.<sup>2</sup> In a sense, the quark forms a “bound state” with the background plasma and the excitation of the transverse fluctuation modes on the bulk string corresponds to excited bound states.

We study this motion of a string in the probe approximation where we ignore its backreaction on the background geometry. We also assume that there is no  $B$ -field in the background. In the black hole geometry, the transverse fluctuation modes of the string get excited due to Hawking radiation [64]. If the string coupling  $g_s$  is small, we can ignore the interaction between the transverse modes on the string and the thermal gas of closed strings in the bulk of the AdS space. This is because the magnitude of Hawking radiation (for both string transverse modes and the bulk closed strings) is controlled by  $G_N \propto g_s^2$ , and the effect of the interaction between the transverse modes on the string and the bulk modes is further down by  $g_s^2$ .

Let the string be along the  $r$  direction and consider small fluctuations of it in the transverse directions  $X^I$ . The action for the string is simply the Nambu–Goto action in the absence of a  $B$ -field. In the gauge where the world-sheet coordinates are identified with the spacetime coordinates  $x^\mu = t, r$ , the transverse fluctuations  $X^I$  become functions of  $x^\mu$ :  $X^I = X^I(x)$ . By expanding the Nambu–Goto action up to quadratic order in  $X^I$ , we obtain

$$S_{\text{NG}} = -\frac{1}{2\pi\alpha'} \int d^2x \sqrt{-\det \gamma_{\mu\nu}} \approx \frac{1}{4\pi\alpha'} \int dt dr \left[ \frac{(\partial_t X^I)^2}{f} - r^4 f (\partial_r X^I)^2 \right] \equiv S_0, \quad (3.13)$$

where  $\gamma_{\mu\nu}$  is the induced metric. In the second approximate equality we also dropped the constant term that does not depend on  $X^I$ . This quadratic approximation is valid as long as the scalars  $X^I$  do not fluctuate too far from their equilibrium value (taken here to be  $X^I = 0$ ). This corresponds to taking a non-relativistic limit for the transverse fluctuations. We will be concerned with the validity of this quadratic approximation later. The equation of motion derived from (3.13) is

$$[f^{-1}\omega^2 + \partial_r(r^4 f \partial_r)]X^I = 0, \quad (3.14)$$

---

<sup>2</sup>For a recent discussion on this non-Abelian “dressing”, see [78].

where we set  $X^I(r, t) \propto e^{-i\omega t}$ . Because  $X^I$  with different polarizations  $I$  are independent and equivalent, we will consider only one of them, say  $X^1$ , and simply call it  $X$  henceforth.

The quadratic action (3.13) and the equation of motion (3.14) derived from it are similar to those for a Klein–Gordon scalar. Therefore, the quantization of this theory can be done just the same way, by expanding  $X$  in a basis of solutions to (3.14). Because  $t$  is an isometry direction of the geometry (3.11), we can take the frequency  $\omega$  to label the basis of solutions. So, let  $\{u_\omega(x)\}$ ,  $\omega > 0$  be a basis of positive-frequency modes. Then we can expand  $X$  as

$$X^I(x) = \int_0^\infty \frac{d\omega}{2\pi} [a_\omega u_\omega(x) + a_\omega^\dagger u_\omega(x)^*]. \quad (3.15)$$

If we normalize  $u_\omega(x)$  by introducing an appropriate norm (see Appendix 3.A), the operators  $a, a^\dagger$  satisfy the canonical commutation relation

$$[a_\omega, a_{\omega'}] = [a_\omega^\dagger, a_{\omega'}^\dagger] = 0, \quad [a_\omega, a_{\omega'}^\dagger] = 2\pi\delta(\omega - \omega'). \quad (3.16)$$

To determine the basis  $\{u_\omega(x)\}$ , we need to impose some boundary condition at  $r = \infty$ . The usual boundary condition in Lorentzian AdS/CFT is to require normalizability of the modes at  $r = \infty$  [48] but, in the present case, that would correspond to an infinitely long string extending to  $r = \infty$ , which would mean that the mass of the external quark is infinite and there would be no Brownian motion. So, instead, we introduce a UV cut-off<sup>3</sup> near the boundary to make the mass very large but finite. Specifically, we implement this by means of a Neumann boundary condition

$$\partial_r X = 0 \quad \text{at} \quad r = r_c \gg r_H, \quad (3.17)$$

where  $r = r_c$  is the cut-off surface.<sup>4</sup> The relation between this UV cut-off  $r = r_c$  and the mass  $m$  of the external particle is easily computed from the tension of the string:

$$m = \frac{1}{2\pi\alpha'} \int_{r_H}^{r_c} dr \sqrt{g_{tt} g_{rr}} = \frac{r_c - r_H}{2\pi\alpha'} \approx \frac{r_c}{2\pi\alpha'}. \quad (3.18)$$

Before imposing a boundary condition, the wave equation (3.14) in general has two solutions, which are related to each other by  $\omega \leftrightarrow -\omega$ . Denote these solutions by  $g_{\pm\omega}(r)$ . They are related by  $g_\omega(r)^* = g_{-\omega}(r)$ . These solutions are easy to obtain in the near horizon region  $r \approx r_H$ , where the wave equation reduces to

$$(\omega^2 + \partial_{r_*}^2) X_\omega \approx 0. \quad (3.19)$$

<sup>3</sup>We use the terms ‘‘UV’’ and ‘‘IR’’ with respect to the boundary energy. In this terminology, in the bulk, UV means near the boundary and IR means near the horizon.

<sup>4</sup>In the AdS/QCD context, one can think of the cut-off being determined by the location of the flavour brane, whose purpose again is to introduce dynamical (finite mass) quarks into the field theory.



Here,  $r_*$  is the tortoise coordinate defined by

$$dr_* = \frac{dr}{r^2 f(r)}. \quad (3.20)$$

Near the horizon, we have

$$r_* \sim \frac{1}{(d-1)r_H} \log\left(\frac{r-r_H}{r_H}\right) \quad (3.21)$$

up to an additive numerical constant. Normally this constant is fixed by setting  $r_* = 0$  at  $r = \infty$ , but we will later find that some other choice is more convenient. From (3.19), we see that, in the near horizon region  $r = r_H$ , we have the following outgoing and ingoing solutions:

$$g_\omega(r) \approx e^{i\omega r_*} : \text{outgoing}, \quad g_{-\omega}(r) \approx e^{-i\omega r_*} : \text{ingoing}. \quad (3.22)$$

The boundary condition (3.17) dictates that we take the linear combination

$$f_\omega(r) = g_\omega(r) + e^{i\theta_\omega} g_{-\omega}(r), \quad e^{i\theta_\omega} = -\frac{\partial_r g_\omega(r_c)}{\partial_r g_{-\omega}(r_c)}. \quad (3.23)$$

We can show that  $\theta_\omega$  is real using the fact that  $g_{-\omega} = g_\omega^*$ .

The normalized modes  $u_\omega(t, r)$  are essentially given by  $f_\omega(r)$ ; namely,  $u_\omega(t, r) \propto e^{-i\omega t} f_\omega(r)$ . A short analysis of the norm (see Appendix 3.A) shows that the correctly normalized mode expansion is given by

$$X(t, r) = \frac{\sqrt{2\pi\alpha'}}{r_H} \int_0^\infty \frac{d\omega}{2\pi} \frac{1}{\sqrt{2\omega}} [f_\omega(r) e^{-i\omega t} a_\omega + f_\omega(r)^* e^{i\omega t} a_\omega^\dagger], \quad (3.24)$$

where  $f_\omega(r)$  behaves near the horizon as

$$f_\omega(r) \rightarrow e^{i\omega r_*} + e^{i\theta_\omega} e^{-i\omega r_*}, \quad r \rightarrow r_H \quad (r_* \rightarrow -\infty). \quad (3.25)$$

If we can find such  $f_\omega(r)$ , then  $a, a^\dagger$  satisfy the canonically normalized commutation relation (3.16).

We identify the position  $x(t)$  of the boundary Brownian particle with  $X(t, r)$  at the cutoff  $r = r_c$ :

$$x(t) \equiv X(t, r_c) = \frac{\sqrt{2\pi\alpha'}}{r_H} \int_0^\infty \frac{d\omega}{2\pi} \frac{1}{\sqrt{2\omega}} [f_\omega(r_c) e^{-i\omega t} a_\omega + f_\omega(r_c)^* e^{i\omega t} a_\omega^\dagger]. \quad (3.26)$$

The equation (3.26) relates the correlation functions of  $x(t)$  to those of  $a, a^\dagger$ . Because the quantum field  $X(t, r)$  is immersed in a black hole background, its modes Hawking radiate [64]. This can be seen from the fact that, near the horizon, the worldsheet action (3.13) is the same as that of a Klein-Gordon field near a two-dimensional black hole. The standard quantization of fields

in curved spacetime [79] shows that the field gets excited at the Hawking temperature. At the semiclassical level, the excitation is purely thermal:

$$\langle a_{\omega}^{\dagger} a_{\omega'} \rangle = \frac{2\pi\delta(\omega - \omega')}{e^{\beta\omega} - 1}. \quad (3.27)$$

Using (3.26) and (3.27), one can compute the correlators of  $x$  to show that it undergoes Brownian motion [67], having both the ballistic and diffusive regimes.

In the AdS<sub>3</sub> ( $d = 3$ ) case, we can carry out the above procedure very explicitly. In this case, the metric (3.11) becomes the nonrotating BTZ black hole:

$$ds^2 = -(r^2 - r_H^2) dt^2 + \frac{dr^2}{r^2 - r_H^2} + r^2 dX^2. \quad (3.28)$$

For the usual BTZ black hole,  $X$  is written as  $X = \phi$  where  $\phi \cong \phi + 2\pi$ , but here we are taking  $X \in \mathbb{R}$ , corresponding to a “planar” black hole. The Hawking temperature (3.12) is, in this case,

$$T \equiv \frac{1}{\beta} = \frac{r_H}{2\pi}. \quad (3.29)$$

In terms of the tortoise coordinate  $r_*$ , the metric (3.28) becomes

$$ds^2 = (r^2 - r_H^2)(-dt^2 + dr_*^2) + r^2 dX^2, \quad r_* \equiv \frac{1}{2r_H} \ln \left( \frac{r - r_H}{r + r_H} \right). \quad (3.30)$$

The linearly independent solutions to (3.14) are given by  $g_{\pm\omega}(r)$ , where

$$g_{\omega}(r) = \frac{1}{1 + i\nu} \frac{\rho + i\nu}{\rho} \left( \frac{\rho - 1}{\rho + 1} \right)^{i\nu/2} = \frac{1}{1 + i\nu} \frac{\rho + i\nu}{\rho} e^{i\omega r_*}. \quad (3.31)$$

Here we introduced

$$\rho \equiv \frac{r}{r_H}, \quad \nu \equiv \frac{\omega}{r_H} = \frac{\beta\omega}{2\pi}. \quad (3.32)$$

The linear combination that satisfies the Neumann boundary condition (3.17) is

$$f_{\omega} = g_{\omega}(\rho) + e^{i\theta_{\omega}} g_{-\omega}(\rho), \quad (3.33)$$

$$e^{i\theta_{\omega}} = -\frac{\partial_r g_{\omega}(r_c)}{\partial_r g_{-\omega}(r_c)} = \frac{1 - i\nu}{1 + i\nu} \frac{1 + i\rho_c\nu}{1 - i\rho_c\nu} \left( \frac{\rho_c - 1}{\rho_c + 1} \right)^{i\nu},$$

where  $\rho_c \equiv r_c/r_H$ . This has the correct near-horizon behavior (3.25) too.

By analyzing the correlators of  $x(t)$  using the bulk Brownian motion, one can determine the admittance  $\mu(\omega)$  defined in (3.7) for the dual boundary Brownian motion [67]. Although the result for general frequency  $\omega$  is difficult

to obtain analytically for general dimensions  $d$ , its low-frequency behavior is relatively easy to find; this was done in [67] and the result for  $\text{AdS}_d/\text{CFT}_{d-1}$  is

$$\mu(\omega) = \frac{(d-1)^2 \alpha' \beta^2 m}{8\pi} + \mathcal{O}(\omega). \quad (3.34)$$

This agrees with the results obtained by drag force computations [35,38,39,41]. For later use, let us also record the low-frequency behavior of the random force correlator obtained in [67]:

$$G^{(R)}(t_1, t_2) \equiv \langle \mathcal{T}[R(t_1)R(t_2)] \rangle, \quad (3.35)$$

$$G^{(R)}(\omega_1, \omega_2) = 2\pi\delta(\omega_1 + \omega_2) \left[ \frac{16\pi}{(d-1)^2 \alpha' \beta^3} + \mathcal{O}(\omega) \right], \quad (3.36)$$

where  $\mathcal{T}$  is the time ordering operator.

### 3.2.3 Generalizations

In the above, we considered the simple case of neutral black holes, corresponding to neutral plasmas in field theory. More generally, however, we can consider situations where the field theory plasmas carry nonvanishing conserved charges. For example, the quark-gluon plasma experimentally produced by heavy ion collision has net baryon number. Field theory plasmas charged under such global  $U(1)$  symmetries correspond on the AdS side to black holes charged under  $U(1)$  gauge fields.

On the gravity side of the correspondence, we do not just have  $\text{AdS}_d$  space but also some internal manifold on which higher-dimensional string/M theory has been compactified.  $U(1)$  gauge fields in the  $\text{AdS}_d$  space can be coming from (i) form fields in higher dimensions upon compactification on the internal manifold, or (ii) the off-diagonal components of the higher dimensional metric with one index along the internal manifold. In the former case (i), a charged CFT plasma corresponds to a charged black hole, *i.e.* a Reissner–Nordström black hole (or a generalization thereof to form fields) in the full spacetime. In this case, the analysis in the previous subsections applies almost unmodified, because a fundamental string is not charged under such form fields (except for the  $B$ -field which is assumed to vanish in the present chapter) and its motion is not affected by the existence of those form fields. Namely, the same configuration of a string—stretching straight between the AdS boundary and the horizon and trivial in the internal directions—is a solution of the Nambu–Goto action. Therefore, as far as the fluctuation in the  $\text{AdS}_d$  directions is concerned, we can forget about the internal directions and the analysis in the previous subsections goes through unaltered, except that the metric (3.11) must be replaced by an appropriate AdS black hole metric deformed by the existence of charges.

The latter case (ii), on the other hand, corresponds to having a rotating black hole (Kerr black hole) in the full spacetime. A notable example is the STU black hole which is a non-rotating black hole solution of five-dimensional AdS supergravity charged under three different  $U(1)$  gauge fields [80]. From the point of view of 10-dimensional Type IIB string theory in  $AdS_5 \times S^5$ , this black hole is a Kerr black hole with three angular momenta in the  $S^5$  directions [81]. This solution can also be obtained by taking the decoupling limit of the spinning D3-brane metric [81–83]. Analyzing the motion of a fundamental string in such a background spacetime in general requires a 10-dimensional treatment, because the string gets affected by the angular momentum of the black hole in the internal directions [40, 84, 85]. So, to study the bulk Brownian motion in such situations, we have to find a background solution in the full 10-dimensional spacetime and consider fluctuation around that 10-dimensional configuration. The background solution is straight in the AdS part as before but can be nontrivial in the internal directions due to the drag by the geometry.

In either case, to study the transverse fluctuation of the string around a background configuration, we do not need the full 10- or 11-dimensional metric. For simplicity, let us focus on the transverse fluctuation in one of the  $AdS_d$  directions. Then we only need the three-dimensional line element along the directions of the background string configuration and the direction of the fluctuation. Let us write the three-dimensional line element in general as

$$ds^2 = -h_t(r)f(r)dt^2 + \frac{h_r(r)}{f(r)}dr^2 + G(r)dX^2. \quad (3.37)$$

$X$  is one of the spatial directions in  $AdS_d$ , parallel to the boundary. It is assumed that  $X(t, r) = 0$  is a solution to the Nambu–Goto action in the full (10- or 11-dimensional) spacetime, and we are interested in the fluctuations around it.<sup>5</sup> The nontrivial effects in the internal directions have been incorporated in this metric (3.37). We will see how such a line element arises in the explicit example of the STU black hole in section 3.6. In this subsection, we will briefly discuss the random motion of a string in general backgrounds using the metric (3.37).

In the metric (3.37), the horizon is at  $r = r_H$  where  $r_H$  is the largest positive solution to  $f(r) = 0$ . The functions  $h_t(r)$  and  $h_r(r)$  are assumed to be regular and positive in the range  $r_H \leq r < \infty$ . Near the horizon  $r \approx r_H$ , expand  $f(r)$  as

$$f(r) \approx 2k_H(r - r_H), \quad k_H \equiv \frac{1}{2}f'(r_H). \quad (3.38)$$

---

<sup>5</sup>Note that, under this assumption in a static spacetime, the three-dimensional line element can be always written in the form of (3.37). The  $(t, r)$  and  $(t, X)$  components should vanish by the assumption that  $X(t, r) = 0$  is a solution, and the  $(t, r)$  component can be eliminated by a coordinate transformation.

The Hawking temperature of the black hole,  $T_H$ , is given by

$$T_H = \frac{1}{\beta} = \frac{k_H}{2\pi} \sqrt{\frac{h_t(r_H)}{h_r(r_H)}}. \quad (3.39)$$

For the metric to asymptote to AdS near the boundary, we have

$$h_t f \sim \frac{r^2}{l^2}, \quad \frac{h_r}{f} \sim \frac{l^2}{r^2} \quad \text{as} \quad r \rightarrow \infty, \quad (3.40)$$

where we reinstated the AdS radius  $l$ . Also, because the  $X$  direction (3.37) is assumed to be one of the spatial directions of the  $\text{AdS}_d$  directions parallel to the boundary,  $G(r)$  must go as

$$G \sim \frac{r^2}{l^2} \quad \text{as} \quad r \rightarrow \infty. \quad (3.41)$$

We demand that  $G(r)$  be regular and positive in the region  $r_H \leq r < \infty$ . Note that the parametrization of the two metric components  $g_{tt}, g_{rr}$  using three functions  $h_t, h_r, f$  is redundant and thus has some arbitrariness.

Consider fluctuation around the background configuration  $X(t, r) = 0$  in the static gauge where  $t, r$  are the worldsheet coordinates. Just as in (3.13), the quadratic action obtained by expanding the Nambu–Goto action in  $X$  is

$$S_0 = -\frac{1}{4\pi\alpha'} \int d\sigma^2 \sqrt{-g} G g^{\mu\nu} \partial_\mu X \partial_\nu X, \quad (3.42)$$

where  $g_{\mu\nu}$  is the  $t, r$  part of the metric (3.37) (i.e., the induced worldsheet metric for the background configuration  $X(t, r) = 0$ ), and  $g = \det g_{\mu\nu}$ . The equation of motion derived from the quadratic action (3.42) is

$$-\ddot{X} + \sqrt{\frac{h_t}{h_r}} \frac{f}{G} \partial_r \left( \sqrt{\frac{h_t}{h_r}} f G X' \right) = 0, \quad (3.43)$$

where  $\dot{\phantom{x}} = \partial_t, \phantom{x}' = \partial_r$ . In terms of the tortoise coordinate  $r_*$  defined by

$$dr_* = \frac{1}{f} \sqrt{\frac{h_r}{h_t}} dr, \quad (3.44)$$

(3.43) becomes a Schrodinger-like wave equation [86]:

$$\left[ \frac{d^2}{dr_*^2} + \omega^2 - V(r) \right] X_\omega(r) = 0, \quad (3.45)$$

where we set  $X(t, r) = e^{-i\omega t} \eta(r) X_\omega(r)$  and the “potential”  $V(r)$  is given by

$$V(r) = -\eta \frac{dr}{dr_*} \frac{d}{dr} \left[ \frac{1}{\eta^2} \frac{dr}{dr_*} \frac{d\eta}{dr} \right], \quad \eta = G^{-1/2}. \quad (3.46)$$

The potential  $V(r)$  vanishes at the horizon and will become more and more important as we move towards the boundary  $r \rightarrow \infty$  where  $V(r) \sim 2r^2/l^4$ .

Just as in the previous subsection, let the two solutions to the wave equation (3.45) be  $g_\omega(r)$  and  $g_{-\omega}(r) = g_\omega(r)^*$ . Near the horizon where  $V(r) = 0$ , the wave equation (3.45) takes the same form as (3.19) and therefore  $g_{\pm\omega}(r)$  can be taken to have the following behavior near the horizon

$$g_{\pm\omega}(r) \rightarrow e^{\pm i\omega r_*} \quad \text{as } r \rightarrow r_H. \quad (3.47)$$

If we introduce a UV cutoff at  $r = r_c$  as before, the solution  $f_\omega(r)$  satisfying the Neumann boundary condition (3.17) at  $r = r_c$  is a linear combination of  $g_{\pm\omega}(r)$  and can be written as (3.23). Using this  $f_\omega(r)$ , we can expand the fluctuation field  $X(t, r)$  as

$$X(t, r) = \sqrt{\frac{2\pi\alpha'}{G(r_H)}} \int_0^\infty \frac{d\omega}{2\pi} \frac{1}{\sqrt{2\omega}} [f_\omega(r) e^{-i\omega t} a_\omega + f_\omega(r)^* e^{i\omega t} a_\omega^\dagger], \quad (3.48)$$

where  $a_\omega, a_\omega^\dagger$  are canonically normalized to satisfy (3.16). As before, the value of  $X(t, r)$  at the UV cutoff  $r = r_c$  is interpreted as the position  $x(t)$  of the boundary Brownian motion:  $X(t, r_c) \equiv x(t)$ . By assuming that the modes Hawking radiate thermally as in (3.27), we can determine the parameters of the boundary Brownian motion such as the admittance  $\mu(\omega)$ .

In general, solving the wave equation (3.45) and obtaining explicit analytic expressions for  $g_{\pm\omega}, f_\omega$  is difficult. However, in the low frequency limit  $\omega \rightarrow 0$ , it is possible to determine their explicit forms as explained in [67] or in Appendix 3.B and, based on that, one can compute the low frequency limit of  $\mu(\omega)$  following the procedure explained in [67]. The result is

$$\mu(\omega) = \frac{2m\pi\alpha'}{G(r_H)} + \mathcal{O}(\omega). \quad (3.49)$$

From this, we can derive the low frequency limit of the random force correlator as follows:

$$G^{(R)}(\omega_1, \omega_2) = 2\pi\delta(\omega_1 + \omega_2) \left[ \frac{G(r_H)}{\pi\alpha'\beta} + \mathcal{O}(\omega) \right]. \quad (3.50)$$

## 3.3 Time scales

### 3.3.1 Physics of time scales

In Eq. (3.5), we introduced the relaxation time  $t_{\text{relax}}$  which characterizes the thermalization time of the Brownian particle. From Brownian motion, we can read off other physical time scales characterizing the interaction between the Brownian particle and plasma.

One such time scale, the microscopic (or collision duration) time  $t_{\text{coll}}$ , is defined to be the width of the random force correlator function  $\kappa(t)$ . Specifically, let us define

$$t_{\text{coll}} = \int_0^\infty dt \frac{\kappa(t)}{\kappa(0)}. \quad (3.51)$$

If  $\kappa(t) = \kappa(0)e^{-t/t_{\text{coll}}}$ , the right hand side of this precisely gives  $t_{\text{coll}}$ . This  $t_{\text{coll}}$  characterizes the time scale over which the random force is correlated, and thus can be interpreted as the time elapsed in a single process of scattering. In usual situations,

$$t_{\text{relax}} \gg t_{\text{coll}}. \quad (3.52)$$

Another natural time scale is the mean-free-path time  $t_{\text{mfp}}$  given by the typical time elapsed between two collisions. In the usual kinetic theory, this mean free path time is typically  $t_{\text{coll}} \ll t_{\text{mfp}} \ll t_{\text{relax}}$ ; however in the case of present interest, this separation no longer holds, as we will see. For a schematic explanation of the timescales  $t_{\text{coll}}$  and  $t_{\text{mfp}}$ , see Figure 3.2.

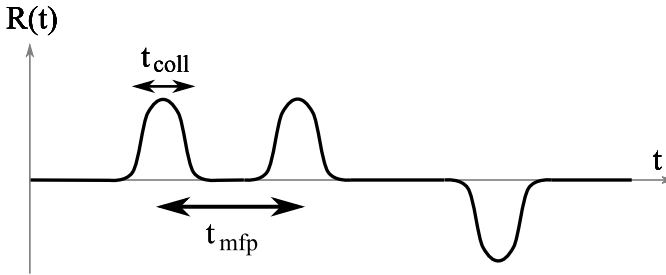


Figure 3.2: A sample of the stochastic variable  $R(t)$ , which consists of many pulses randomly distributed.

### 3.3.2 A simple model

The collision duration time  $t_{\text{coll}}$  can be read off from the random force 2-point function  $\kappa(t) = \langle R(t)R(0) \rangle$ . To determine the mean-free-path time  $t_{\text{mfp}}$ , we need higher point functions and some microscopic model which relates those higher point functions with  $t_{\text{mfp}}$ . Here we propose a simple model<sup>6</sup> which relates  $t_{\text{mfp}}$  with certain 4-point functions of the random force  $R$ .

For simplicity, we first consider the case with one spatial dimension. Consider a stochastic quantity  $R(t)$  whose functional form consists of many pulses

<sup>6</sup>This is a generalization of the discussion given in Appendix D.1 of [67]. For somewhat similar models (binary collision models), see [87] and references therein.

randomly distributed.  $R(t)$  is assumed to be a classical quantity (c-number). Let the form of a single pulse be  $P(t)$ . Furthermore, assume that the pulses come with random signs. If we have  $k$  pulses at  $t = t_i$  ( $i = 1, 2, \dots, k$ ), then  $R(t)$  is given by

$$R(t) = \sum_{i=1}^k \epsilon_i P(t - t_i), \quad (3.53)$$

where  $\epsilon_i = \pm 1$  are random signs.

Let the distribution of pulses obey the Poisson distribution, which is a physically reasonable assumption if  $R$  is caused by random collisions. This means that the probability that there are  $k$  pulses in an interval of length  $\tau$ , say  $[0, \tau]$ , is given by

$$P_k(\tau) = e^{-\mu\tau} \frac{(\mu\tau)^k}{k!}. \quad (3.54)$$

Here,  $\mu$  is the number of pulses per unit time. In other words,  $1/\mu$  is the average distance between two pulses. We do not assume that the pulses are well separated; namely, we do *not* assume  $\Delta \ll 1/\mu$ . If we identify  $R(t)$  with the random force in the Langevin equation,  $t_{\text{mfp}} = 1/\mu$ .

The 2-point function for  $R$  can be written as

$$\langle R(t)R(t') \rangle = \sum_{k=1}^{\infty} e^{-\mu\tau} \frac{(\mu\tau)^k}{k!} \sum_{i,j=1}^k \langle \epsilon_i \epsilon_j P(t - t_i) P(t' - t_j) \rangle_k, \quad (3.55)$$

where we assumed  $t, t' \in [0, \tau]$  and  $\langle \rangle_k$  is the statistical average when there are  $k$  pulses in the interval  $[0, \tau]$ . Because  $k$  pulses are randomly and independently distributed in the interval  $[0, \tau]$  by assumption, this expectation value is computed as

$$\begin{aligned} & \sum_{i,j=1}^k \langle \epsilon_i \epsilon_j P(t - t_i) P(t' - t_j) \rangle_k \\ &= \frac{1}{\tau^k} \int_0^\tau dt_1 \cdots dt_k \left[ \sum_{i=1}^k P(t - t_i) P(t' - t_i) + \sum_{i \neq j}^k \langle \epsilon_i \epsilon_j \rangle_k P(t - t_i) P(t' - t_j) \right]. \end{aligned} \quad (3.56)$$

Here, the second term vanishes because  $\langle \epsilon_i \epsilon_j \rangle_k = 0$  for  $i \neq j$ . Therefore, one readily computes

$$\begin{aligned} \sum_{i,j=1}^k \langle \epsilon_i \epsilon_j P(t - t_i) P(t' - t_j) \rangle_k &= \frac{k}{\tau} \int_0^\tau dt_1 P(t - t_1) P(t' - t_1) \\ &\approx \frac{k}{\tau} \int_{-\infty}^{\infty} dt_1 P(t - t_1) P(t' - t_1). \end{aligned} \quad (3.57)$$



Here, in going to the second line, we took  $\tau$  to be much larger than the support of  $P(t)$ , which is always possible because  $\tau$  is arbitrary. Substituting this back into (3.55), we find

$$\langle R(t)R(t') \rangle = \mu \int_{-\infty}^{\infty} dt_1 P(t-t_1)P(t'-t_1). \quad (3.58)$$

In a similar way, one can compute the following 4-point function:

$$\begin{aligned} & \langle R(t)R(t')R(t'')R(t''') \rangle \\ &= \sum_{k=1}^{\infty} e^{-\mu\tau} \frac{(\mu\tau)^k}{k!} \sum_{i,j,m,n=1}^k \langle \epsilon_i \epsilon_j \epsilon_m \epsilon_n P(t-t_i)P(t'-t_j)P(t''-t_m)P(t'''-t_n) \rangle_k. \end{aligned} \quad (3.59)$$

Again, the expectation value  $\langle \epsilon_i \epsilon_j \epsilon_m \epsilon_n \rangle_k$  vanishes unless some of  $i, j, m, n$  are equal. The possibilities are  $i = j \neq m = n$ ,  $i = m \neq j = n$ ,  $i = n \neq j = m$ , and  $i = j = m = n$ . Taking into account all these possibilities, in the end we have

$$\langle R(t)R(t')R(t'')R(t''') \rangle = \langle R(t)R(t')R(t'')R(t''') \rangle_{\text{disc}} + \langle R(t)R(t')R(t'')R(t''') \rangle_{\text{conn}}, \quad (3.60)$$

where

$$\begin{aligned} \langle R(t)R(t')R(t'')R(t''') \rangle_{\text{disc}} &= \langle R(t)R(t') \rangle \langle R(t'')R(t''') \rangle + \langle R(t)R(t'') \rangle \langle R(t')R(t''') \rangle \\ &+ \langle R(t)R(t''') \rangle \langle R(t')R(t'') \rangle, \end{aligned} \quad (3.61)$$

$$\langle R(t)R(t')R(t'')R(t''') \rangle_{\text{conn}} = \mu \int_{-\infty}^{\infty} du P(t-u)P(t'-u)P(t''-u)P(t'''-u). \quad (3.62)$$

We can think of (3.61) as the “disconnected part” and (3.62) as the “connected part”, or non-Gaussianity of the random force statistics.

In the Fourier space, the expressions for these correlation functions simplify:

$$\langle R(\omega_1)R(\omega_2) \rangle = 2\pi\mu\delta(\omega_1 + \omega_2)P(\omega_1)P(\omega_2), \quad (3.63)$$

$$\begin{aligned} \langle R(\omega_1) \cdots R(\omega_4) \rangle_{\text{disc}} &= (2\pi\mu)^2 [\delta(\omega_1 + \omega_2)\delta(\omega_3 + \omega_4) + \delta(\omega_1 + \omega_3)\delta(\omega_2 + \omega_4) \\ &+ \delta(\omega_1 + \omega_4)\delta(\omega_2 + \omega_3)] P(\omega_1) \cdots P(\omega_4), \end{aligned} \quad (3.64)$$

$$\langle R(\omega_1) \cdots R(\omega_4) \rangle_{\text{conn}} = 2\pi\mu\delta(\omega_1 + \cdots + \omega_4)P(\omega_1) \cdots P(\omega_4). \quad (3.65)$$

In particular, for small  $\omega_i$ ,

$$\langle R(\omega_1)R(\omega_2) \rangle \approx 2\pi\mu\delta(\omega_1 + \omega_2)P(\omega = 0)^2 \quad (3.66)$$

$$\langle R(\omega_1)R(\omega_2)R(\omega_3)R(\omega_4) \rangle_{\text{conn}} \approx 2\pi\mu\delta(\omega_1 + \omega_2 + \omega_3 + \omega_4)P(\omega = 0)^4. \quad (3.67)$$

Therefore, from the small frequency behavior of 2-point function and connected 4-point function, we can separately read off the mean-free-path time  $t_{\text{mfp}} \sim 1/\mu$  and  $P(\omega = 0)$ , the impact per collision.

The discussion thus far has been focused on the case with one spatial dimension, but generalization to  $n = d - 2$  spatial dimensions is straightforward. In this case, the random force becomes an  $n$ -dimensional vector  $R^I(t)$ ,  $I = 1, 2, \dots, n$ . Generalizing (3.53), let us model the random force to be given by a sum of pulses:

$$R^I(t) = \sum_{i=1}^k \epsilon_i^I P(t - t_i). \quad (3.68)$$

Here, for each value of  $i$ ,  $\epsilon_i^I$  is a stochastic variable taking random values in the  $(n - 1)$ -dimensional sphere  $S^{n-1}$ . We also assume that  $\epsilon_i^I$  for different values of  $i$  are independent of each other. Then we can readily compute the following statistical average:

$$\langle \epsilon_i^I \epsilon_i^J \rangle = \frac{\delta^{IJ}}{n}, \quad \langle \epsilon_i^I \epsilon_i^J \epsilon_i^K \epsilon_i^L \rangle = \frac{\delta^{IJ} \delta^{KL} + \delta^{IK} \delta^{JL} + \delta^{IL} \delta^{JK}}{n(n+2)}. \quad (3.69)$$

From this, we can derive the following  $R$ -correlators:

$$\langle R^I(\omega_1) R^J(\omega_2) \rangle = \frac{2\pi\mu}{n} \delta^{IJ} \delta(\omega_1 + \omega_2) P(\omega_1) P(\omega_2), \quad (3.70)$$

$$\begin{aligned} \langle R^I(\omega_1) R^J(\omega_2) R^K(\omega_3) R^L(\omega_4) \rangle &= \langle R^I(\omega_1) R^J(\omega_2) R^K(\omega_3) R^L(\omega_4) \rangle_{\text{conn}} \\ &\quad + \langle R^I(\omega_1) R^J(\omega_2) R^K(\omega_3) R^L(\omega_4) \rangle_{\text{disc}}, \end{aligned} \quad (3.71)$$

where

$$\begin{aligned} \langle R^I(\omega_1) R^J(\omega_2) R^K(\omega_3) R^L(\omega_4) \rangle_{\text{disc}} &= \langle R^I(\omega_1) R^J(\omega_2) \rangle \langle R^K(\omega_3) R^L(\omega_4) \rangle \\ &\quad + \langle R^I(\omega_1) R^K(\omega_3) \rangle \langle R^J(\omega_2) R^L(\omega_4) \rangle \\ &\quad + \langle R^I(\omega_1) R^L(\omega_4) \rangle \langle R^J(\omega_2) R^K(\omega_3) \rangle, \end{aligned} \quad (3.72)$$

$$\begin{aligned} \langle R^I(\omega_1) R^J(\omega_2) R^K(\omega_3) R^L(\omega_4) \rangle_{\text{conn}} &= \frac{2\pi\mu}{n(n+2)} (\delta^{IJ} \delta^{KL} + \delta^{IK} \delta^{JL} + \delta^{IL} \delta^{JK}) \\ &\quad \times \delta(\omega_1 + \dots + \omega_4) P(\omega_1) \dots P(\omega_4). \end{aligned} \quad (3.73)$$

These are essentially the same as the  $n = 1$  results (3.63), (3.65) and we can compute the mean-free-path time  $t_{\text{mfp}} \sim 1/\mu$  from the small  $\omega$  behavior of 2- and 4-point functions.

We will use these relations to read off  $t_{\text{mfp}}$  for the Brownian particle in CFT plasma using the bulk Brownian motion.

### 3.3.3 Non-Gaussian random force and Langevin equation

In the above, we argued that the time scale  $t_{\text{mfp}}$  that characterizes the statistical properties of the random force  $R$  is related to the nontrivial part (connected part) of the 4-point function of  $R$ . Namely, it is related to the non-Gaussianity of the random force. Here, let us briefly discuss the relation between non-Gaussianity and the non-linear Langevin equation.

In subsection 3.2.1, we discussed the linear Langevin equation (3.2) for which the friction is proportional to the momentum  $p$ . In other words, the friction coefficient  $\gamma(t)$  did not contain  $p$ . Furthermore, the random force  $R$  was assumed to be Gaussian. In many real systems, Gaussian statistics for the random force gives a good approximation, and the linear Langevin equation provides a useful approach to study the systems. However, this idealized physical situation does not describe nature in general. For example, even the simplest case of a Brownian particle interacting with the molecules of a solvent is rather thought to obey a Poissonian than a Gaussian statistics (just like the simple model discussed in subsection 3.3.2). It is only in the weak collision limit where energy transfer is relatively small compared to the energy of the system that the central limit theorem says that the statistics can be approximated as Gaussian [88, 89]. Furthermore, due to the non-linear fluctuation-dissipation relations [90], the non-Gaussianity of random force and the non-linearity of friction are closely related. An extension of the phenomenological Langevin equation that incorporates such non-linear and non-Gaussian situations is an issue that has not yet been completely settled (for a recent discussion, see [89]).

However, the relation between time scales  $t_{\text{coll}}$ ,  $t_{\text{mfp}}$  and  $R$  correlators derived in subsection 3.3.2 does not depend on the existence of such an extension of the Langevin equation. Below, we will compute  $R$  correlators using the AdS/CFT correspondence and derive expressions for the time scale  $t_{\text{mfp}}$ , but that derivation will not depend on the existence of an extended Langevin equation either.<sup>7</sup> It would be interesting to use the concrete AdS/CFT setup for Brownian motion to investigate the above issue of a non-linear non-Gaussian Langevin equation. We leave it for future research.

## 3.4 Holographic computation of the $R$ -correlator

In the last section, we saw that  $t_{\text{mfp}}$  can be read off if we know the low-frequency limit of the 2- and 4-point functions of the random force. For

---

<sup>7</sup>More precisely, the computation in subsection 3.4.2 is independent of the existence of any Langevin equation, because we directly compute the  $R$  correlators using the fact that the total force  $F$  equals  $R$  in the  $m \rightarrow \infty$  limit. On the other hand, in subsection 3.4.1, we compute the  $R$  correlators directly, but use the relation (3.77) derived from the linear Langevin equation. So, the latter computation is assuming that a Langevin equation exists at least to the linear order.

the connected 4-point function to be nonvanishing, we need more than the quadratic term  $S_0$  in (3.13) or (3.42). Such terms will arise if we keep higher order terms in the expansion of the Nambu–Goto action. This amounts to taking into account the relativistic correction to the motion of the “cloud” around the quark mentioned in subsection 3.2.2. In the case of the neutral black holes discussed in subsection 3.2.2, if we keep up to quartic terms (and drop a constant), the action becomes

$$S = S_0 + S_{\text{int}}, \quad (3.74)$$

$$S_{\text{int}} = \frac{1}{16\pi\alpha'} \int dt dr \left( \frac{\dot{X}^2}{f} - r^4 f X'^2 \right)^2, \quad (3.75)$$

where the quadratic (free) part  $S_0$  is as given before in (3.13).

There are two ways to compute correlation functions in the presence of the quartic term (3.75). The first one, which is perhaps more intuitive, is to regard the theory with the action  $S_0 + S_{\text{int}}$  as a field theory of the worldsheet field  $X$  at temperature  $T$  and compute the  $X$  correlators using the standard technique of thermal field theory as in section 1.6. The second one, which is perhaps more rigorous but technically more involved, is to use the GKPW prescription and holographic renormalization, see section 1.4.1, to compute the correlator for the force acting on the boundary Brownian particle.

The two approaches give essentially the same result in the end, as they should. In the following, we will first describe the first approach and then briefly discuss the the second approach, relegating the technical details to Appendix 3.D. In this section and the next, for the simplicity of presentation, we will focus on the neutral black holes of subsection 3.2.2.

### 3.4.1 Thermal field theory on the worldsheet

The Brownian string we are considering is immersed in a black hole background which has temperature  $T$  given by (3.12). Therefore, we can think of the string described by the action (3.74) just as a field theory of  $X(t, r)$  at temperature  $T$ , for which the standard thermal perturbation theory (see section 1.6) is applicable.

For the thermal field theory described by (3.74), let us compute the real-time connected 4-point function

$$\begin{aligned} G_{\text{conn}}^{(x)}(t_1, t_2, t_3, t_4) &= \langle \mathcal{T}[x(t_1)x(t_2)x(t_3)x(t_4)] \rangle_{\text{conn}} \\ &= \langle \mathcal{T}[X(t_1, r_c)X(t_2, r_c)X(t_3, r_c)X(t_4, r_c)] \rangle_{\text{conn}}, \end{aligned} \quad (3.76)$$

where  $\mathcal{T}$  is the time ordering operator and  $x(t) = X(t, r_c)$  is the position of the boundary Brownian particle. In the absence of external force,  $K(\omega) = 0$ , (3.7)

relates  $x$  and random force  $R$  by

$$R(\omega) = -\frac{im\omega x(\omega)}{\mu(\omega)}. \quad (3.77)$$

Therefore, using the low-frequency expression for  $\mu(\omega)$  given in (3.34), we can compute the 4-point function of  $R$  from the one for  $x$  in (3.76).

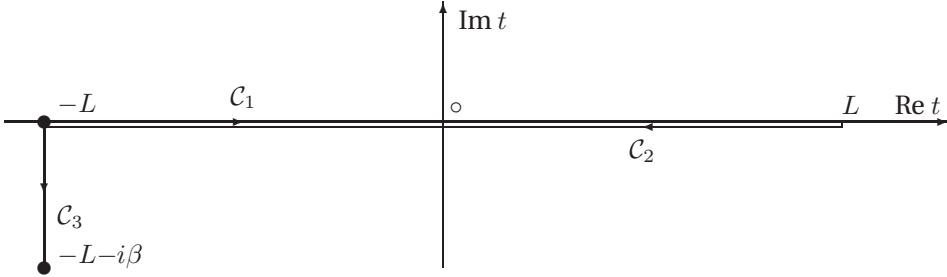


Figure 3.3: The contour for computing real-time correlators at finite temperature.

As is standard, we can compute such real-time correlators at finite temperature  $T$  by analytically continuing the time  $t$  to a complex time  $z$  and performing path integration on the complex  $z$  plane along the contour  $C = C_1 + C_2 + C_3$ , where  $C_i$  are oriented intervals

$$C_1 = [-L, L], \quad C_2 = [L, -L], \quad C_3 = [-L, -L - i\beta] \quad (3.78)$$

as shown in Figure 3.3.  $L$  is a large positive number which is sent to infinity at the end of computation. We can parametrize the contour  $C$  by a real parameter  $\lambda$  which increases along  $C$  as

$$\begin{aligned} C_1 : & \quad z = \lambda - L & (0 \leq \lambda \leq 2L) \\ C_2 : & \quad z = 3L - \lambda & (2L \leq \lambda \leq 4L) \\ C_3 : & \quad z = -L + i(4L - \lambda) & (4L \leq \lambda \leq 4L + \beta) \end{aligned} \quad (3.79)$$

The field  $X$  is defined for all values of  $\lambda$ . Another convenient parametrization of  $C$  is

$$\begin{aligned} C_1 : & \quad z = t, & (-L \leq t \leq L), \\ C_2 : & \quad z = t, & (-L \leq t \leq L), \\ C_3 : & \quad z = -L - i\tau, & (0 \leq \tau \leq \beta). \end{aligned} \quad (3.80)$$

We will denote by  $X_{[i]}$  ( $i = 1, 2, 3$ ) the field  $X$  on the segment  $C_i$  parametrized by  $t$  and  $\tau$  in (3.80). Henceforth, we will use the subscript  $[i]$  for a quantity associated with  $C_i$ .

The path integral is now performed over  $X_{[1]}(t)$ ,  $X_{[2]}(t)$ , and  $X_{[3]}(\tau)$ , but in the  $L \rightarrow \infty$  limit the path integral over  $X_{[3]}$  factorizes and can be dropped [25]. Therefore, with the parametrization (3.80), the path integral becomes

$$\int \mathcal{D}X e^{iS} \rightarrow \int \mathcal{D}X_{[1]} \mathcal{D}X_{[2]} e^{i(S_{[1]} - S_{[2]})}, \quad (3.81)$$

where  $S_{[i]}$ ,  $i = 1, 2$  are obtained by replacing  $X$  with  $X_{[i]}$  in (3.74). The negative sign in front of  $S_{[2]}$  in (3.81) is because the direction of the parameter  $t$  we took in (3.80) is opposite to that of  $C_2$ .

The correlator (3.76) can be written as

$$G_{\text{conn}}^{(x)}(t_1, t_2, t_3, t_4) = \langle \mathcal{T}_C[X_{[1]}(t_1, r_c)X_{[1]}(t_2, r_c)X_{[1]}(t_3, r_c)X_{[1]}(t_4, r_c)] \rangle_{\text{conn}}, \quad (3.82)$$

where  $\mathcal{T}_C$  is ordering along  $C$  (in other words, with respect to the parameter  $\lambda$ ), and can be computed in perturbation theory by treating  $S_0$  as the free part and  $S_{\text{int}}$  as an interaction. In doing that, we have to take into account both the type-1 fields  $X_{[1]}$  and the type-2 fields  $X_{[2]}$ . Namely, we have to introduce propagators not just for  $X_{[1]}$  but also between  $X_{[1]}$  and  $X_{[2]}$  as follows

$$\begin{aligned} D_{[11]}(t - t', r, r') &= \langle \mathcal{T}_C[X_{[1]}(t, r)X_{[1]}(t', r')] \rangle_0 = D_F(t - t', r, r'), \\ D_{[21]}(t - t', r, r') &= \langle \mathcal{T}_C[X_{[2]}(t, r)X_{[1]}(t', r')] \rangle_0 = D_W(t - t', r, r'). \end{aligned} \quad (3.83)$$

Here,  $\langle \rangle_0$  is the expectation value for the free theory with action  $S_0$  at temperature  $T$ . We see that the propagators  $D_{[11]}$  and  $D_{[21]}$  are equal, respectively, to the usual time-ordered (Feynman) propagator  $D_F$  and the Wightman propagator  $D_W$  of the field  $X(t, r)$ . We must also remember that we have not only interaction vertices that come from  $S_{[1]}^{\text{int}}$  and involve  $X_{[1]}$ , but also ones that come from  $S_{[2]}^{\text{int}}$  and involve  $X_{[2]}$ . The second type of vertices come with an extra minus sign.

Using the propagators (3.83), the connected 4-point function is evaluated, at leading order in perturbation theory, to be

$$\begin{aligned} G_{\text{conn}}^{(x)}(\omega_1, \omega_2, \omega_3, \omega_4) &= \frac{i}{16\pi\alpha'} 2\pi\delta(\omega_1 + \dots + \omega_4) \int_{r_H}^{r_c} dr \\ &\times \left\{ \sum_{\substack{\text{perm} \\ (ijkl)}} \left[ \frac{\omega_i\omega_j}{f} D_{[11]}(\omega_i)D_{[11]}(\omega_j) + r^4 f \partial_r D_{[11]}(\omega_i) \partial_r D_{[11]}(\omega_j) \right] \right. \\ &\quad \times \left[ \frac{\omega_k\omega_l}{f} D_{[11]}(\omega_k)D_{[11]}(\omega_l) + r^4 f \partial_r D_{[11]}(\omega_k) \partial_r D_{[11]}(\omega_l) \right] \\ &\quad \left. - (D_{[11]} \rightarrow D_{[21]}) \right\}. \end{aligned} \quad (3.84)$$

Here, we wrote down the result in the Fourier space and used a shorthand notation  $D_{[11]}(\omega_i) \equiv D_{[11]}(\omega_i, r, r_c)$ . The summation is over permutations  $(ijkl)$  of  $(1234)$ .

We are interested in the low frequency limit of this correlator. In that limit, the propagators simplify and can be explicitly written down. In Appendix 3.C, we study the low-frequency propagators, and the resulting expressions are

$$D_{[11]}(\omega, r, r_c) = D_F(\omega, r, r_c) = \frac{2\pi\alpha'}{r_H^2} \left[ \frac{e^{i\omega r_*} + e^{-i\omega r_*}}{\omega(1 - e^{-\beta\omega})} - \frac{e^{i\omega r_*}}{\omega} \right], \quad (3.85)$$

$$D_{[21]}(\omega, r, r_c) = D_W(\omega, r, r_c) = \frac{2\pi\alpha'}{r_H^2} \frac{e^{i\omega r_*} + e^{-i\omega r_*}}{\omega(1 - e^{-\beta\omega})},$$

where  $r_*$  is the tortoise coordinate introduced in (3.20). As explained in (3.179), the precise low frequency limit we are taking is

$$\omega_i \rightarrow 0, \quad \beta, \omega_i r_* : \text{fixed}. \quad (3.86)$$

The reason why we have to keep  $\omega_i r_*$  fixed is that, no matter how small  $\omega_i$  is, we can consider a region very close to the horizon ( $r_* = -\infty$ ) such that  $\omega_i r_* = \mathcal{O}(1)$ . If we insert the expressions (3.85) into (3.84) and keep the leading term in the small  $\omega_i$  expansion in the sense of (3.86), we obtain

$$G_{\text{conn}}^{(x)}(\omega_1, \omega_2, \omega_3, \omega_4) \sim \frac{i\alpha'^3 \beta^5}{\omega_1 \omega_2 \omega_3 \omega_4} \delta(\omega_1 + \dots + \omega_4) \times \sum_{1 \leq i < j \leq 4} (\omega_i + \omega_j) \int_{-\infty}^0 dr_* \frac{r_*^2}{f} e^{-2i(\omega_i + \omega_j)r_*} + \mathcal{O}(\omega^{-2}), \quad (3.87)$$

where we ignored numerical factors. Using (3.77) and (3.34), we can finally derive the expression for the  $R$  correlator:

$$G_{\text{conn}}^{(R)}(\omega_1, \omega_2, \omega_3, \omega_4) \sim \frac{i}{\alpha' \beta^3} \delta(\omega_1 + \dots + \omega_4) \times \sum_{1 \leq i < j \leq 4} (\omega_i + \omega_j) \int_{-\infty}^0 dr_* \frac{r_*^2}{f} e^{-2i(\omega_i + \omega_j)r_*} + \mathcal{O}(\omega^2). \quad (3.88)$$

Let us look at the IR part of (3.87), namely the contribution from the near-horizon region (large negative  $r_*$ ). Because  $f \sim (d-1)e^{(d-1)r_H r_*}$  near the horizon, the  $r_*$  integral in (3.87) is

$$\int_{-\infty}^0 dr_* \frac{r_*^2}{f} e^{-2i(\omega_i + \omega_j)r_*} \sim \frac{r_H^2}{d-1} \int_{-\infty}^0 dr_* e^{-(d-1)r_H r_*} e^{-2i(\omega_i + \omega_j)r_*} \quad (3.89)$$

which diverges because of the contribution from the near horizon region,  $r_* \rightarrow -\infty$ . We will discuss the nature of this IR divergence later.

### 3.4.2 Holographic approach

Next, let us discuss another way to compute the correlators of the boundary Brownian motion, following the standard GKPW procedure as in section 1.4.1. For this approach, we send the UV cutoff  $r_c \rightarrow \infty$  and let the string extend all the way to the AdS boundary  $r = \infty$ . The boundary value of  $X(t, r)$  is the position of the boundary Brownian particle:  $x(t) = X(t, r \rightarrow \infty)$ . The boundary operator dual to the bulk field  $X(t, r)$  is  $F(t)$ , the total force (friction plus random force) acting on the boundary Brownian particle. The AdS/CFT dictionary

$$\left\langle e^{i \int dt F(t)x(t)} \right\rangle_{\text{CFT}} = e^{i S_{\text{bulk}}[x(t)]} \quad (3.90)$$

says that, to compute boundary correlators for  $F$ , we should consider bulk configurations for which  $X(t, r)$  asymptotes to a given function  $x(t)$  at  $r = \infty$ , evaluate the bulk action, and functionally differentiate the result with respect to  $x(t)$ . Note that, in the limit  $r_c \rightarrow \infty$  or  $m \rightarrow \infty$  that we take, friction is ignorable as compared to random force  $R$ , and  $F$  correlators are the same as  $R$  correlators [41]. Roughly speaking, because the Brownian particle does not move in the  $m \rightarrow \infty$  limit, there will be no friction and thus  $R = F$ .

In the end, the resulting 4-point function  $\langle FFFF \rangle$  is essentially given by the interaction term in the action, with the  $X$  fields replaced by the boundary-bulk propagators. Namely,

$$\begin{aligned} \langle \mathcal{T}[F(t_1)F(t_2)F(t_3)F(t_4)] \rangle &\sim \frac{1}{16\pi\alpha'} \int dt dr \\ &\sum_{\text{perm}} \left[ -\frac{\partial_t K(t_i) \partial_t K(t_j)}{f} + r^4 f \partial_r K(t_i) \partial_r K(t_j) \right] \\ &\times \left[ -\frac{\partial_t K(t_k) \partial_t K(t_l)}{f} + r^4 f \partial_r K(t_k) \partial_r K(t_l) \right], \end{aligned} \quad (3.91)$$

where  $K(t_i) \equiv K(t, r|t_i)$  is the boundary-bulk propagator from the boundary point  $t_i$  to the bulk point  $(t, r)$ . This is the Witten diagram rule that we naively expect. However, because the worldvolume theory of a string is different from, e.g. a Klein–Gordon scalar, a careful consideration of holographic renormalization is necessary. Indeed, the naive expression is (3.91) is UV divergent and needs regularization. Furthermore, our black hole spacetime is a Lorentzian geometry and we should apply the rules of Lorentzian AdS/CFT of section 1.7.2. As is explained in Appendix 3.D, after all the dust has been settled, the  $F$  correlator gives exactly the same IR divergence as the naive computation of the  $R$  correlator, (3.88). This implies that this IR divergence we are finding is not an artifact but a real thing to be interpreted physically.<sup>8</sup>

<sup>8</sup>Although the IR parts are the same, the result obtained in the previous subsection 3.4.1 using



It is worth pointing out that the result (3.91) has a similar structure to the one we saw in the toy model (3.62), with the propagator  $K(t)$  roughly corresponding to  $P(t)$ . It would be interesting to find an improved toy model which precisely reproduces the structure (3.91).

In Appendix 3.D.5, we also computed the *retarded* 4-point function of random force. The expression is free from both IR and UV divergences and the final result is finite. However, because we do not know how to relate the retarded 4-point function and  $t_{\text{mfp}}$ , this cannot be used to compute  $t_{\text{mfp}}$ . It would be interesting to find a microscopic model that directly relates retarded correlators and  $t_{\text{mfp}}$ .

### 3.4.3 General polarizations

The argument so far has been as if there were only one field  $X$  and the associated random force  $R$ . However, in the general  $d > 3$  case we have  $n = d - 2 > 1$  fields  $X^I$ ,  $I = 1, 2, \dots, n$ . Considering all  $X^I$ , the bulk action (3.75) actually becomes

$$S_{\text{int}} = \frac{1}{16\pi\alpha'} \int dt dr \left[ \frac{(\dot{X}^I)^2}{f} - r^4 f (X^{I'})^2 \right]^2. \quad (3.92)$$

The associated random force  $R^I$  has  $n$  components too.

The computation of 4-point functions in this multi-component case can be done completely in parallel with the one-component case. Let us define

$$G_{\text{conn}}^{(x)IJKL}(t_1, t_2, t_3, t_4) \equiv \langle \mathcal{T}[X^I(t_1, r_c)X^J(t_2, r_c)X^K(t_3, r_c)X^L(t_4, r_c)] \rangle. \quad (3.93)$$

This is nonvanishing only if some indices are identical. More precisely, the only nonvanishing cases are (i) all indices are identical,  $I = J = K = L$ , or (ii) indices are pairwise identical,  $I = J \neq K = L$ ,  $I = K \neq J = L$ , or  $I = L \neq J = K$ .

In case (i), the resulting 4-point function is exactly the same as the one-component case (3.84). Consequently, the IR form of the random force correlator  $G_{\text{conn}}^{(R)IIII}$  is the same as the one-component case (3.88).

---

the worldsheet thermal field theory is not quite the same as the one obtained in this subsection 3.4.2 using holographic renormalization, due to the counter terms added to the latter at the UV cutoff  $r = r_c$ .

In case (ii), on the other hand, the 4-point function becomes

$$\begin{aligned}
G_{\text{conn}}^{(x)IIJJ}(\omega_1, \omega_2, \omega_3, \omega_4) &= \frac{i}{16\pi\alpha'} 2\pi\delta(\omega_1 + \dots + \omega_4) \int_{r_H}^{r_c} dr \\
&\times \left\{ 8 \left[ \frac{\omega_1\omega_2}{f} D_{[11]}(\omega_1) D_{[11]}(\omega_2) + r^4 f \partial_r D_{[11]}(\omega_1) \partial_r D_{[11]}(\omega_2) \right] \right. \\
&\quad \times \left[ \frac{\omega_3\omega_4}{f} D_{[11]}(\omega_3) D_{[11]}(\omega_4) + r^4 f \partial_r D_{[11]}(\omega_3) \partial_r D_{[11]}(\omega_4) \right] \\
&\quad \left. - (D_{[11]} \rightarrow D_{[21]}) \right\}. \tag{3.94}
\end{aligned}$$

The IR form of the random force correlator is

$$\begin{aligned}
G_{\text{conn}}^{(R)IIJJ}(\omega_1, \omega_2, \omega_3, \omega_4) &\sim \frac{i}{\alpha'\beta^3} \delta(\omega_1 + \dots + \omega_4) \int_{-\infty}^0 dr_* \frac{r_*^2}{f} \\
&\quad \times \sum_{1 \leq i \leq 2, 3 \leq j \leq 4} (\omega_i + \omega_j) e^{-2i(\omega_i + \omega_j)r_*} + \mathcal{O}(\omega^2). \tag{3.95}
\end{aligned}$$

Comparing this with the expectation from the field theory side, (3.73) we observe the same structure. Namely, the connected 4-point functions are nonvanishing only when the polarization indices are all or pairwise identical. The precise relative values of the nonvanishing 4-point functions are model-dependent and not important; in the simple model of subsection 3.3.2, it depends on our choice of the expectation values (3.69).

### 3.5 The IR divergence

In the last section, we computed the connected 4-point function for the random force  $R$  and found that the low-frequency expression,

$$\begin{aligned}
G_{\text{conn}}^{(R)}(\omega_1, \omega_2, \omega_3, \omega_4) &\sim \frac{i}{\alpha'\beta^3} \delta(\omega_1 + \dots + \omega_4) \\
&\quad \times \sum_{1 \leq i < j \leq 4} (\omega_i + \omega_j) \int_{-\infty}^0 dr_* \frac{r_*^2}{f} e^{-2i(\omega_i + \omega_j)r_*}, \tag{3.96}
\end{aligned}$$

has an IR divergence coming from the integral in the near horizon region. What is the physical reason for this divergence? Very near the horizon, the expansion of the Nambu–Goto action in the transverse fluctuation  $X$  breaks down because the proper temperature becomes higher and higher as one approaches the horizon and, as a result, the string fluctuation gets wilder and

wilder. The correct thing to do in principle is to consider the full non-linear Nambu–Goto action, but this is technically very difficult. Instead, a physically reasonable estimate of the result is the following. Let us introduce an IR cutoff near the horizon at

$$r_s = r_H + \epsilon, \tag{3.97}$$

where  $\epsilon \ll r_H$ . We take this cutoff  $r_s$  to be the radius where the expansion of the Nambu–Goto action becomes bad. Then, in IR-divergent expressions such as (3.88), we simply throw away the contribution from the region  $r < r < r_s$  by taking the integral to be only over  $r > r_s$ . Of course, to obtain a more precise result, we should include the contribution from the region  $r_H < r < r_s$  with the higher order terms in the expansion of the Nambu–Goto action taken into account. However, we expect that the contribution from this region  $r_H < r < r_s$  will be of the same order as the contribution from the region  $r > r_s$  and, therefore, we can estimate the full result by just keeping the latter contribution.

With this physical expectation in mind, let us evaluate the mean-free-path time  $t_{\text{mfp}}$  by introducing the IR cutoff (3.97). The parameter  $\epsilon$  appearing in (3.97) can be related to the proper distance from the horizon,  $s$ , as follows:

$$s = \int_{r_H}^{r_H+\epsilon} \frac{dr}{r\sqrt{f}} \sim \int_{r_H}^{r_H+\epsilon} \frac{dr}{\sqrt{(d-1)r_H(r-r_H)}} = \sqrt{\frac{2\epsilon}{(d-1)r_H}}. \tag{3.98}$$

Therefore

$$\epsilon \sim s^2 r_H, \tag{3.99}$$

where we dropped numerical factors. In the tortoise coordinate  $r_*$ , the cutoff is at

$$r_*^s \sim -\frac{1}{(d-1)r_H} \log s^2, \tag{3.100}$$

where we used (3.21).

The introduction of an IR cutoff of the geometry near the horizon also means that the resulting expressions such as (3.96), with the IR cutoff imposed, is valid only for frequencies larger than a certain cutoff frequency  $\omega_s$ . We can relate  $\omega_s$  with the geometric cutoff  $r_*^s$  as follows. If we cut off the geometry at  $r_* = r_*^s$ , we have to impose some boundary condition there (just as for the brick wall model). For example, let us impose a Neumann boundary condition. As was shown in (3.177), for very low frequencies, the solutions to the wave equation behave as

$$f_\omega(r) \sim e^{i\omega r_*} + e^{-i\omega r_*}. \tag{3.101}$$

For this to satisfy Neumann boundary condition  $\partial_{r_*} f_\omega(r)|_{r_*=r_*^s} = 0$ , we need  $\omega = n\pi/r_*^s$  where  $n \in \mathbb{Z}$ . Namely, the frequency has been discretized in units of  $\pi/|r_*^s|$ . Therefore, the smallest possible frequency is

$$\omega_s \sim \frac{1}{|r_*^s|} \sim \frac{1}{\beta \log(1/s)}. \quad (3.102)$$

If we use (3.100) and (3.102), the correlator (3.96) becomes

$$\begin{aligned} G_{\text{conn}}^{(R)}(\omega_1, \omega_2, \omega_3, \omega_4) &\sim \frac{i}{\alpha' \beta^3} \delta(\omega_1 + \dots + \omega_4) \omega_s r_H^2 \int_{r_*^s} dr_* e^{-(d-1)r_H r_*} \\ &\sim \frac{i}{\alpha' \beta^3} \delta(\omega_1 + \dots + \omega_4) \omega_s r_H^2 \frac{e^{-(d-1)r_H r_*^s}}{r_H} \\ &\sim \frac{is^2 \omega_s}{\alpha' \beta^4} \delta(\omega_1 + \dots + \omega_4) \sim \frac{is^2}{\alpha' \beta^5 \log(1/s)} \delta(\omega_1 + \dots + \omega_4). \end{aligned} \quad (3.103)$$

On the other hand, from (3.36), the 2-point function is

$$G^{(R)}(\omega_1, \omega_2) \sim \frac{1}{\alpha' \beta^3} \delta(\omega_1 + \omega_2) \quad (3.104)$$

Comparing above results and the toy model results (3.66), (3.67), we obtain

$$t_{\text{mf}p} \sim \frac{1}{\mu} \sim \frac{\alpha' \beta}{s^2 \log(1/s)}, \quad P(\omega = 0) \sim \frac{1}{\beta s \sqrt{\log(1/s)}}. \quad (3.105)$$

Now the question is how to determine the length  $s$ . This must be the place where the expansion (3.74) of the Nambu–Goto action becomes bad. One can show that this occurs a proper length  $\sim \sqrt{\alpha'}$  away from the horizon due to thermal fluctuation (Hawking radiation) in the black hole background (for an argument in more general setups see subsection 3.6.1). This leads us to set

$$s \sim \sqrt{\alpha'}. \quad (3.106)$$

At this point, the local proper temperature becomes of the order of the Hagedorn temperature,  $\sim 1/\sqrt{\alpha'}$ . The above condition must be the same as the condition that the loop correction of the worldsheet theory to the 4-point function  $\langle F^4 \rangle$  becomes of the same order as the tree level contribution.

If we substitute (3.106) into (3.105), we obtain

$$t_{\text{mf}p} \sim \frac{1}{T \log \lambda}, \quad P(\omega = 0) \sim \frac{T \lambda^{1/4}}{\sqrt{\log \lambda}} \quad (3.107)$$

where, following the convention of the  $d = 5$  (AdS<sub>5</sub>) case, we defined the “t Hooft coupling” by

$$\lambda \equiv \frac{l^4}{\alpha'^2}, \quad (3.108)$$

where we restored the AdS radius  $l$  which we have been setting to one.

The result (3.107) is quite interesting. In [67], the collision duration time  $t_{\text{coll}}$  was determined to be

$$t_{\text{coll}} \sim \frac{1}{T}. \tag{3.109}$$

Therefore,  $t_{\text{mfp}}$  given in (3.107) implies that a plasma particle can be thought of as in interaction with roughly  $\log \lambda$  other particles simultaneously.

Even if we take into account the fact that  $X^I$  has in general more than one component ( $I = 1, 2, \dots, n = d - 2$ ) and use the results such as (3.73), (3.95), we end up the same estimate for  $t_{\text{mfp}}$  as far as its order is concerned.

## 3.6 Generalizations

In the previous section, we derived using AdS/CFT the expression for the mean-free-path time  $t_{\text{mfp}}$  for the simple case of neutral plasma. In this section, we sketch how this generalizes to the more general metric (3.37) and present the expression for the mean-free-path time for more general systems such as charged plasmas. As an example, we will apply the result to the STU black hole.

### 3.6.1 Mean-free-path time for the general case

We are interested in computing the mean-free-path time in field theory by analyzing the motion of a Brownian string in the metric (3.37). For that, as has been explained in section 3.3 for the neutral case, we need to compute the 4-point function of the random force in addition to the 2-point function.

Expanding the Nambu–Goto action in the background metric (3.37) up to quartic order, the action for the string in the tortoise coordinate defined in (3.44) is given as follows:

$$S = S_0 + S_{\text{int}}, \tag{3.110}$$

$$S_0 = \frac{1}{4\pi\alpha'} \int dt dr_* G (\dot{X}^2 - X'^2), \tag{3.111}$$

$$S_{\text{int}} = \frac{1}{16\pi\alpha'} \int dt dr_* \frac{G^2}{h_{tf}} (\dot{X}^2 - X'^2)^2, \tag{3.112}$$

where we dropped a constant independent of the field  $X$ , and  $\dot{\phantom{x}} = \partial_t$ ,  $' = \partial_{r_*}$ . As we discussed in subsection 3.4.2 for the simple neutral case, we can use  $S_{\text{int}}$  as the interaction term and apply the usual GKPW rule to compute correlators for the random force<sup>9</sup>  $F$  dual to the bulk field  $X$ . As before, the naive

---

<sup>9</sup>Recall that in this setup the force  $F$  is equal to the random force  $R$ .

result from the GKPW prescription includes both UV and IR divergences. Using holographic renormalization, which is discussed in Appendix 3.D for the neutral case, we can remove the UV divergence by adding counter terms to the action. The IR divergence, on the other hand, signals the breakdown of the quartic approximation (3.110). We regulate this divergence by introducing an IR cutoff at  $r_* = r_*^s$  near to the horizon, whose physical motivation was explained in section 3.5.

Following the same analysis as in section 3.5 now with the interaction term (3.112), we obtain an expression similar to (3.88) for the connected random force 4-point function. The dominant contribution comes from the near-horizon region and is given in frequency space by

$$\langle T[F^4] \rangle_{\text{conn}} \sim \frac{i}{\alpha' \beta^3} \delta(\omega_1 + \dots + \omega_4) \int_{r_*^s} dr_* \frac{G^2}{f h_t} \sum_{1 \leq i < j \leq 4} (\omega_i + \omega_j) e^{-2i(\omega_i + \omega_j)r_*}, \quad (3.113)$$

where  $r_*^s$  is the aforementioned IR cutoff (in the tortoise coordinate). Let the IR cutoff in the  $r$  coordinate be at  $r = r_H + \epsilon \equiv r_s$ . The parameter  $\epsilon$  is related to the proper distance  $s$  from the horizon as

$$s = \int_{r_H}^{r_H + \epsilon} \sqrt{\frac{h_r}{f}} dr \approx \sqrt{\frac{2\epsilon h_r(r_H)}{k_H}}, \quad \epsilon \approx \frac{s^2 k_H}{2h_r(r_H)}. \quad (3.114)$$

Using the relation (3.44) between  $r_s$  and  $r_*^s$ , we can estimate the cut-off integral (3.113) as

$$\langle T[F^4] \rangle \sim \frac{G^2(r_H) \omega_s}{\alpha' s^2} \delta(\omega_1 + \dots + \omega_4), \quad (3.115)$$

where  $\omega_s$  is the smallest frequency for which the expansion (3.110) is valid. Combining this with the result (3.50) for the 2-point function, the mean-free-path time is estimated as

$$t_{\text{mfp}} \sim \frac{\alpha' \beta^2 \omega_s}{s^2}. \quad (3.116)$$

Now, let us determine the IR cutoff parameters  $s$  (or equivalently  $\epsilon$ ) and  $\omega_s$  appearing in (3.116). As before, we take the IR cutoff to be the location where  $S_0$  and  $S_{\text{int}}$  become of the same order. As is clear from (3.111), (3.112), the expansion of the Nambu–Goto action becomes bad at the location where

$$\frac{G}{h_t f} \dot{X}^2, \frac{G}{h_t f} X'^2 \sim 1. \quad (3.117)$$

So, we would like to estimate  $\dot{X}$ ,  $X'$ . Near the horizon,  $r \approx r_H$ , we can write the action (3.111) as

$$S_0 \sim \frac{1}{2} \int dt dr_* (\dot{\tilde{X}}^2 - \tilde{X}'^2), \quad \tilde{X} \equiv \sqrt{\frac{G(r_H)}{2\pi\alpha'}} X. \quad (3.118)$$

There being no dimensional quantity in the problem other than the temperature  $T$ , we must have  $\tilde{X}, \tilde{X}' \sim T$ , namely  $|\dot{X}|, |X'| \sim \sqrt{2\pi\alpha'/G(r_H)} T$ . So, the condition (3.117) determines the IR cutoff to be at

$$r - r_H = \epsilon \sim \frac{\alpha' T^2}{k_H h_t(r_H)}. \quad (3.119)$$

In term of  $s$ , the IR cutoff is at the string length:

$$s \sim \sqrt{\alpha'}. \quad (3.120)$$

It is more subtle to determine the parameter  $\omega_s$ . In Appendix 3.B (around Eq. (3.174)), the following was shown. Let us we choose the tortoise coordinate  $r_*$  to be related to  $r$  near the horizon as

$$r_* \approx \frac{1}{4\pi T} \log \left( \frac{r - r_H}{L_H} \right), \quad (3.121)$$

where  $L_H$  is defined through the following integral

$$\int_{\infty}^r \frac{dr}{fG} \sqrt{\frac{h_r}{h_t}} = \frac{1}{4\pi G_H T} \log \left( \frac{r - r_H}{L_H} \right) + \mathcal{O}(r - r_H) \quad (3.122)$$

for  $r \approx r_H$ . Then the solution  $f_\omega(r)$  to the wave equation (3.43), satisfying a normalizable boundary condition at infinity, will have the form

$$f_\omega(r) \sim e^{i\omega r_*} - e^{-i\omega r_*} \quad (3.123)$$

for small  $\omega$ . More precisely, we have

$$f_\omega(r) \sim e^{i\omega r_*} - e^{i\alpha_\omega} e^{-i\omega r_*}, \quad \alpha_\omega = \mathcal{O}(\omega^2). \quad (3.124)$$

Now, let us we impose some boundary condition at  $r_*^s$ , such as a Neumann boundary condition  $\partial_{r_*} f_\omega = 0$ , then the frequency  $\omega$  gets discretized in units of  $\Delta\omega = \pi/|r_*^s|$ . Note that, if  $\alpha_\omega = \mathcal{O}(\omega)$  as  $\omega \rightarrow 0$ , then the coefficient of the  $\mathcal{O}(\omega)$  term will affect the value of  $\Delta\omega$ ; this is why (3.124) was important. This motivates the following choice for the minimum frequency:

$$\omega_s \sim \Delta\omega \sim \frac{1}{|r_*^s|} \sim \frac{1}{\beta \log \left( \frac{L_H}{\epsilon} \right)} \sim \frac{1}{\beta \log \left( \frac{\beta L_H}{s^2} \sqrt{h_t(r_H) h_r(r_H)} \right)}. \quad (3.125)$$

Substituting in the above expressions for  $s, \omega_s$ , the mean-free-path time (3.116) is

$$t_{\text{mfp}} \sim \frac{1}{T \log(\eta\sqrt{\lambda})}, \quad \eta \equiv \frac{L_H}{T} \sqrt{h_t(r_H) h_r(r_H)}, \quad (3.126)$$

where  $\lambda$  is the ‘t Hooft coupling’ defined in (3.108). Note that the nontrivial effect of charge only enters through the logarithm and hence the dependence of  $t_{\text{mfp}}$  on it is very mild in the strongly coupled case  $\lambda \gg 1$ .

### 3.6.2 Application: STU black hole

The AdS/CFT correspondence has been successfully used to extract the properties of field theory plasmas. A particularly interesting case is a 4-dimensional charged plasma, because it is relevant for the experimentally generated quark-gluon plasma with net baryon charge. One notable situation to realize 4-dimensional charged plasmas in the AdS/CFT setup is the spinning D3-brane, which in the decoupling limit gives  $d = 4$ ,  $\mathcal{N} = 4$  SYM with nonvanishing  $R$ -charges. We can have three different  $R$ -charges corresponding three Cartan generators of the  $SU(4) \cong SO(6)$   $R$ -symmetry group. As already mentioned in subsection 3.2.3, on the gravity side this corresponds to a Kerr black hole in  $\text{AdS}_5 \times S^5$  with three angular momenta in the  $S^5$  directions [82, 83]. Upon compactifying on  $S^5$ , this reduces to the so-called STU black hole of the five-dimensional supergravity [80, 81]. From this five-dimensional perspective, the STU black hole is a non-rotating black hole with three  $U(1)$  charges. There has been much study [40, 84, 85, 91–94] on the properties of the  $R$ -charged field theory plasma using the STU black hole. Here, we would like to apply the machineries we have developed in the previous sections to the computation of the mean-free-path time for the Brownian particle in  $R$ -charged plasma dual to the STU black hole.

#### The STU black hole

The 10-dimensional metric of the STU black hole is given by [80]:<sup>10</sup>

$$\begin{aligned}
 ds_{10}^2 &= \sqrt{\Delta} ds_5^2 + \frac{l^2}{\sqrt{\Delta}} \sum_{i=1}^3 X_i^{-1} \left[ d\mu_i^2 + \mu_i^2 \left( d\psi_i + \frac{A^i}{l} \right)^2 \right], & (3.127) \\
 ds_5^2 &= -\frac{f}{\mathcal{H}^{2/3}} dt^2 + \mathcal{H}^{1/3} \left( \frac{dr^2}{f} + r^2 (dX^I)^2 \right), \\
 f(r) &= \frac{r^2}{l^2} \mathcal{H} - \frac{m}{r^2}, \quad \mathcal{H} = H_1 H_2 H_3, \quad H_i = 1 + \frac{q_i}{r^2}, \\
 X_i &= H_i^{-1} \mathcal{H}^{1/3}, \quad A^i = \sqrt{\frac{m}{q_i}} (1 - H_i^{-1}) dt, \quad \Delta = \sum_{i=1}^3 X_i \mu_i^2, \\
 \mu_1 &= \sin \theta_1, \quad \mu_2 = \cos \theta_1 \sin \theta_2, \quad \mu_3 = \cos \theta_1 \cos \theta_2
 \end{aligned}$$

with  $i = 1, 2, 3$ . Here,  $X^I$ ,  $I = 1, 2, 3$  are spatial directions along the boundary and  $l$  is the AdS radius. The four parameters  $m, q_i$  are related to the mass and three electric charges of the STU black hole. It is convenient to introduce the

<sup>10</sup>The horizon of the STU black hole can be either  $S^3, \mathbb{R}^3$ , or  $H^3$ , but we are focusing on the planar  $\mathbb{R}^3$  case, corresponding to a charged plasma in flat  $\mathbb{R}^3$ .



dimensionless quantities

$$\kappa_i = \frac{q_i}{r_H^2}, \quad i = 1, 2, 3. \quad (3.128)$$

The horizon is at  $r = r_H$  where  $r_H$  is the largest solution to  $f(r) = 0$ . The latter equation relates  $m$  to  $r_H$  and  $\kappa_i$  as

$$m = \frac{r_H^4}{l^2} \mathcal{H}(r_H) = \frac{r_H^4}{l^2} (1 + \kappa_1)(1 + \kappa_2)(1 + \kappa_3). \quad (3.129)$$

The Hawking temperature is given by

$$T = \frac{r_H}{2\pi} \frac{2 + \kappa_1 + \kappa_2 + \kappa_3 - \kappa_1\kappa_2\kappa_3}{\sqrt{(1 + \kappa_1)(1 + \kappa_2)(1 + \kappa_3)}}. \quad (3.130)$$

From the five-dimensional point of view, the STU black hole is electrically charged under the gauge fields  $A^i$  and the associated chemical potentials are

$$\Phi^i = \frac{1}{\kappa_5^2} [A_t^i(r = \infty) - A_t^i(r = r_H)] = -\frac{r_H^2}{\kappa_5^2 l} \frac{\sqrt{\kappa_i} \prod_{j=1}^3 (1 + \kappa_j)}{1 + \kappa_i}. \quad (3.131)$$

Here  $\kappa_5^2 = 8\pi G_5$  is the five-dimensional Newton constant and

$$G_5 = \frac{G_{10}}{V_{S^5}} = \frac{8\pi^6 g_s^2 \alpha'^4}{\pi^3 l^5} = \frac{\pi l^3}{2N^2}, \quad (3.132)$$

where  $N$  is the rank of the boundary gauge theory. For expressions for other physical quantities, such as energy density, entropy density, and charge density, see *e.g.* [95]. From thermodynamical stability, the parameters  $\kappa_i$  are restricted to the range [96]

$$2 - \kappa_1 - \kappa_2 - \kappa_3 + \kappa_1\kappa_2\kappa_3 > 0. \quad (3.133)$$

We can shift the gauge potential  $A^i$  so that its value on the horizon is zero:

$$\mathcal{A}^i(r) \equiv A^i(r) - A^i(r_H). \quad (3.134)$$

If we accordingly shift the angular variable by

$$\tilde{\psi}_i \equiv \psi_i + A_t^i(r_H) \quad (3.135)$$

then the metric (3.127) becomes

$$ds_{10}^2 = \sqrt{\Delta} ds_5^2 + \frac{R^2}{\sqrt{\Delta}} \sum_{i=1}^3 X_i^{-1} [d\mu_i^2 + \mu_i^2 (d\tilde{\psi}_i + \mathcal{A}^i/R)^2]. \quad (3.136)$$

### Background configuration

We first want to find a background configuration of a string in the 10 dimensional geometry (3.127) or (3.136), so that we can start expanding the Nambu-Goto action around it. If we restrict ourselves to configurations with trivial  $\theta_a$  dependence, the relevant line element can be written as

$$ds^2 = -\alpha dt^2 + \beta dr^2 + \gamma(dX^I)^2 + \sum_{i=1}^3 \epsilon_i (d\tilde{\psi}_i + \phi_i dt)^2. \quad (3.137)$$

Here  $\alpha, \beta, \gamma, \epsilon_i, \phi_i$  are functions of  $r$  and  $\theta_a$  which can be read off from (3.136). For example,  $\alpha = \Delta^{1/2} f \mathcal{H}^{-2/3}$ . Parametrize the worldsheet by  $t, r$  and take the following ansatz:

$$X^I(t, r) = 0, \quad \tilde{\psi}_i(t, r) = \tilde{\omega}_i t + \varphi_i(r). \quad (3.138)$$

The string is straight in the  $\text{AdS}_5$  part of the spacetime. On the other hand, the angular momenta in the  $S^5$  directions are expected to drag the string in these directions and  $\tilde{\omega}_i, \varphi_i$  correspond to nontrivial drifting/trailing of the string [40, 84, 85]. The Euler-Lagrange equation for  $\varphi(r)$  states that  $\pi_{\varphi_i}^r \equiv \partial L_{\text{NG}} / \partial(\partial_r \tilde{\psi}_i) = \partial L_{\text{NG}} / \partial \varphi_i$  is constant along the string. The quantity  $\pi_{\varphi_i}^r$  corresponds to the inflow of angular momenta (or, from the five-dimensional point of view, electric charges) from the ‘‘flavor D-brane’’ at the UV cutoff  $r = r_c$ , and how to choose them depends on the physical situation one would like to consider [85]. Here, let us focus on the case where the string endpoint on the ‘‘flavor D-brane’’ is free and there is no inflow, *i.e.*,  $\pi_{\varphi_i}^r = 0$ . This corresponds to a boundary Brownian particle neutral under the  $R$ -symmetry. This is physically appropriate because we want to compute the random force correlators unbiased by the effects of the charge of the probe itself. It is not difficult to see that setting  $\pi_{\varphi_i}^r = 0$  leads to  $\varphi_i = 0$  by examining the Euler-Lagrange equations.

Let us next turn to the angular velocity  $\tilde{\omega}_i$ . Given  $\varphi_i = 0$ , the induced metric on the worldsheet is

$$ds_{ind}^2 = -\alpha dt^2 + \beta dr^2 + \sum_{i=1}^3 \epsilon_i (\tilde{\omega}_i + \phi_i)^2 dt^2. \quad (3.139)$$

The determinant of this induced metric is

$$\det g \propto -\alpha + \sum_{i=1}^3 \epsilon_i (\tilde{\omega}_i + \phi_i)^2. \quad (3.140)$$

This must be always non-positive for the configuration to physically make sense. This condition is most stringent at the horizon  $r = r_H$  where  $\alpha \propto f = 0$ ,

$\phi_i = \mathcal{A}_t^i(r_H)/l = 0$ . So, we need

$$\sum_i \epsilon_i \tilde{\omega}_i^2 \leq 0. \tag{3.141}$$

Since  $\epsilon_i \geq 0$ , this means that

$$\tilde{\omega}_i = 0. \tag{3.142}$$

Namely, the background configuration is simply

$$X^I(t, r) = \tilde{\psi}_i(t, r) = 0. \tag{3.143}$$

Note that the angular motion is trivial only in the  $\tilde{\psi}_i$  coordinates and in the original  $\psi_i$  coordinates there is non-vanishing angular drift.

So far we have been treating  $\theta_a$  as constant. However, this is not correct and an arbitrary choice of  $\theta_a$  will not satisfy the full equations of motion. Below, we will consider the following three cases:

- (i) 1-charge case:  $\kappa_1 = \kappa \neq 0, \kappa_2 = \kappa_3 = 0; \theta_1 = \pi/2$ ,
- (ii) 2-charge case:  $\kappa_1 = 0, \kappa_2 = \kappa_3 = \kappa \neq 0; \theta_1 = 0$ ,
- (iii) 3-charge case:  $\kappa_1 = \kappa_2 = \kappa_3 = \kappa \neq 0; \theta_1, \theta_2$ : arbitrary.

It can be shown [85] that the above values of  $\theta_a$  are necessary for all the equations of motion to be satisfied. These values make sense physically since, if the angular momentum around an axis is nonvanishing, the string wants to orbit along the circle of the largest possible radius around that axis. This is achieved by the above choices of  $\theta_a$ .

**Friction coefficient**

Before proceeding to the computation of the mean-free-path time, let us check that the low-frequency friction coefficient for the STU black hole that we can compute using the formula (3.49) is consistent with the result found in the literature [85]. In the present case of the metric (3.137), the formula (3.49) gives

$$\mu(\omega) = \frac{2m\pi\alpha'}{\gamma(r_H)} + \mathcal{O}(\omega). \tag{3.144}$$

On the other hand, the drag force computed in [85] is<sup>11</sup>

$$\mathcal{F} = -\frac{\gamma(r_{ws})}{2\pi\alpha'} v, \tag{3.145}$$

---

<sup>11</sup>This is the drag force for the “non-torque string” of [85] which corresponds to no inflow of at the flavor D-brane; see the discussion below (3.138). See Refs. [40, 84, 85] for the relation between the strings with and without inflow.

where  $v$  is the velocity of the quark and  $r_{ws}$  is the solution to  $\alpha(r_{ws}) - v^2 \gamma(r_{ws}) = 0$ . In the non-relativistic limit,  $v \rightarrow 0$ , the admittance read off from (3.145) should become the same as the low-frequency result (3.144). Using the fact that  $r_{ws} \rightarrow r_H$  and  $p = mv$  in the  $v \rightarrow 0$  limit, it is easy to see that (3.145) indeed reproduces the admittance (3.144).

### Mean-free-path time

For the three cases (i)–(iii) described above, let us use the formula (3.126) and compute  $t_{\text{mfp}}$ . Consider the  $n$ -charge case ( $n = 1, 2, 3$ ). For the background configuration (3.143), the 10-dimensional metric of the STU black hole (3.136) induces the following metric:

$$ds^2 = -fH^{-\frac{n+1}{2}}(1 - f^{-1}H^2\mathcal{A}_t^2)dt^2 + H^{\frac{n-1}{2}}\left(\frac{dr^2}{f} + r^2(dX^I)^2\right), \quad (3.146)$$

$$\mathcal{A}_t = \sqrt{mq}\left(\frac{1}{r^2 + q} - \frac{1}{r_H^2 + q}\right), \quad H = 1 + \frac{q}{r^2}, \quad (3.147)$$

where  $q = \kappa r_H^2$ . Here, in addition to the  $t, r$  part, we kept the  $X^I$  part of the metric (3.143) also, because we would like to consider the transverse fluctuations along  $X^I$  directions. Comparing this metric with the general expression (3.37), we find

$$h_t = H^{-\frac{n+1}{2}}(1 - f^{-1}H^2\mathcal{A}_t^2), \quad h_r = H^{\frac{n-1}{2}}, \quad G = r^2H^{\frac{n-1}{2}}. \quad (3.148)$$

Therefore, from (3.126),

$$t_{\text{mfp}} \sim \frac{1}{T \log(\eta\sqrt{\lambda})}, \quad \eta = \frac{L_H}{T\sqrt{H(r_H)}} = \frac{L_H}{T\sqrt{1 + \kappa}}. \quad (3.149)$$

The computation of  $\eta$ , particularly  $L_H$  in it, is slightly complicated. So, we delegate the details of the calculation to Appendix 3.E and simply present the

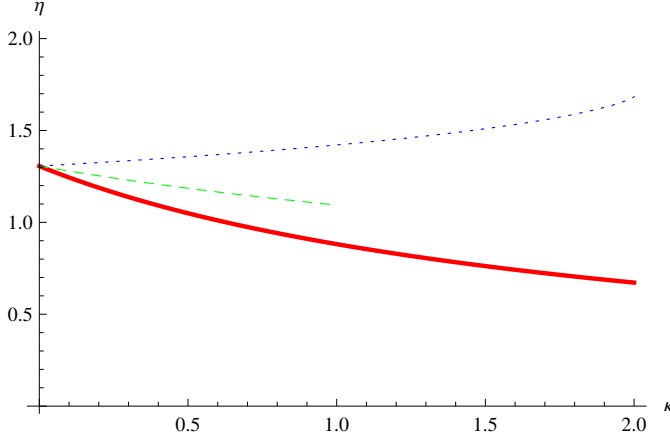


Figure 3.4: Behavior of  $\eta$  versus  $\kappa$ , for 1-charge (solid red), 2-charge (dashed green), and 3-charge (dotted blue) cases. The range of  $\kappa$  is determined by the thermodynamical stability (3.133) to be  $\kappa < 2$  for the 1- and 3-charge cases while  $\kappa < 1$  for 2-charge case.

results. For 1-, 2-, and 3-charge cases,  $\eta$  is given respectively by

$$\eta = \frac{4\pi}{2 + \kappa} \exp \left\{ -2(2 + \kappa) \int_{\infty}^1 \frac{d\rho}{\rho^2 - 1} \left[ \frac{1}{\sqrt{(\rho^2 + 1 + \kappa)((1 + \kappa)\rho^2 + 1)}} - \frac{1}{2 + \kappa} \right] \right\} \quad (3.150)$$

$$\eta = \frac{2\pi}{\sqrt{1 + \kappa}} \exp \left\{ -4\sqrt{1 + \kappa} \int_{\infty}^1 \frac{d\rho}{\rho^2 - 1} \left[ \frac{1}{\sqrt{(\rho^2 + 1)(\rho^2 + 1 + 2\kappa)}} - \frac{1}{2\sqrt{1 + \kappa}} \right] \right\} \quad (3.151)$$

$$\eta = \frac{4\pi}{(1 + \kappa)(2 - \kappa)} \exp \left\{ -2(1 + \kappa)^{3/2}(2 - \kappa) \int_{\infty}^1 \frac{d\rho}{\rho^2 - 1} \right. \\ \left. \times \left[ \frac{\rho}{\sqrt{(\rho^2 + 1 + \kappa - \kappa^2)(\rho^4 + (1 + 3\kappa)\rho^2 - \kappa^3)}} - \frac{1}{(1 + \kappa)^{3/2}(2 - \kappa)} \right] \right\} \quad (3.152)$$

The small  $\kappa$  expansion of  $\eta$  is presented in (3.263)–(3.265).

In Figure 3.4, we have plotted the behavior of  $\eta$  as we change  $\kappa$ . Because  $\eta$  appears in the denominator of the expression for  $t_{\text{mfp}}$ , we observe the following: for the 1- and 2-charge cases,  $t_{\text{mfp}}$  gets longer as we increase the chemical potential keeping  $T$  fixed, while for the 3-charge case,  $t_{\text{mfp}}$  gets shorter as we increase the chemical potential keeping  $T$  fixed.

One may find it counter-intuitive that  $t_{\text{mfp}}$  increases as we increase chemical potential with  $T$  fixed in the 1- and 2-charge cases, based on the intuition that a larger chemical potential means higher charge density and thus more constituents to obstruct the motion of the Brownian particle. However, such intuition is not correct. What we know instead is that, if we increase the charge with the mass fixed, then the entropy decreases, as one can see from the entropy formula for charged black holes. So, if we interpret entropy as the number of “active” degrees of freedom which can obstruct the motion of the Brownian particle, then this suggests that  $t_{\text{mfp}}$  should increase as we increase the charge with the mass fixed. We did numerically check that this is indeed true for all the 1-, 2- and 3-charge cases.

### 3.7 Discussion

We studied Brownian motion in the AdS/CFT setup and computed the time scales characterizing the interaction between the Brownian particle and the CFT plasma, such as the mean-free-path time  $t_{\text{mfp}}$ , by relating them to the 2- and 4-point functions of random force. We found that there is an IR divergence in the computation of  $t_{\text{mfp}}$  which we regularized by introducing an IR cutoff near the horizon. Here let us discuss the issues involved in the procedure and the implication of the result.

The first question that arises is:  $t_{\text{mfp}}$  is the mean-free-path time for what particle? First of all, one can wonder whether this is really a mean-free-path time in the first place, because the nontrivial 4-point function was obtained by expanding the Nambu–Goto action to the next leading order, which is a relativistic correction to the motion of the bulk string. So, isn’t this a relativistic correction to the kinetic term in the Langevin equation, not to the random force? However, recall the “cloud” picture of the Brownian particle mentioned before; the very massive quark we inserted is dressed with a cloud of polarized plasma constituents. The position of the quark corresponds to the boundary endpoint of the bulk string, while the cloud degrees of freedom correspond to the fluctuation modes of the bulk string. So, we are incorporating relativistic corrections to these cloud degrees freedom (fluctuations) but not to the quark which gets very heavy in the large  $m$  limit and thus remains non-relativistic.

So, what is happening is the following. First, the constituents of the background plasma kick the cloud degrees of freedom randomly and, consequently, those cloud degrees of freedom undergo random motion, to which we have incorporated relativistic corrections. Then these cloud degrees of freedom, in turn, kick the quark, which is recorded as the random force  $F$  felt by the quark.  $F$  is non-Gaussian, or has a nontrivial 4-point function, because the cloud that is interacting with the quark is relativistic. The quark’s motion, which is what is observed in experiments, is certainly governed by the non-Gaussian random  $F$  and the frequency of collision events is given by  $1/t_{\text{mfp}}$ .

However, it is worth emphasizing that this  $t_{\text{mfp}}$  is not a mean-free-path time for the plasma constituents themselves.<sup>12</sup>

We focused on the fluctuations in the noncompact AdS directions. However, for example, in the case of STU black holes, the full spacetime is  $\text{AdS}_5 \times S^5$  and the string can fluctuate in the internal  $S^5$  directions as well. Let us denote the fluctuations of the string in the internal directions by  $Y$ , while the fluctuations in the AdS directions continue to be denoted by  $X$ . One may wonder if the computations of the random force correlators such as  $\langle \mathcal{O}_X \mathcal{O}_X \mathcal{O}_X \mathcal{O}_X \rangle$  are affected by the  $Y$  fields. Here, we denoted the force by  $\mathcal{O}_X$  to remind ourselves that the force is an operator conjugate to the bulk field  $X$ . The  $Y$  fields do contribute to such quantities, because the Nambu–Goto action expanded up to quartic order involves terms of the form  $X^2 Y^2$ . However, as long as we are interested in quantities with all external lines being  $\mathcal{O}_X$ , such as  $\langle \mathcal{O}_X \mathcal{O}_X \mathcal{O}_X \mathcal{O}_X \rangle$ , they only make loop contributions, which are down by factors of  $\alpha'$ . Therefore, our leading order results do not change.

In the present chapter, we focused on the case where the plasma has no net momentum. More generally, one can consider the case where the plasma carries net amount of momentum and insert a quark in it. The Brownian motion in such situations were studied in [69, 71] (see also [70]) in AdS/CFT setups. It is interesting to generalize our computation of  $t_{\text{tmp}}$  to such cases. Note the following, however: in general, in the presence of a net background momentum, the string will “trail back” because it is pushed by the flow. Unless one applies an external force, the string will start to move and ultimately attain the same velocity as the background plasma. This final state is simply a boost of the static situation studied in the present chapter. So, the result of the current chapter applies to this last situation too (after rescaling due to Lorentz contraction).

The resulting expression for the mean-free-path time, e.g. (3.107), is quite interesting because of the logarithm. As mentioned around (3.109), this means that the Brownian particle is experiencing  $\sim \log \lambda$  collision events at the same time. Because  $\lambda \propto N$ , this is reminiscent of the fast scrambler proposal [98, 99] which claims that, in theories that have gravity dual,  $\sim \log N$  degrees of freedom are in interaction with each other simultaneously.

In our previous paper [67], we claimed that  $t_{\text{mfp}} \sim 1/T$  based on dimensional analysis, but (3.107) says that there is an extra factor which cannot be deduced on dimensional grounds. Of course, we have to note the fact that  $t_{\text{mfp}}$  we computed in the present chapter is not the time scale of the constituents but of the Brownian particle (see also footnote 12). In our previous paper [67], we had  $t_{\text{relax}}^{\text{old}} \sim m/(T^2 \sqrt{\lambda})$ ,  $t_{\text{mfp}}^{\text{old}} \sim 1/(T \sqrt{\lambda})$  instead, which were nice because if we set  $m \rightarrow T$  in  $t_{\text{relax}}^{\text{old}}$  we get  $t_{\text{mfp}}^{\text{old}}$ . In the (3.107), this is no longer the case, but now the relation between  $t_{\text{relax}}$  and  $t_{\text{mfp}}$  is not so simple as we can see

<sup>12</sup>Ref. [97] estimates the mean-free-path of the plasma constituents to be  $l_{\text{mfp}} \sim 1/T$  from the parameters of the hydrodynamics that one can read off from the bulk gravity.

from the fact that there is a nontrivial  $\lambda$  dependence in the impact per collision,  $P(\omega = 0)$  (Eq. (3.107)). It would be interesting to find an improved microscopic toy model which can relate  $t_{relax}$  and  $t_{mfp}$ .

Probably the most controversial issue in our computations is the IR cutoff. When regulating integrals such as (3.96), we cut off the geometry at a proper distance  $s \sim l_s$  away from the horizon, assuming that the contribution from the rest of the integral is of the same order. This seems physically reasonable, but we do not have a proof. One could also have tried to put a cutoff at the point where the backreaction of the fundamental string on the black hole geometry becomes important. Since the interaction of the string with the background is suppressed by additional powers of the string coupling constant, the resulting cutoff is presumably closer to the Planck length than the string length.

Related to the above statement, it is interesting to note that the mean-free-path at weak coupling [100]

$$\lambda_{mfp,weak} \sim \frac{1}{g_{YM}^4 T \ln(1/g_{YM}^2)} \quad (3.153)$$

has a form tantalizingly similar to (3.105). In particular, the log in (3.153) is coming from an IR divergence cut off by non-perturbative magnetic effects [100], while the log in (3.105) was also coming from an IR divergence that we regularized by introducing an IR cutoff. It would be interesting to study whether there is a relation between the weakly and strongly coupled descriptions of the IR divergences and the physical interpretation of the IR cutoffs.

### 3.A Normalizing solutions to the wave equation

As explained in subsection 3.2.2 or more generally in subsection 3.2.3, the normalized modes  $\{u_\omega\}$  are proportional to  $f_\omega$  of the form (3.23); namely,  $u_\omega(t, r) \propto e^{-i\omega t} f_\omega(r)$ . Here, we fix the normalization and derive the expansion (3.24) or more generally (3.48).

The analogue of the Klein–Gordon inner product for functions  $f(t, r), g(t, r)$  satisfying the equation of motion (3.43) is [67]

$$(f, g)_\Sigma = -\frac{i}{2\pi\alpha'} \int_\Sigma \sqrt{\tilde{g}} n^\mu G (f \partial_\mu g^* - \partial_\mu f g^*), \quad (3.154)$$

where  $\Sigma$  is a Cauchy surface in the  $t, r$  part of the metric (3.37).  $\tilde{g}$  is the induced metric on  $\Sigma$  and  $n^\mu$  is the future-pointing unit normal to  $\Sigma$ .

We want to normalize  $f_\omega$  using this norm (3.154). In the present case, there is the following simplification to this procedure. Near the horizon  $r \sim r_H$ , the action (3.42) reduces to

$$S_0 \approx \frac{G(r_H)}{4\pi\alpha'} \int dt dr_* [(\partial_t X)^2 - (\partial_{r_*} X)^2]. \quad (3.155)$$



Therefore, in this region and in the tortoise coordinate system,  $X$  is just like a massless Klein–Gordon scalar in flat space. Correspondingly, the contribution to the norm (3.154) from the near horizon region is

$$-\frac{iG(r_H)}{2\pi\alpha'} \int_{r_* \sim -\infty} dr_* (f \partial_t g^* - \partial_t f g^*), \quad (3.156)$$

where as  $\Sigma$  we took the constant  $t$  surface. This is the usual Klein–Gordon inner product for the theory (3.155), up to overall normalization. Of course, there is a contribution to the inner product from regions away from the horizon. However, because the near-horizon region is semi-infinite in the tortoise coordinate  $r_*$  (recall that  $r = r_H$  corresponds to  $r_* = -\infty$ ), the normalization of solutions is completely determined by this region where the inner product is simply (3.156). This means that the canonically normalized mode expansion is given by

$$X(t, r) = \sqrt{\frac{2\pi\alpha'}{G(r_H)}} \int_0^\infty \frac{d\omega}{2\pi} \frac{1}{\sqrt{2\omega}} [f_\omega(r) e^{-i\omega t} a_\omega + f_\omega(r)^* e^{i\omega t} a_\omega^\dagger]. \quad (3.157)$$

where  $f_\omega(r)$  behaves near the horizon as

$$f_\omega(r) \rightarrow e^{i\omega r_*} + e^{i\theta_\omega} e^{-i\omega r_*}, \quad r \rightarrow r_H \quad (r_* \rightarrow -\infty) \quad (3.158)$$

with some  $\theta_\omega \in \mathbb{R}$ . If we can find such  $f_\omega(r)$ , then  $a, a^\dagger$  satisfy the canonically normalized commutation relation (3.16).

### 3.B Low energy solutions to the wave equation

Here, we study the solution to the wave equation (3.14), or more generally (3.43), satisfying an appropriate boundary condition (the Neumann boundary condition (3.17) or normalizable boundary condition at infinity), for very small frequencies  $\omega$ . We see that the solutions become trivial plane waves in the limit.

The general wave equation (3.43) can be written in the frequency space as

$$\left[ \omega^2 + \sqrt{\frac{\hbar_t}{\hbar_r}} \frac{f}{G} \partial_r \left( \sqrt{\frac{\hbar_t}{\hbar_r}} f G \partial_r \right) \right] X_\omega(r) = 0. \quad (3.159)$$

Very close to the horizon, this becomes

$$[\omega^2 + 16\pi^2 T^2 (r - r_H) \partial_r ((r - r_H) \partial_r)] X_\omega(r) = 0. \quad (3.160)$$

This means that the linearly independent solutions are

$$g_{\pm\omega} = \exp \left[ \pm i \frac{\omega}{4\pi T} \log \left( \frac{r - r_H}{L_1} \right) \right] \quad (3.161)$$

where  $L_1$  is a length scale which is arbitrary at this point. The  $\pm$  signs here correspond to outgoing and ingoing waves. We are considering the small  $\omega$  limit but, no matter how small  $\omega$  is, we can always consider a region very close to the horizon so that  $\frac{\omega}{4\pi T} \log\left(\frac{r-r_H}{L_1}\right) = \mathcal{O}(1)$ , namely  $\frac{r-r_H}{L_1} \lesssim e^{-4\pi T/\omega}$ . In such a region, we cannot expand the exponential and should keep the full exponential expression (3.161). In other words, the precise limit we are taking is

$$\omega \rightarrow 0, \quad \frac{\omega}{T} \log\left(\frac{r-r_H}{L_1}\right) : \text{fixed.} \quad (3.162)$$

Now, consider the region not so close to the horizon. For small  $\omega$ , we can ignore the  $\omega^2$  term in (3.159), obtaining

$$X_\omega = B_1 + B_2 \int_\infty^r \frac{dr'}{f(r')G(r')} \sqrt{\frac{h_r(r')}{h_t(r')}} + \mathcal{O}(\omega^2), \quad (3.163)$$

where  $B_1, B_2$  are constant. For  $r \approx r_H$ , this gives

$$X_\omega = B_1 + \frac{B_2}{4\pi T G(r_H)} \log\left(\frac{r-r_H}{L_H}\right) + \mathcal{O}(r-r_H) \quad (r \sim r_H). \quad (3.164)$$

Here, we defined the constant  $L_H$  by

$$\int_\infty^r \frac{dr}{fG} \sqrt{\frac{h_r}{h_t}} = \frac{1}{4\pi T G(r_H)} \log\left(\frac{r-r_H}{L_H}\right) + \mathcal{O}(r-r_H). \quad (3.165)$$

Because it will turn out to be convenient to choose  $L_H = L_1$ , we will set  $L_H = L_1$  henceforth. On the other hand, for large  $r$ , (3.163) gives (assuming the large  $r$  behavior (3.40), (3.41) of functions  $h_t, h_r, G$ ),

$$X_\omega = B_1 - \frac{B_2}{3r^3} + \mathcal{O}(\omega^2). \quad (3.166)$$

We can determine  $B_1, B_2$  by comparing these small-frequency solutions between the very-near-horizon region and the not-so-near-horizon region. For small frequencies  $\omega$ , (3.161) becomes

$$X_\omega \approx 1 \pm i \frac{\omega}{4\pi T} \log\left(\frac{r-r_H}{L_H}\right) + \mathcal{O}(\omega^2). \quad (3.167)$$

Comparing this with (3.164), we determine

$$B_1 = 1 + \mathcal{O}(\omega^2), \quad B_2 = \pm i\omega G(r_H) + \mathcal{O}(\omega^2). \quad (3.168)$$

Therefore, the linearly independent (outgoing/ingoing) solutions are

$$g_{\pm\omega}(r) = \begin{cases} \exp\left[\pm i \frac{\omega}{4\pi T} \log\left(\frac{r-r_H}{L_H}\right)\right] & r \sim r_H \\ 1 \pm \frac{i\omega G(r_H)}{3r^3} & r \gg r_H \end{cases} \quad (3.169)$$

The general solution  $X_\omega$  is given by the linear combination of the outgoing and ingoing solutions  $g_{\pm\omega}$ . If we want to construct a normalizable solution that vanishes as  $r \rightarrow \infty$  then, from the  $r \gg r_H$  behavior of (3.169), the linear combination to take is

$$X_\omega^{(\text{norm})} = g_\omega - g_{-\omega}. \quad (3.170)$$

If we did not take  $L_1 = L_H$ , the two terms would be multiplied by  $\exp[\mp i \frac{\omega}{4\pi T} \log(\frac{L_H}{L_1})]$  respectively. Note that our expressions are correct up to  $\mathcal{O}(\omega^2)$  terms. The near-horizon behavior of this is

$$X_\omega^{(\text{norm})} \approx \exp\left[i \frac{\omega}{4\pi T} \log\left(\frac{r - r_H}{L_H}\right)\right] - \exp\left[-i \frac{\omega}{4\pi T} \log\left(\frac{r - r_H}{L_H}\right)\right]. \quad (3.171)$$

Therefore, if define the tortoise coordinate  $r_*$  to have the following behavior the horizon:

$$r_* \approx \frac{1}{4\pi T} \log\left(\frac{r - r_H}{L_H}\right) \quad (3.172)$$

then the near-horizon behavior (3.171) simply becomes

$$X_\omega^{(\text{norm})} \approx e^{i\omega r_*} - e^{-i\omega r_*} \quad (r \approx r_H). \quad (3.173)$$

Let us elaborate on this point slightly more. In the near horizon region, in general we can have

$$X_\omega^{(\text{norm})} \approx e^{i\omega r_*} - e^{i\alpha_\omega} e^{-i\omega r_*}. \quad (3.174)$$

where  $\alpha_\omega$  is some phase. The fact that (3.173) is correct up to  $\mathcal{O}(\omega)$  means is that, if we take  $r_*$  to be given by (3.172), then  $\alpha_\omega = \mathcal{O}(\omega^2)$  as  $\omega \rightarrow 0$ . In particular, unless we choose  $L_H$  to be the one given by (3.165), the  $\omega \rightarrow 0$  behavior of  $\alpha_\omega$  will contain an  $\mathcal{O}(\omega)$  term.

Next, let us consider imposing a Neumann boundary condition  $\partial_r X = 0$  at  $r = r_c \gg r_H$  instead. Set the general solution to be

$$X_\omega = g_\omega + C g_{-\omega}. \quad (3.175)$$

then the Neumann boundary condition  $X'_\omega(r_c) = 0$  gives

$$C = -\frac{g'_\omega(r_c)}{g'_{-\omega}(r_c)} = -\frac{-\frac{i\omega G(r_H)}{r_c^4} + \mathcal{O}(\omega^2)}{\frac{i\omega G(r_H)}{r_c^4} + \mathcal{O}(\omega^2)} = 1 + \mathcal{O}(\omega), \quad (3.176)$$

where we used the second equation in (3.169). Comparing this result with (3.22) and (3.25), we find that the modes  $f_\omega$  satisfying the Neumann boundary condition are given by, at low frequencies,

$$g_\omega(r) = e^{i\omega r_*}, \quad \theta_\omega = 0, \quad f_\omega(r) = e^{i\omega r_*} + e^{-i\omega r_*}. \quad (3.177)$$

This is consistent with the explicit result for AdS<sub>3</sub> in (3.31), (3.33). So, for very small  $\omega$ , the solution  $f_\omega(r)$  is a simple sum of outgoing and ingoing waves, which are just plane waves.<sup>13</sup> Because  $g_\pm(r) \rightarrow 1$  as  $r \rightarrow \infty$ , we have

$$f_\omega(r = r_c) \approx 2. \quad (3.178)$$

Because of the  $\mathcal{O}(\omega)$  ambiguity in (3.176),  $\theta_\omega = \mathcal{O}(\omega)$  as  $\omega \rightarrow 0$  (cf. comments below (3.174)).

In the tortoise coordinate, the limit (3.162) we are taking can be written as

$$\omega \rightarrow 0, \quad \beta, \omega r_* : \text{fixed}. \quad (3.179)$$

### 3.C Various propagators and their low frequency limit

The quadratic action for a string embedded in the AdS<sub>d</sub> black hole spacetime

$$ds^2 = -h_t(r)f(r)dt^2 + \frac{h_r(r)}{f(r)}dr^2 + G(r)dX^2, \quad (3.180)$$

(Eq. (3.37)) is given by

$$S_0 = \frac{1}{4\pi\alpha'} \int dt dr \left[ \sqrt{\frac{h_r}{h_t}} \frac{G}{f} (\partial_t X)^2 - \sqrt{\frac{h_t}{h_r}} G f (\partial_r X)^2 \right]. \quad (3.181)$$

We would like to regard this system as a thermal field theory at temperature  $T$ , and derive the relation among various propagators (Green functions) and the solutions to the wave equation. We present the result for the general metric (3.37), but if one wants the results for the simpler neutral case (3.11), set  $f = r^2 h$ ,  $h_t = h_r = 1$ ,  $G = r^2$ .

Let us define Wightman, Feynman, retarded, and advanced propagators as

$$\begin{aligned} D_W(t - t', r, r') &= \langle X(t, r) X(t', r') \rangle, \\ D_F(t - t', r, r') &= \langle \mathcal{T}[X(t, r) X(t', r')] \rangle, \\ D_{\text{Ret}}(t - t', r, r') &= \theta(t - t') \langle [X(t, r), X(t', r')] \rangle, \\ D_{\text{Adv}}(t - t', r, r') &= -\theta(t' - t) \langle [X(t, r), X(t', r')] \rangle. \end{aligned} \quad (3.182)$$

We impose a Neumann boundary condition for  $X(r, t)$  at  $r = r_c$ , so the propagators satisfy the same Neumann boundary condition. Using the wave equation

$$\left[ -\frac{G}{h_t f} \partial_t^2 + \frac{1}{\sqrt{h_t h_r}} \partial_r \left( \sqrt{\frac{h_t}{h_r}} G f \partial_r \right) \right] X = 0 \quad (3.183)$$

<sup>13</sup>For related observations on the triviality of the solution in the low frequency limit, see [101].

and the canonical commutation relation

$$[X(t, r), \partial_t X(t, r')] = 2\pi i \alpha' \sqrt{\frac{\hbar_t}{\hbar_r}} \frac{f}{G} \delta(r - r'), \quad (3.184)$$

we can show that these propagators satisfy

$$\left[ -\frac{G}{\hbar_t f} \partial_t^2 + \frac{1}{\sqrt{\hbar_t \hbar_r}} \partial_r \left( \sqrt{\frac{\hbar_t}{\hbar_r}} G f \partial_r \right) \right] D_W(t - t', r, r') = 0, \quad (3.185)$$

$$\left[ -\frac{G}{\hbar_t f} \partial_t^2 + \frac{1}{\sqrt{\hbar_t \hbar_r}} \partial_r \left( \sqrt{\frac{\hbar_t}{\hbar_r}} G f \partial_r \right) \right] D_I(t - t', r, r') = \frac{2\pi i \alpha'}{\sqrt{-g}} \delta(t - t') \delta(r - r'), \quad (3.186)$$

with  $I = F, \text{Ret}, \text{Adv}$  and  $\sqrt{-g} = \sqrt{\hbar_t \hbar_r}$ .

As in (3.157), the field  $X$  can be expanded as

$$X(t, r) = \sqrt{\frac{2\pi\alpha'}{G(r_H)}} \int_0^\infty \frac{d\omega}{2\pi} \frac{1}{\sqrt{2\omega}} [f_\omega(r) e^{-i\omega t} a_\omega + f_\omega(r)^* e^{i\omega t} a_\omega^\dagger], \quad (3.187)$$

where

$$f_\omega(r) = g_\omega(r) + e^{i\theta_\omega} g_{-\omega}(r) \quad (3.188)$$

and  $g_\omega(r)$  behaves near the horizon as

$$g_\omega(r) \approx e^{i\omega r^*} \quad (r \sim r_H). \quad (3.189)$$

The phase  $\theta_\omega$  is determined by the Neumann boundary condition at  $r = r_c$  that  $f_\omega$  satisfies. Since the system is at temperature  $T$ , the expectation value of  $a, a^\dagger$  is given by (3.26). It is then easy to show that the Wightman propagator can be written as

$$D_W(\omega, r, r') = \frac{2\pi\alpha'}{G(r_H)} \frac{f_\omega(r) f_{-\omega}(r')}{2\omega(1 - e^{-\beta\omega})}, \quad (3.190)$$

where  $f_{-\omega} = f_\omega^*$ .

We would like to express other propagators  $D_{\text{Adv}, \text{Ret}, F}$  in terms of  $f_\omega, g_\omega$ . Note that

$$D_F(\omega, r, r') = D_W(\omega, r, r') + D_{\text{Adv}}(\omega, r, r') = D_W(-\omega, r', r) + D_{\text{Ret}}(\omega, r, r'). \quad (3.191)$$

Because we have already obtained  $D_W$  in (3.190), if we know one of  $D_F, D_{\text{Ret}}$ , and  $D_{\text{Adv}}$ , we can obtain all other propagators. Here, let us consider  $D_{\text{Adv}}$ . From (3.186),  $D_{\text{Adv}}(\omega, r, r')$  should satisfy

$$\left[ \frac{G}{\hbar_t f} \omega^2 + \frac{1}{\sqrt{\hbar_t \hbar_r}} \partial_r \left( \sqrt{\frac{\hbar_t}{\hbar_r}} G f \partial_r \right) \right] D_{\text{Adv}}(\omega, r, r') = \frac{2\pi i \alpha'}{\sqrt{-g}} \delta(r - r'). \quad (3.192)$$

If  $r \neq r'$ , this is the same as the wave equation that  $f_\omega, g_\omega$  satisfy. Therefore, take the ansatz

$$D_{Adv}(\omega, r, r') = A[\theta(r - r')g_\omega(r')f_\omega(r) + \theta(r' - r)g_\omega(r)f_\omega(r')]. \quad (3.193)$$

This satisfies the correct boundary condition (Neumann) at  $r, r' = r_c$  and furthermore satisfies the purely outgoing boundary condition at the horizon, which is appropriate for an advanced correlator. Using the fact that both  $f, g$  satisfy the wave equation, we find

$$\left[ \frac{G}{h_t f} \omega^2 + \frac{1}{\sqrt{h_t h_r}} \partial_r \left( \sqrt{\frac{h_t}{h_r}} G f \partial_r \right) \right] D_{Adv} = \frac{A \delta(r - r')}{h_r} G f (g_\omega \partial_r f_\omega - \partial_r g_\omega f_\omega). \quad (3.194)$$

Therefore,

$$A = 2\pi i \alpha' \sqrt{\frac{h_r}{h_t}} \frac{1}{G f} \frac{1}{g_\omega \partial_r f_\omega - \partial_r g_\omega f_\omega} = \frac{2\pi i \alpha'}{G(r_H) (g_\omega \partial_{r_*} f_\omega - \partial_{r_*} g_\omega f_\omega)}. \quad (3.195)$$

Using the wave equation for  $f_\omega, g_\omega$ , it is easy to show that this expression does not depend on  $r$ . By taking  $r \rightarrow r_H$  and using (3.188), (3.189),

$$A = -\frac{\pi \alpha' e^{-i\theta_\omega}}{G(r_H) \omega}. \quad (3.196)$$

So, the advanced propagator is given by

$$D_{Adv}(\omega, r, r') = -\frac{\pi \alpha' e^{-i\theta_\omega}}{G(r_H) \omega} [\theta(r - r')g_\omega(r')f_\omega(r) + \theta(r' - r)g_\omega(r)f_\omega(r')]. \quad (3.197)$$

In the low frequency limit, the expressions for the propagators simplify, as we saw in Appendix 3.B. The precise limit we are considering is (3.179). First, the Wightman propagator (3.190) becomes, because of (3.177),

$$D_W(\omega, r, r') = \frac{\pi \alpha'}{G(r_H)} \frac{(e^{i\omega r_*} + e^{-i\omega r_*})(e^{i\omega r'_*} + e^{-i\omega r'_*})}{\omega(1 - e^{-\beta\omega})} \quad (\text{small } \omega). \quad (3.198)$$

Similarly, the advanced propagator (3.197) becomes

$$\begin{aligned} D_{Adv}(\omega, r, r') &= -\frac{\pi \alpha'}{G(r_H) \omega} \left[ \theta(r_* - r'_*) e^{i\omega r'_*} (e^{i\omega r_*} + e^{-i\omega r_*}) \right. \\ &\quad \left. + \theta(r'_* - r_*) e^{i\omega r_*} (e^{i\omega r'_*} + e^{-i\omega r'_*}) \right] \\ &= -\frac{\pi \alpha'}{G(r_H)} \frac{e^{i\omega(r_* + r'_*)} + e^{-i\omega|r_* - r'_*|}}{\omega} \quad (\text{small } \omega). \end{aligned} \quad (3.199)$$

Using the relation (3.191), the Feynman propagator is

$$D_F(\omega, r, r') = \frac{\pi\alpha'}{G(r_H)} \left[ \frac{(e^{i\omega r_*} + e^{-i\omega r_*})(e^{i\omega r'_*} + e^{-i\omega r'_*})}{\omega(1 - e^{-\beta\omega})} - \frac{e^{i\omega(r_*+r'_*)} + e^{-i\omega|r_*-r'_*|}}{\omega} \right] \quad (\text{small } \omega). \quad (3.200)$$

In particular, consider the case where one of the points is at the UV cutoff,  $r' = r_c$ . From (3.178), we have

$$D_F(\omega, r, r_c) = \frac{2\pi\alpha'}{G(r_H)} \left[ \frac{e^{i\omega r_*} + e^{-i\omega r_*}}{\omega(1 - e^{-\beta\omega})} - \frac{e^{i\omega r_*}}{\omega} \right], \quad (3.201)$$

$$D_W(\omega, r, r_c) = \frac{2\pi\alpha'}{G(r_H)} \frac{e^{i\omega r_*} + e^{-i\omega r_*}}{\omega(1 - e^{-\beta\omega})}.$$

### 3.D Holographic renormalization and Lorentzian AdS/CFT

In this Appendix, we discuss how to compute correlation function using the AdS/CFT dictionary for the total force  $F$  which is dual to the worldsheet field  $X$ . As we explained in subsection 3.4.2, this involves holographic renormalization of the worldsheet action. Furthermore, if we want to compute real time correlation functions in a black hole (finite temperature) geometry, we should apply the rules of Lorentzian AdS/CFT [73, 74], see section 1.7.2.

#### 3.D.1 Holographic renormalization

First, let us consider the holographic renormalization of the worldsheet action. For this, only the asymptotic behavior of the action near the boundary is relevant. Therefore, as the background geometry, we can consider the Poincaré AdS geometry obtained by setting  $T = 0$  (3.11):

$$ds^2 = -r dt^2 + \frac{dr^2}{r^2} + r^2(dX^I)^2. \quad (3.202)$$

for which the worldsheet action becomes

$$S_{\text{bare}} = S_0 + S_{\text{int}}, \quad (3.203)$$

$$S_0 = \frac{1}{4\pi\alpha'} \int_{\Sigma} dt dr (\dot{X}^2 - r^4 X'^2), \quad S_{\text{int}} = \frac{1}{16\pi\alpha'} \int_{\Sigma} dt dr (\dot{X}^2 - r^4 X'^2)^2. \quad (3.204)$$

Here, we considered only one of the polarizations, say  $X^1$ , and denoted it by  $X$ .  $\Sigma$  is the worldsheet,

$$\Sigma = \{(t, r) \mid t \in \mathbb{R}, 0 \leq r \leq r_c\}, \quad (3.205)$$

and  $\dot{\phantom{x}} = \partial_t$ ,  $\prime = \partial_r$ .  $r_c$  is a UV cutoff. For computational convenience, let us rescale  $X \rightarrow \sqrt{2\pi\alpha'} X$  and set  $\kappa = \pi\alpha'$ , so that

$$S_0 = \frac{1}{2} \int_{\Sigma} dt dr (\dot{X}^2 - r^4 X'^2), \quad S_{\text{int}} = \frac{\kappa}{4} \int_{\Sigma} dt dr (\dot{X}^2 - r^4 X'^2)^2. \quad (3.206)$$

The equation of motion is

$$-\partial_t^2 X + \partial_r(r^4 \partial_r X) = \kappa[-\partial_t(H \partial_t X) + \partial_r(H r^4 \partial_r X)], \quad H \equiv -\dot{X}^2 + r^4 X'^2. \quad (3.207)$$

Let us solve the equation of motion (3.207) by expanding  $X(t, r)$  in the coupling  $\kappa$  as

$$X(t, r) = Y(t, r) + \kappa Z(t, r) + \mathcal{O}(\kappa^2) \quad (3.208)$$

and furthermore expanding  $Y, Z$  around  $r = \infty$  as

$$\begin{aligned} Y(t, r) &= y_{(0)}(t) + \frac{y_{(1)}(t)}{r} + \frac{y_{(2)}(t)}{r^2} + \frac{y_{(3)}(t)}{r^3} + \dots, \\ Z(t, r) &= z_{(0)}(t) + \frac{z_{(1)}(t)}{r} + \frac{z_{(2)}(t)}{r^2} + \frac{z_{(3)}(t)}{r^3} + \dots. \end{aligned} \quad (3.209)$$

Henceforth, we will ignore quantities of  $\mathcal{O}(\kappa^2)$ . The expansion for  $X$  itself is

$$X(t, r) = x_{(0)}(t) + \frac{x_{(1)}(t)}{r} + \frac{x_{(2)}(t)}{r^2} + \frac{x_{(3)}(t)}{r^3} + \dots, \quad x_{(i)} = y_{(i)} + \kappa z_{(i)}. \quad (3.210)$$

By substituting this expansion into (3.207) and comparing coefficients, one readily finds that the following is a solution:

$$y_{(0)} = \text{any} \equiv J, \quad y_{(1)} = 0, \quad y_{(2)} = -\frac{1}{2}\ddot{J}, \quad y_{(3)} = \text{any}, \quad (3.211a)$$

$$z_{(0)} = 0, \quad z_{(1)} = 0, \quad z_{(2)} = -j^2 \ddot{J}, \quad z_{(3)} = \text{any}. \quad (3.211b)$$

The expression for  $X$  is

$$x_{(0)} = J, \quad x_{(1)} = 0, \quad x_{(2)} = -\frac{1}{2}\ddot{J} - \kappa j^2 \ddot{J}, \quad x_{(3)} = \text{any}. \quad (3.212)$$

Note that  $X(r, t) \rightarrow J(t)$  as  $r \rightarrow \infty$ ; namely,  $J$  is the non-normalizable mode which can be thought of as a source for the dual operator  $\mathcal{O}_X = F$  on the



boundary. On the other hand,  $x_{(3)}$  is the normalizable mode which roughly corresponds to the expectation value of the operator  $F$ . We will make this latter statement more precise below.

If we plug the solution (3.212) into the action (3.206), we obtain the following on-shell action:

$$\begin{aligned}
 S_{\text{bare,on-shell}} &= \frac{\kappa}{2} \int_{\Sigma} d^2x J J^2 \ddot{J} + \int_{\partial\Sigma} dt \left[ \left( -\frac{1}{2} r J \ddot{J} - \kappa r J J^2 \ddot{J} \right) - \frac{\kappa}{4} r J J^2 \ddot{J} \right] \\
 &\sim \int_{\partial\Sigma} dt \left[ -\frac{1}{2} r J \ddot{J} - \frac{3\kappa}{4} r J J^2 \ddot{J} \right] + (\text{finite}) \\
 &\sim \int_{\partial\Sigma} dt \left[ \frac{1}{2} r J^2 + \frac{\kappa}{4} J^4 \right] + (\text{finite}). \tag{3.213}
 \end{aligned}$$

In going to the second line we performed the  $r$  integration, and in going to the last line we integrated by parts. This is divergent, but the divergence can be canceled by introducing the following counter terms:

$$S_{\text{ct}} = \int_{\partial\Sigma} dt \sqrt{-\gamma} \left[ \frac{1}{2} r^2 (\nabla_{\gamma} X)^2 - \frac{\kappa}{4} (r^2 (\nabla_{\gamma} X)^2)^2 \right], \tag{3.214}$$

where  $\square_{\gamma} = -\frac{1}{r^2} \partial_t^2$  is the Laplacian for the metric  $\gamma$  induced on the boundary  $r = r_c$ . Likewise,  $(\nabla_{\gamma} X)^2 = -\frac{1}{r^2} (\partial_t X)^2$ . If we define the metric  $\gamma'$  induced on the boundary of the worldsheet at  $r$ , then  $\gamma'_{tt} = -r^2(1 - \dot{X}^2)$  and  $\int dt \sqrt{-\gamma'_{tt}}$  reproduces (3.214) (also recall that we have rescaled  $X \rightarrow \sqrt{2\pi\alpha'} X$ ).

To remove the divergence from the “bare” action (3.206), we take  $S_{\text{ren}} = S_{\text{bare}} + S_{\text{ct}}$  as our total action. The on-shell variation of this total action evaluates to

$$\begin{aligned}
 \delta S_{\text{ren,on-shell}} &= \int_{\partial\Sigma} dt \sqrt{-\gamma} \left( \kappa r^4 [(\nabla X)^2 \partial_n X + 3(\nabla_{\gamma} X)^2 \square_{\gamma} X] \right. \\
 &\quad \left. - r^2 (\partial_n X + \square_{\gamma} X) \right) \delta X, \tag{3.215}
 \end{aligned}$$

where  $\partial_n$  is the normal derivative with respect to the worldsheet boundary  $\partial\Sigma$ . Therefore,

$$\begin{aligned}
 \frac{\delta S_{\text{ren,on-shell}}}{\delta J} &= \sqrt{-\gamma} \left( -G(\partial_n X + \square_{\gamma} X) + \kappa G^2 [(\nabla X)^2 \partial_n X + 3(\nabla_{\gamma} X)^2 \square_{\gamma} X] \right) \\
 &= 3x_{(3)}(1 + \kappa J^2) + \mathcal{O}(1/r). \tag{3.216}
 \end{aligned}$$

In the second equality, we plugged in the explicit expansion (3.212). Therefore, by the GKPW rule as in section 1.4.1, the expectation value of the operator  $\mathcal{O}_X = F$  dual to  $X$  in the presence of source  $x_{(0)} \equiv J$  is given by, up to  $\mathcal{O}(\kappa^2)$  terms,

$$\langle F \rangle_J = 3x_{(3)}(1 + \kappa J^2) = 3y_{(3)} + 3\kappa \left( z_{(3)} + y_{(3)} J^2 \right). \tag{3.217}$$

The  $j^2$  term may appear strange, but we will see that this term gets canceled in the final expression for the 4-point function. Actually, there is a further contribution to (3.217), but we will discuss it later (see below (3.241)).

Although our discussion above was based on the pure AdS space (3.202) for the simplicity of the argument, the final expression (3.217) is valid for general asymptotically AdS space, including the AdS black hole (3.11). Below, we will use (3.217) to compute correlation functions for the AdS black hole background (3.11).

### 3.D.2 Propagators and correlators

To compute the expectation value  $\langle F \rangle_J$  using the formula (3.217), we need to know  $x_{(3)} = y_{(3)} + \kappa z_{(3)} + \mathcal{O}(\kappa^2)$ . This can be determined if we know the propagators that satisfy appropriate boundary conditions in the inside of the AdS space as we discuss below.

If we substitute the expansion (3.208) into the wave equation (3.14) and compare the coefficients, we obtain

$$[-h^{-1}\partial_t^2 + \partial_r(r^4 h \partial_r)]Y = 0, \quad (3.218a)$$

$$[-h^{-1}\partial_t^2 + \partial_r(r^4 h \partial_r)]Z = \rho, \quad (3.218b)$$

where we are now considering the AdS black hole spacetime (3.11) and the “source”  $\rho$  is defined by

$$\rho \equiv -\partial_t(H_0 h^{-1} \partial_t Y) + \partial_r(H_0 r^4 h \partial_r Y), \quad H_0 \equiv -h^{-1}(\partial_t Y)^2 + r^4 h (\partial_r Y)^2. \quad (3.219)$$

We solve (3.218a) under the asymptotic condition  $Y(r, t) \rightarrow J(t)$  as  $r \rightarrow \infty$  and (3.218b) under the condition  $Z(r, t) \rightarrow 0$  as  $r \rightarrow \infty$ . Let us solve these using propagators. First, let  $K(r, t|t')$  be the boundary-bulk propagator, namely the solution to the zeroth-order wave equation (3.218a) satisfying the boundary condition

$$K(r, t|t') \rightarrow \delta(t - t') \quad \text{as } r \rightarrow \infty. \quad (3.220)$$

Then the solution to (3.218a) is

$$Y(t, r) = \int dt' K(r, t|t') J(t'). \quad (3.221)$$

From this, we can read off  $y_{(3)}$  as

$$y_{(3)}(t) = \int dt' [K(r, t|t')]_{r^{-3}} J(t'). \quad (3.222)$$

where  $[\ ]_{r^{-3}}$  means to take the coefficient of the  $r^{-3}$  term in the  $1/r$  expansion.

Let us move on to the next order equation (3.218b) to determine  $z_{(3)}$ . Let  $D(r, t|r', t')$  be the bulk propagator, namely the solution to

$$[-h^{-1}\partial_t^2 + \partial_r(r^4 h \partial_r)]D(t, r|t', r') = \delta(t - t')\delta(r - r') \quad (3.223)$$

that vanishes as  $r, r' \rightarrow \infty$ . Then the solution to the next order equation (3.218b) can be written as

$$Z(t, r) = \int dt' dr' D(t, r|t', r')\rho(t', r'). \quad (3.224)$$

It is easy to see that the  $Z$  given by (3.224) has the expected behavior (3.211b). To see it, let us explicitly construct the bulk propagator satisfying (3.223), or in the frequency space,

$$[h^{-1}\omega^2 + \partial_r(r^4 h \partial_r)]D(\omega, r, r') = \delta(r - r'). \quad (3.225)$$

The solution to this can be constructed<sup>14</sup> from the solution to (3.218a), which can be written in the frequency space as

$$[h^{-1}\omega^2 + \partial_r(r^4 h \partial_r)]Y_\omega = 0. \quad (3.226)$$

As discussed above the equation (3.19), this wave equation (3.226) has two solutions; let us denote them by  $\phi_{\pm\omega}(r)$ .<sup>15</sup> These are related to each other by  $\phi_\omega(r)^* = \phi_{-\omega}(r)$ . As one can see from (3.211a), we can take them to have the following large  $r$  expansion:

$$\phi_{\pm\omega}(r) = 1 + \frac{\omega^2}{r^2} + \frac{c_{\pm\omega}}{r^3} + \dots, \quad (3.227)$$

where  $c_{\pm\omega}$  are some constants ( $c_\omega^* = c_{-\omega}$ ). For example, in the AdS<sub>3</sub> case ( $d = 3$ ),

$$\phi_{\pm\omega}(r) = \left(1 \pm \frac{i\omega}{r}\right) \left(\frac{r - r_H}{r + r_H}\right)^{i\omega/2r_H} = 1 + \frac{\omega^2}{2r^2} \mp \frac{i\omega(r_H^2 + \omega^2)}{3r^3} + \dots \quad (3.228)$$

For  $r \neq r'$ , the equation (3.225) is the same as (3.226) and therefore  $D(\omega, r, r')$  is given by a linear combination of  $\phi_\omega(r)$  and  $\phi_{-\omega}(r)$ . Taking into account the  $r \leftrightarrow r'$  symmetry, the bulk propagator  $D$  can be written as

$$D(\omega, r, r') = A \left[ \phi_\omega^>(r)\phi_\omega^<(r')\theta(r - r') + \phi_\omega^>(r')\phi_\omega^<(r)\theta(r' - r) \right]. \quad (3.229)$$

<sup>14</sup>The following argument is analogous to the one given around (3.192).

<sup>15</sup> $\phi_{\pm\omega}(r)$  are different from  $g_{\pm\omega}(r)$  defined around (3.19) only by normalization;  $\phi_{\pm\omega}(r) \rightarrow 1$  as  $r \rightarrow \infty$ , while  $g_{\pm\omega}(r) \rightarrow e^{\pm i\omega r_*}$  as  $r \rightarrow r_c$  ( $r_* \rightarrow -\infty$ ). These agree in the small  $\omega$  limit.

Here  $A$  is constant and we defined

$$\begin{aligned}\phi_\omega^>(r) &\equiv \phi_\omega(r) - \phi_{-\omega}(r) = \frac{c_\omega - c_{-\omega}}{r^3} + \mathcal{O}(r^{-4}), \\ \phi_\omega^<(r) &\equiv \alpha\phi_\omega(r) + (1 - \alpha)\phi_{-\omega}(r) = 1 + \frac{\omega^2}{2r^2} + \frac{\alpha c_\omega + (1 - \alpha)c_{-\omega}}{r^3} + \mathcal{O}(r^{-4}).\end{aligned}\tag{3.230}$$

The fact that  $\phi_\omega^>(r) \rightarrow 0$  as  $r \rightarrow 0$  correctly gives the asymptotic condition for  $D$ , namely  $D \rightarrow 0$  as  $r, r' \rightarrow \infty$ . On the other hand, we do not specify the boundary condition of  $D$  as  $r, r' \rightarrow r_H$ . The unknown number  $\alpha$  parametrizes possible boundary conditions which is to be determined by some physical requirement. But we leave  $\alpha$  arbitrary and therefore (3.229) is valid regardless of the boundary condition. Because  $\phi_\omega^<(r) \rightarrow 1$  as  $r \rightarrow \infty$ , it is actually equal to the bulk-boundary propagator in the frequency space;

$$\phi_\omega^<(r) = K(\omega, r).\tag{3.231}$$

By substituting (3.229) into the equation (3.225), we obtain

$$A = \frac{1}{r^4 h[\phi_\omega^>(\partial_r \phi_\omega^<) - (\partial_r \phi_\omega^>) \phi_\omega^<]}\tag{3.232}$$

(this is the same as (3.195)). Since this does not depend on  $r$  (see below (3.195)), by taking  $r \rightarrow \infty$  and using the asymptotic behavior (3.230), we find  $A = (c_\omega - c_{-\omega})^{-1}$ . Therefore, the bulk propagator is found to be

$$D(\omega, r, r') = (c_\omega - c_{-\omega})^{-1} [\phi_\omega^>(r)\phi_\omega^<(r')\theta(r - r') + \phi_\omega^>(r')\phi_\omega^<(r)\theta(r' - r)],\tag{3.233}$$

where we used (3.231). The  $r \rightarrow \infty$  behavior of this is, using the asymptotic behavior (3.230),

$$D(\omega, r, r') = -\frac{1}{3r^3}K(\omega, r')\theta(r - r') - \frac{1}{3r'^3}\theta(r' - r) + \mathcal{O}(r^{-4}) \quad (r \rightarrow \infty).\tag{3.234}$$

Using (3.211a), we can show that the source  $\rho$  (defined in Eq. (3.219)) goes as  $\rho = 2\dot{J}^2\ddot{J} + \mathcal{O}(r^{-2})$ . Then, from (3.224) and (3.234) we can read off  $z_{(3)}$  as follows:

$$z_{(3)}(t) = \lim_{r \rightarrow \infty} \left[ -\frac{1}{3} \int_{r_H}^r dt' dr' K(t', r'|t) \rho(t', r') + \frac{2}{3} r \dot{J}(t)^2 \ddot{J}(t) \right].\tag{3.235}$$

The second term cancels the divergent contribution corresponding to  $z_{(2)}$  in (3.211b).

So, we succeeded in expressing  $y_{(3)}, z_{(3)}$  appearing in the formula (3.217) using propagators; the resulting expressions are (3.222) and (3.235). Using

these, we can compute the boundary correlators for  $F$ . First, at the first order in  $\kappa$  that we are working in, the 2-point function gets contribution only from  $y_{(3)}$  in (3.222) and

$$\langle \mathcal{T}[F(t_1)F(t_2)] \rangle = \frac{\delta}{\delta J(t_2)} \langle F(t_1) \rangle \Big|_{J=0} = 3 \frac{\delta}{\delta J(t_2)} y_{(3)}(t_1) = 3[K(t_1, r|t_2)]|_{r=3}. \quad (3.236)$$

In the frequency space,

$$\langle F(\omega_1)F(\omega_2) \rangle = 2\pi\delta(\omega_1 + \omega_2) 3K(\omega_2, r)|_{r=3}. \quad (3.237)$$

To obtain 4-point functions, we take functional derivatives of (3.217) three times. Therefore, only the second term  $3\kappa(z_{(3)} + y_{(3)}\dot{J}^2)$  in (3.217) is relevant for the computation. Let us write the source  $\rho$  appearing in (3.235) as

$$\rho = \partial_t \rho^t + \partial_r \rho^r, \quad \rho^t \equiv -H_0 h^{-1} \partial_t Y, \quad \rho^r \equiv H_0 r^4 h \partial_r Y. \quad (3.238)$$

Then, by partial integration, (3.235) becomes

$$\begin{aligned} z_{(3)}(t) = \lim_{r \rightarrow \infty} \left\{ \frac{1}{3} \int_{r_H}^r dt' dr' \left[ \rho^t(t', r') \partial_{t'} K(t', r'|t) + \rho^r(t', r') \partial_{r'} K(t', r'|t) \right] \right. \\ \left. - \frac{1}{3} \int dt' \left[ K(t', r|t) \rho^r(t', r) - K(t', r_H|t) \rho^r(t', r_H) \right] \right. \\ \left. + \frac{2}{3} r \dot{J}(t)^2 \ddot{J}(t) \right\}. \quad (3.239) \end{aligned}$$

We dropped the boundary terms at  $t = \pm\infty$ . The first term in the second line can be evaluated using the expansion

$$K(t', r|t) = \delta(t - t') + \mathcal{O}(r^{-2}), \quad \rho^r(t, r) = r \dot{J}^2 \ddot{J} + 3y_{(3)} \dot{J}^2 + \mathcal{O}(r^{-1}). \quad (3.240)$$

As a result, in the combination appearing in (3.217), the term involving  $y_{(3)} \dot{J}^2$  cancels out:

$$\begin{aligned} 3\kappa \left[ z_{(3)}(t) + y_{(3)}(t) \dot{J}(t)^2 \right] = \kappa \lim_{r \rightarrow \infty} \left\{ \int_{r_H}^r dt' dr' \left[ \rho^t(t', r') \partial_{t'} K(t', r'|t) \right. \right. \\ \left. \left. + \rho^r(t', r') \partial_{r'} K(t', r'|t) \right] \right. \\ \left. + \int dt' K(t', r_H|t) \rho^r(t', r_H) + r \partial_t [\dot{J}(t)^3] \right\}. \quad (3.241) \end{aligned}$$

The second last term in (3.241) gets canceled by the extra contribution alluded to below (3.217). Let us now discuss what this extra contribution is. The on-shell variation of the action, which we used to compute the expectation value

$\langle F \rangle_J$ , is given by (3.215). Because we are regarding the region  $r_H \leq r \leq r_c$  as our spacetime, there actually is contribution from the “boundary”  $r = r_H$  to this expression. In the AdS black hole spacetime, this extra contribution to  $\delta S_{\text{ren,on-shell}}$  becomes

$$\delta S_{\text{ren,on-shell}} \supset - \int_{r=r_H} dt r^4 h (\partial_r Y + \kappa H_0 \partial_r Y) \delta Y, \quad (3.242)$$

where we dropped  $\mathcal{O}(\kappa^2)$  terms and “ $\supset$ ” means that the left hand side includes the expression on the right hand side. Note that, because the counter term  $S_{\text{ct}}$  (3.214) was added only for the boundary at infinity, the second and the fourth terms in (3.215) did not contribute to this expression. Since  $h \rightarrow 0$  as  $r \rightarrow r_H$ , this becomes

$$\delta S_{\text{ren,on-shell}} \supset -\kappa \int_{r=r_H} dt r^4 h H_0 \partial_r Y \delta Y \quad (3.243)$$

(note that  $H_0$  involves  $h^{-1}$ ). Therefore, by taking functional derivative, we find that there is the following extra contribution to  $\langle F \rangle_J$ :

$$\langle F(t) \rangle_J = \frac{\delta S_{\text{ren,on-shell}}}{\delta J(t)} \supset -\kappa \int_{r'=r_H} dt' r'^4 h H_0 \partial_r Y K(t', r'|t). \quad (3.244)$$

This precisely cancels the second last term in (3.241). Therefore, the terms relevant for computing 4-point functions is

$$\begin{aligned} \langle F(t) \rangle_J \supset \kappa \lim_{r \rightarrow \infty} \left\{ \int_{r_H}^r dt' dr' \left[ j_t(t', r') \partial_{t'} K(t', r'|t) + j_r(t', r') \partial_{r'} K(t', r'|t) \right] \right. \\ \left. + r \partial_t [J(t)^3] \right\}. \end{aligned} \quad (3.245)$$

By taking functional derivatives of (3.245), we find that

$$\begin{aligned} G^F(t_1, t_2, t_3, t_4) = \langle \mathcal{T}[F(t_1)F(t_2)F(t_3)F(t_4)] \rangle &= \frac{\delta^3}{\delta J(t_2) \delta J(t_3) \delta J(t_4)} \langle F(t_1) \rangle_J \Big|_{J=0} \\ &= \kappa \left\{ \frac{1}{4} \sum \int_{r_H}^r dt dr \left( -\frac{1}{h} \dot{K}_i \dot{K}_j + r^4 h K'_i K'_j \right) \right. \\ &\quad \times \left( -\frac{1}{h} \dot{K}_k \dot{K}_l + r^4 h K'_k K'_l \right) \\ &\quad \left. + 6r \partial_{t_1} \left[ \dot{\delta}(t_1 - t_2) \dot{\delta}(t_1 - t_3) \dot{\delta}(t_1 - t_4) \right] \right\}, \end{aligned} \quad (3.246)$$

where the  $r \rightarrow \infty$  limit is understood. Also,  $K_i \equiv K(t, r|t_i)$  and the summation

is over permutations  $(ijkl)$  of  $(1234)$ . The expression in the Fourier space is

$$\begin{aligned}
 G^F(\omega_1, \omega_2, \omega_3, \omega_4) &= 2\pi\kappa\delta(\omega_1 + \omega_2 + \omega_3 + \omega_4) \\
 &\times \left\{ \frac{1}{4} \sum_{\substack{\text{perm} \\ (ijkl)}} \int_{r_H}^r dr (\omega_i\omega_j K_i K_j + r^4 h K'_i K'_j) (\omega_k\omega_l K_k K_l + r^4 h K'_k K'_l) \right. \\
 &\quad \left. - 6r\omega_1\omega_2\omega_3\omega_4 \right\}, \tag{3.247}
 \end{aligned}$$

where now  $K_i \equiv K(\omega_i, r)$ . Note that the first term in (3.247) is the expression for the 4-point function we would obtain from the naive GKPW rule. The last term is there to cancel the UV divergence coming from the first term due to the fact that  $K_i = 1 + \mathcal{O}(r^{-2})$ .

### 3.D.3 Lorentzian AdS/CFT

So far we have not fully taken into account the fact that our spacetime is a Lorentzian spacetime, for which we have to use the Lorentzian AdS/CFT prescription [73, 74] as in section 1.7.2.

On the boundary side, to compute real time correlators, we have to take the time to run along the contour on the complex plane, as we discussed in subsection 3.4.1; see Figure 3.3 on page 64. The Lorentzian AdS/CFT prescription is simply to consider a bulk spacetime which “fills in” this contour. Then the bulk spacetime will have no boundary and there is no ambiguity in boundary conditions (although we have to impose certain gluing condition for fields across different patches). Following [74], we take the bulk spacetime to be the union of three patches  $M_i$  with  $i = 1, 2, 3$ , each of which fills in the corresponding contour  $C_i$  in (3.78). First, we take  $M_1$  to be the  $-L \leq t \leq L, r_H \leq r < \infty$  part of the Lorentzian AdS black hole (3.11).  $M_2$  is taken to be the same as  $M_1$  metric-wise, but the orientation is taken to be opposite to  $M_1$ , corresponding to the fact that  $C_1$  and  $C_2$  has opposite orientations.  $M_3$  is taken to be the Euclidean version of the black hole (3.11),

$$ds_E^2 = \frac{r^2}{l^2} [h(r)d\tau^2 + (dX^I)^2] + \frac{l^2}{r^2 h(r)} dr^2. \tag{3.248}$$

The Euclidean time  $\tau$  is taken to be  $0 \leq \tau \leq \beta$  where  $\beta$  is the inverse Hawking temperature in (3.12). For a schematic explanation of the patches  $M_{1,2,3}$ , see Figure 3.5. The way that three patches  $M_{1,2,3}$  are glued together is simply the bulk extension of the way that the contours  $C_{1,2,3}$  are glued together; see Figure 3.6.

Because now our spacetime is not just  $M_1$  but  $M = M_1 + M_2 + M_3$ , the action have contributions from all of  $M_{1,2,3}$ , just as the boundary (3.81). Therefore, the bulk integration appearing e.g. in (3.247) should be now over all  $M_i$ , with

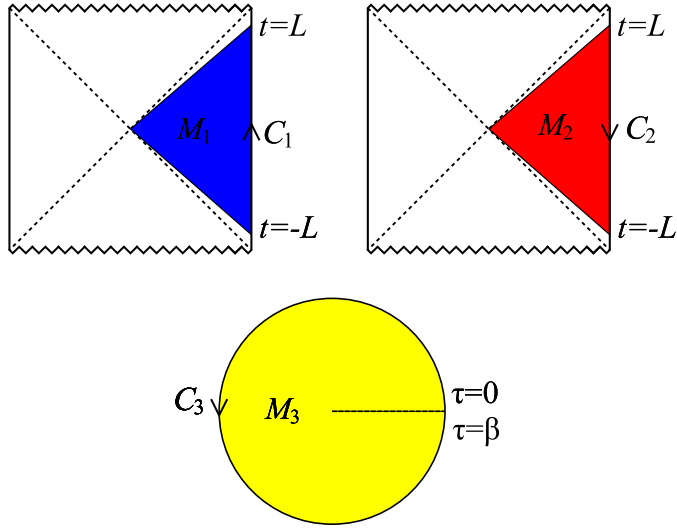


Figure 3.5: The bulk geometry  $M = M_1 + M_2 + M_3$  that “fills in” the boundary contour  $C = C_1 + C_2 + C_3$ . For  $d > 3$ , the Penrose diagrams for the Lorentzian patches drawn above are not accurate because the zigzag singularity lines must actually be not horizontal but bent inwards [102].

the signs correctly taken into account:

$$\begin{aligned}
 G^F(\omega_1, \omega_2, \omega_3, \omega_4) &= 2\pi\kappa\delta(\omega_1 + \omega_2 + \omega_3 + \omega_4) \\
 &\times \left\{ \frac{1}{4} \sum_{\substack{\text{perm} \\ (ijkl)}} \int_{r_H}^r dr \left[ \left( \frac{\omega_i \omega_j K_{[11]i} K_{[11]j}}{h} + r^4 h K'_{[11]i} K'_{[11]j} \right) \right. \right. \\
 &\quad \times \left( \frac{\omega_k \omega_l K_{[11]k} K_{[11]l}}{h} + r^4 h K'_{[11]k} K'_{[11]l} \right) \\
 &\quad - \left( \frac{\omega_i \omega_j K_{[21]i} K_{[21]j}}{h} + r^4 h K'_{[21]i} K'_{[21]j} \right) \\
 &\quad \left. \times \left( \frac{\omega_k \omega_l K_{[21]k} K_{[21]l}}{h} + r^4 h K'_{[21]k} K'_{[21]l} \right) \right] \\
 &\quad \left. - 6r\omega_1\omega_2\omega_3\omega_4 \right\}. \tag{3.249}
 \end{aligned}$$

Here,  $K_{[ab]i} = K_{[ab]}(\omega_i, r)$  and  $K_{[ab]}(\omega, r)$  is the boundary-bulk propagator from the boundary  $\partial M_b$  to the bulk  $M_a$ . The second line corresponds to the integration over  $M_1$  and the third line to the integration over  $M_2$ . Because we are taking the  $L \rightarrow \infty$  limit, the contribution from  $M_3$  has been dropped. The counter



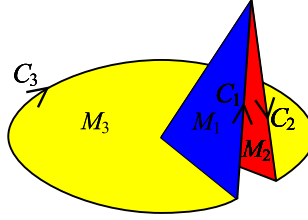


Figure 3.6: How to patch together the bulk patches  $M_1, M_2, M_3$ .

term  $-6r\omega_1\omega_2\omega_3\omega_4$  is added only for  $M_1$ , because the source is inserted only on  $\partial M_1$  ( $K_{[21]}(\omega, r)$  vanishes as  $r \rightarrow \infty$ ).

Because the spacetime  $M = M_1 + M_2 + M_3$  has no boundary inside, the boundary-bulk propagator can be determined without having to worry about boundary conditions. Carefully matching the values across different patches following [73, 74], we find the boundary-bulk propagators as follows:

$$\begin{aligned}
 K_{[11]}(\omega, r) &= \frac{1}{e^{\beta\omega} - 1} [-\phi_\omega(r) + e^{\beta\omega} \phi_{-\omega}(r)], \\
 K_{[21]}(\omega, r) &= \frac{e^{\beta\omega}}{e^{\beta\omega} - 1} [-\phi_\omega(r) + \phi_{-\omega}(r)], \\
 K_{[31]}(\omega, r) &= \frac{e^{(iL+\beta)\omega}}{e^{\beta\omega} - 1} [-\phi_\omega(r) + \phi_{-\omega}(r)],
 \end{aligned}
 \tag{3.250}$$

where  $\phi_{\pm\omega}(r)$  is the solution to the wave equation (3.226) satisfying the boundary condition (3.227). By substituting these propagators into (3.249), we can finally obtain the 4-point function for  $F$ .

### 3.D.4 Low frequency correlators

We are interested in the low frequency behavior of the correlation functions. As we discussed in Appendix 3.B, the solution  $\phi_{\pm\omega}(r)$  simplifies in the low frequency limit as<sup>16</sup>

$$\phi_{\pm\omega}(r) \sim e^{\pm i\omega r_*}.
 \tag{3.251}$$

If we apply this to (3.249) and (3.250), we obtain the following low frequency behavior:

$$\begin{aligned}
 G^F(\omega_1, \dots, \omega_4) &\sim \frac{\kappa}{\beta^3} \delta(\omega_1 + \dots + \omega_4) \sum_{1 \leq i < j \leq 4} (\omega_i + \omega_j) \int_{-\infty}^0 dr_* \frac{r_*^2}{h} e^{-2i(\omega_i + \omega_j)r_*} \\
 &+ (\text{higher powers in } \omega),
 \end{aligned}
 \tag{3.252}$$

<sup>16</sup>Note that the precise limit we are taking is (3.179).

where we dropped numerical factors. Because we have rescaled  $X$  in (3.206), to obtain the correlator for  $F = \mathcal{O}_X$  dual to the original  $X$  before rescaling, we have to rescale  $F \rightarrow \frac{F}{\sqrt{2\pi\alpha'}}$ . Therefore, in the end, the 4-point function for  $F$  is

$$G^F(\omega_1, \dots, \omega_4) \sim \frac{1}{\alpha'\beta^3} \delta(\omega_1 + \dots + \omega_4) \sum_{1 \leq i < j \leq 4} (\omega_i + \omega_j) \int_{-\infty}^0 dr_* \frac{r^2}{h} e^{-2i(\omega_i + \omega_j)r_*}. \quad (3.253)$$

This is exactly the same as the result (3.88) that we obtained by a more naive method. Namely, this has exactly the same IR divergence as (3.88) that we studied in section 3.5.

### 3.D.5 Retarded 4-point function

In the above, we computed the time-ordered 4-point function for the force  $F$  which turned out to be IR divergence. We can also compute the retarded 4-point function using the above formalism. As was shown in [74], for computing retarded correlators, one uses purely ingoing boundary condition for the boundary-bulk propagator:

$$K_{\text{Ret}}(\omega, r) = \phi_{-\omega}(r). \quad (3.254)$$

If we define

$$G_{\text{Ret}}^F(t_1, t_2, t_3, t_4) = \sum_{\substack{\text{perm} \\ (ijkl)}} \theta(t_i > t_j > t_k > t_l) \langle [[F(t_i), F(t_j)], F(t_k)], F(t_l) \rangle \quad (3.255)$$

then the prescription of [74] gives

$$\begin{aligned} G_{\text{Ret}}^F(\omega_1, \omega_2, \omega_3, \omega_4) &= 2\pi\kappa\delta(\omega_1 + \omega_2 + \omega_3 + \omega_4) \\ &\times \left\{ \frac{1}{4} \sum_{\substack{\text{perm} \\ (ijkl)}} \int_{r_H}^r dr (\omega_i \omega_j K_{\text{Ret},i} K_{\text{Ret},j} + r^4 h K'_{\text{Ret},i} K'_{\text{Ret},j}) \right. \\ &\quad \times (\omega_k \omega_l K_{\text{Ret},k} K_{\text{Ret},l} + r^4 h K'_{\text{Ret},k} K'_{\text{Ret},l}) \\ &\quad \left. - 6r\omega_1\omega_2\omega_3\omega_4 \right\}, \quad (3.256) \end{aligned}$$

where  $K_{\text{Ret},i} = K_{\text{Ret}}(\omega_i, r)$ . The integration effectively becomes only over  $M_1$ .

For definiteness, consider the AdS<sub>3</sub> case where the retarded correlator is

$$K_{\text{Ret}}(\omega, r) = \left(1 - \frac{i\omega}{r}\right) \left(\frac{r - r_H}{r + r_H}\right)^{-i\omega/2r_H}. \quad (3.257)$$

For this case, Eq. (3.256) gives

$$G_{\text{Ret}}^F(\omega_1, \dots, \omega_4) = \kappa 2\pi \delta(\omega_1 + \dots + \omega_4) \omega_1 \omega_2 \omega_3 \omega_4 \left( 2r_H - \frac{16 \sum_{i < j} \omega_i \omega_j}{r_H} \right). \quad (3.258)$$

Note that this is exact; we have not done low frequency approximation. This is both IR and UV finite.

### 3.E Computation of $\eta$ for the STU black hole

In this Appendix, we will compute the mean-free-path time for the STU black hole studied in 3.6.2. The final results have been presented in (3.149) and (3.150)–(3.152).

We will discuss the 1-charge case ( $\kappa_1 = \kappa, \kappa_2 = \kappa_3 = 0$ ) only, because the 2- and 3-charge cases are similar. First, the relations (3.129), (3.130), and (3.131) read, in this case,

$$m = \frac{r_H^4}{l^2} (1 + \kappa), \quad T = \frac{r_H}{2\pi} \frac{2 + \kappa}{\sqrt{1 + \kappa}}, \quad \Phi = -\frac{r_H^2}{\kappa_3^2 l} \sqrt{\kappa}. \quad (3.259)$$

$L_H$  in (3.149) can be computed as follows. From the definition (3.122) and (3.148) for  $n = 1$ , we obtain

$$\begin{aligned} \int_{\infty}^r dr \frac{H^{1/2}}{r^2 f} \frac{1}{\sqrt{1 - f^{-1} H^2 \mathcal{A}_t^2}} &= \int_{\infty}^r \frac{dr}{r^2 - r_H^2} \sqrt{\frac{r_H^2 + \ell^2}{(r^2 + r_H^2 + \ell^2)((r_H^2 + \ell^2)r^2 + r_H^4)}} \\ &= \frac{1}{2r_H^3} \frac{\sqrt{1 + \kappa}}{(2 + \kappa)} \log \frac{r - r_H}{L_H} + \mathcal{O}(r - r_H) \end{aligned} \quad (3.260)$$

The integral in the first line diverges as  $r \rightarrow r_H$ . We can separate this divergent piece by subtracting and adding the term obtained by setting  $r$  to  $r_H$  in the square root. Further setting  $\rho = r/r_H$  and  $\kappa = \ell^2/r_H$ , we have

$$\begin{aligned} \log \frac{r - r_H}{r + r_H} + 2(2 + \kappa) \int_{\infty}^1 \frac{d\rho}{\rho^2 - 1} \left[ \frac{1}{\sqrt{(\rho^2 + 1 + \kappa)((1 + \kappa)\rho^2 + 1)}} - \frac{1}{(2 + \kappa)} \right] \\ \equiv \log \frac{r - r_H}{L_H} + \mathcal{O}(r - r_H). \end{aligned} \quad (3.261)$$

In the second term in the first line, we have set the upper limit of the integral to  $\rho \rightarrow 1$  (which is equivalent to  $r \rightarrow r_H$ ) because the integral is now convergent. By comparing both sides, we obtain

$$L_H = 2r_H \exp \left\{ -2(2 + \kappa) \int_{\infty}^1 \frac{d\rho}{\rho^2 - 1} \left[ \frac{1}{\sqrt{(\rho^2 + 1 + \kappa)((1 + \kappa)\rho^2 + 1)}} - \frac{1}{2 + \kappa} \right] \right\}. \quad (3.262)$$

By using (3.259), we obtain the final expression (3.150). For small  $\kappa$ , it is easy to expand the integrand in (3.150) in  $\kappa$ , and each integral converges. This leads to the following expansion of  $\eta$  in  $\kappa$ :

$$\eta = e^{-\pi/2} \left[ 2\pi - \pi\kappa + \frac{(12 - \pi)\pi}{16} \kappa^2 \right] + \mathcal{O}(\kappa^3) \quad (3.263)$$

This shows that, as  $\kappa$  increases with fixed  $T$ , the mean-free-path time  $t_{mfp}$  increases.

The 2- and 3-charge cases are similar and we obtain (3.151) and (3.152). The small  $\kappa$  expansion of  $\eta$  is

$$\eta = e^{-\pi/2} \left[ 2\pi - \frac{1}{2}(4 - \pi)\pi\kappa + \frac{1}{16}\pi(52 - 19\pi + \pi^2)\kappa^2 + \mathcal{O}(\kappa^3) \right] \quad (3.264)$$

$$\eta = e^{-\pi/2} \left[ 2\pi + (\pi - 3)\pi\kappa + \frac{1}{16}\pi(140 - 57\pi + 4\pi^2)\kappa^2 + \mathcal{O}(\kappa^3) \right] \quad (3.265)$$

for the 2- and 3-charge cases, respectively.



# CHAPTER 4

---

## DRAG FORCE IN 4D KERR-ADS BLACK HOLE

---

### 4.1 Introduction

An important feature of RHIC is the spatial anisotropy of the data correlated with non-zero impact parameter of the colliding ions. The spatial anisotropy translates into a non-zero component of the second Fourier harmonic of the particle distribution in the plane transverse to the collision.<sup>1</sup> This coefficient is known as elliptic flow and has been calculated using hydrodynamic evolution of the sQGP in a stunning agreement with data [104, 105]<sup>2</sup>. Up to now most AdS computations of sQGP have ignored spatial anisotropy: the black hole background is always the standard static isotropic AdS black hole. There is good reason to do so. Transport coefficients such as the viscosity are defined with respect to the isotropic perfect fluid and for other quantities the experimental indication that the system thermalizes rapidly to an almost perfect, i.e. isotropic, fluid means that anisotropy corrections are small. The exceptions are “local temperature/pressure” approximations as in Bhattacharyya et al [57] and Chesler et al [58]. Yet for a number of them, e.g. photon production or jet-quenching, it is the anisotropic component that is experimentally the most accessible.

---

<sup>1</sup>The first Fourier component vanishes by symmetry.

<sup>2</sup>A more detailed discussion on this phenomena and others can be found in [106] and references therein.

In this chapter we make a first step towards the study anisotropic effects on jet-quenching from the string theory point of view. Jet-quenching is a characteristic feature of the sQGP phase in RHIC. It signals the strong energy loss of a highly massive quark moving in hot charged plasma. In the frame work of AdS/CFT, a quark is represented by a string suspended from the boundary of asymptotically AdS space into the interior [65, 107, 108]. This set-up was proposed in the context of  $\mathcal{N} = 4$  supersymmetric Yang-Mills theory at finite temperature [35, 39] and has been explored in detail in [59, 60] with a beautiful extension to trailing wake of the heavy quark in the sQGP dual to the back-reaction of string on the black-hole geometry. The way we shall introduce anisotropy in the system is to consider non-zero angular momentum. The advantage is that the dual description of this system is straightforward: one considers rotating black holes. The drawback is that the anisotropy primarily responsible for elliptic flow is due to the asymmetric almond-shape overlap of the two non-central colliding nuclei rather than angular momentum. As all non-central collisions the total system carries a significant amount of angular momentum, but most of that is carried away by spectator-nuclei not involved in the formation of the sQGP. At RHIC the angular momentum fraction of the total elliptic flow is thought to be less than 10%, although it is expected to increase to 30% at LHC [61, 62] and the references therein. Clearly experimentally more relevant would be a AdS/CFT study of elliptic flow due to non-rotational anisotropy. The problem is that the gravity set-up in this case is unclear. Non-rotational anisotropy dissipates fast as the system equilibrates and isotropizes, and this points to a time-dependent gravity dual, see e.g. Chesler presentation in Amsterdam String Theory Workshop 2010.<sup>3</sup> For that reason we start here with studying anisotropic jet-quenching in a rotating plasma.

## 4.2 Drag force on a string in a global 4D AdS black hole

In global coordinates, the metric of four dimensional AdS-Schwarzschild is given by

$$\begin{aligned}
 ds^2 &= -r^2 h(r) dt^2 + \frac{1}{r^2 h(r)} dr^2 + r^2 (d\theta^2 + \sin^2 \theta d\phi^2), \\
 h(r) &= l^2 + \frac{1}{r^2} - \frac{2M}{r^3},
 \end{aligned} \tag{4.1}$$

where  $M$  is proportional to the mass of the black hole and  $l$  is the radius of curvature. The Hawking temperature of four dimensional AdS-Schwarzschild can be obtained in a simple way by demanding the periodicity of Euclidean

---

<sup>3</sup>Alternatively one could consider 4+1 dimensional hairy black holes to break the anisotropy; we thank H. Ooguri for pointing this out.

time to avoid a conical singularity at  $r = r_H$ . This gives  $T_H = \frac{1}{4\pi} \left( \frac{1}{r_H} + 3r_H l^2 \right)$ , where  $r_H$  is the radius of horizon defined as the zero locus  $h(r_H) = 0$  [109] and can be written explicitly in terms of parameters  $l$  and  $M$ :

$$r_H(l, M) = \frac{(9Ml^4 + \sqrt{3l^6 + 81M^2l^8})^{1/3}}{3^{2/3}l^2} - \frac{1}{3^{1/3} (9Ml^4 + \sqrt{3l^6 + 81M^2l^8})^{1/3}}. \quad (4.2)$$

A string in this background can be described by the following Nambu-Goto action:

$$S = -\frac{1}{2\pi\alpha'} \int d\sigma^2 \sqrt{-\det g_{\alpha\beta}} = \int d\sigma^2 \mathcal{L},$$

$$g_{\alpha\beta} \equiv G_{\mu\nu} \partial_\alpha X^\mu \partial_\beta X^\nu, \quad (4.3)$$

with  $\sigma^\alpha$  are coordinates of string worldsheet,  $X^\mu = X^\mu(\sigma)$  are the embedding of string worldsheet in spacetime, and  $G_{\mu\nu}$  is the spacetime metric (4.1). The equation of motions derived from (4.3) are,

$$\nabla_\alpha P_\mu^\alpha = 0, \quad P_\mu^\alpha \equiv -\frac{1}{2\pi\alpha'} G_{\mu\nu} \partial^\alpha X^\nu = -\frac{1}{2\pi\alpha'} \pi_\mu^\alpha \quad (4.4)$$

with  $P_\mu^\alpha$  is the worldsheet current of spacetime momentum carried by the string, proportional to the canonical worldsheet momentum

$$\pi_\mu^\alpha = -\frac{(2\pi\alpha')}{\sqrt{-g}} \frac{\delta S}{\delta \partial_\alpha X^\mu}, \quad (4.5)$$

with  $g = \det g_{\alpha\beta}$ . The total momentum charge in the direction  $\mu$  carried by the string equals

$$p_\mu = \int d\Sigma_\alpha \sqrt{-g} P_\mu^\alpha, \quad (4.6)$$

where  $\Sigma_\alpha$  is a cross-sectional surface (a line) on the string worldsheet. The proper-force on the string then equals

$$\frac{\partial p_\mu}{\partial \sigma^0} = \sqrt{-g} P_\mu^{\sigma^1} \quad (4.7)$$

which in turn is equal to the canonical worldsheet-momentum

$$\frac{\partial p_\mu}{\partial \sigma^0} = -\frac{1}{2\pi\alpha'} \pi_\mu^{\sigma^1} \quad (4.8)$$

If the configuration is constant in time, the proper force  $\frac{\partial p_\mu}{\partial \sigma^0}$  does not depend on the location  $\sigma^1$  along the worldsheet, thanks to the equation of motion.

$$\frac{\partial}{\partial \sigma^1} \frac{\partial p_\mu}{\partial \sigma^0} = \frac{\partial}{\partial \sigma^1} \sqrt{-g} P_\mu^{\sigma^1} = -\frac{\partial}{\partial \sigma^0} \sqrt{-g} P_\mu^{\sigma^0} \stackrel{\text{static}}{=} 0 \quad (4.9)$$



Using the physical gauge,  $\sigma^\alpha = (t, r)$ , we can write the action (4.3) as follows

$$S = -\frac{1}{2\pi\alpha'} \int d\sigma^2 \sqrt{-g},$$

$$-g = 1 + r^4 h(r) (\theta'^2 + \phi'^2 \sin^2 \theta) - \frac{1}{h(r)} \left( \dot{\theta}^2 + \dot{\phi}^2 \sin^2 \theta \right) - r^4 \sin^2 \theta \left( \dot{\theta}\phi' - \theta'\dot{\phi} \right)^2, \quad (4.10)$$

with  $\dot{\phantom{x}} \equiv \frac{d}{dt}$  and  $' \equiv \frac{d}{dr}$ . The equations of motion are:

$$\begin{aligned} & \frac{\partial}{\partial t} \left( \frac{r^4}{\sqrt{-g}} \sin^2 \theta \left( \dot{\theta}\phi' - \theta'\dot{\phi} \right) \theta' - \frac{\sin^2 \theta}{h(r)\sqrt{-g}} \dot{\phi} \right) \\ & + \frac{\partial}{\partial r} \left( \frac{r^4 h(r) \sin^2 \theta}{\sqrt{-g}} \phi' - \frac{r^4}{\sqrt{-g}} \sin^2 \theta \left( \dot{\theta}\phi' - \theta'\dot{\phi} \right) \dot{\theta} \right) = 0, \end{aligned} \quad (4.11)$$

and

$$\begin{aligned} & \frac{1}{\sqrt{-g}} \left( r^4 h(r) \phi'^2 - \frac{1}{h(r)} \dot{\phi}^2 - r^4 \left( \dot{\theta}\phi' - \theta'\dot{\phi} \right)^2 \right) \sin \theta \cos \theta \\ & + \frac{\partial}{\partial t} \left( \frac{r^4 \sin^2 \theta}{\sqrt{-g}} \left( \dot{\theta}\phi' - \theta'\dot{\phi} \right) \phi' + \frac{1}{h(r)\sqrt{-g}} \dot{\theta} \right) \\ & - \frac{\partial}{\partial r} \left( \frac{r^4 \sin^2 \theta}{\sqrt{-g}} \left( \dot{\theta}\phi' - \theta'\dot{\phi} \right) \dot{\phi} + \frac{r^4 h(r)}{\sqrt{-g}} \theta' \right) = 0. \end{aligned} \quad (4.12)$$

### 4.2.1 Great circle at $\theta = \pi/2$

It easy to see that the metric (4.1) has  $SO(3)$  symmetry. Specially the boundary is the  $S^2$ , and the free motion of a quark on this sphere is a great circle. The motion of string giving arise to a great circle trajectory should therefore reduce to the geodesic equations on the boundary. The simplest solution of the great circles is when we consider the motions in the equatorial coordinates  $\phi = \phi(t, r)$  only, while the other angular coordinate we set  $\theta = \pi/2$ . We take an ansatz for  $\phi(t, r)$  as below<sup>4</sup>

$$\phi(t, r) = \omega t + \eta(r), \quad (4.13)$$

where  $\omega$  is a non-zero constant. Substituting the ansatz (4.13) into the action (4.3), we obtain equation of motion for  $\eta(r)$  which is given by a constant of its

<sup>4</sup>With this ansatz, the dynamical field is effectively given by field  $\eta(r)$ .

momentum conjugate since the Lagrangian is only a functional of  $\eta'(r)$

$$\begin{aligned}\pi_\phi^r &= -2\pi\alpha' \frac{\partial \mathcal{L}}{\partial \eta'(r)} = \frac{r^4 h(r) \eta'(r)}{\sqrt{1 + r^4 h(r) \eta'(r)^2 - \frac{\omega^2}{h(r)}}}, \\ \eta'(r) &= \frac{\pi_\phi^r}{r^4 h(r)} \sqrt{\frac{h(r) - \omega^2}{h(r) - \frac{(\pi_\phi^r)^2}{r^4}}},\end{aligned}\quad (4.14)$$

thus we find  $\pi_\phi^r$  is a constant, by solving the equation of motion, proportional to the momentum conjugate in radial direction. We have chosen positive sign to describe a string that trails out from boundary down to the horizon. In order to make sense of the solution, we have to require that (4.14) must be real everywhere. This requirement gives us a condition

$$\frac{h(r) - \omega^2}{h(r)r^4 - (\pi_\phi^r)^2} \geq 0 \quad (4.15)$$

At the boundary  $r \rightarrow \infty$ , the requirement tells us that there is a bound on the velocity of the particle that  $l^2 \geq \omega^2$ . Because (4.14) ought to be real everywhere for  $r_H \leq r < \infty$ , the only possible choice we can take is for the constant  $(\pi_\phi^r)^2 = \omega^2 r_{Sch}^4$ , with  $r_{Sch} = r_H(\sqrt{l^2 - \omega^2}, M)$  defined to be the point where  $h(r_{Sch}) = \omega^2$ . Then the numerator and denominator in (4.15) change their sign at the same point at  $r = r_{Sch}$ .

The exact solution for equation (4.14) is quite difficult to find but to compute the drag force it is enough just to use the equation (4.14). To compute the flow of momentum  $dp_\phi$  down the string, we use

$$\Delta P_\phi = \int d\Sigma_\alpha P_\phi^\alpha. \quad (4.16)$$

In this static configuration all momentum flow is radial. Thus the total momentum reduces to

$$\Delta P_\phi = \int_{\mathcal{I}} dt \sqrt{-g} P_\phi^r = \frac{dp_\phi}{dt} \Delta t, \quad (4.17)$$

with  $\mathcal{I}$  is some time interval of length  $\Delta t$ . Thus the drag force in  $\phi$  direction is given by

$$\frac{dp_\phi}{dt} = \sqrt{-g} P_\phi^r = -\frac{\pi_\phi^r}{2\pi\alpha'}, \quad (4.18)$$

where the negative value implies that it is the drag force. Explicitly  $\pi_\phi^r = \omega r_{Sch}^2$ , with  $\omega \geq 0$ .

### 4.2.2 General solution of the great circle

In general, great circles are not only the motion in  $\theta = \pi/2$  plane. The great circle can be in an arbitrary plane. We can describe this as follows using coordinates transformation:

$$x = \sin \theta \cos \phi, \quad y = \sin \theta \sin \phi, \quad z = \cos \theta. \quad (4.19)$$

We consider a constrained Nambu-Goto action<sup>5</sup>

$$\begin{aligned} S_{cNG} &= -\frac{1}{2\pi\alpha'} \int d\sigma^2 \sqrt{-g} \left[ 1 + \frac{\lambda^2}{2} (x^i x^i - 1) \right], \\ -g &= r^4 \left( (\dot{x}^i x'^i)^2 - (\dot{x}^i \dot{x}^i - h(r)) \left( x'^i x'^i + \frac{1}{r^4 h(r)} \right) \right), \end{aligned} \quad (4.20)$$

where  $x^i \equiv (x, y, z)$  and  $\lambda$  is a Lagrange multiplier. The equations of motion for this action are given by a constraint equation  $x^i x^i = 1$  and

$$\begin{aligned} \lambda^2 x^i \sqrt{-g} &- \frac{\partial}{\partial t} \left( x'^i \frac{r^4 \dot{x}^j x'^j}{\sqrt{-g}} - \dot{x}^i \frac{\left( r^4 x'^j x'^j + \frac{1}{h(r)} \right)}{\sqrt{-g}} \right) \\ &- \frac{\partial}{\partial r} \left( \dot{x}^i \frac{r^4 \dot{x}^j x'^j}{\sqrt{-g}} - x'^i \frac{r^4 (\dot{x}^j \dot{x}^j - h(r))}{\sqrt{-g}} \right) = 0. \end{aligned} \quad (4.21)$$

Notice that if we substitute the constraint equation back to the action (4.20) then we get back the action (4.3).

#### radial independent ansatz

A simple solution can be described by radial  $r$  independent ansatz,  $x^i = x^i(t)$ , where the equations of motion become

$$\lambda^2 x^i \sqrt{-g} + \frac{\partial}{\partial t} \left( \frac{\dot{x}^i}{h(r) \sqrt{-g}} \right) = 0, \quad (4.22)$$

with  $-g = \frac{1}{h} (h - \dot{x}^i \dot{x}^i)$ . Multiplying with  $x^i$  and using constraint  $x^i \dot{x}^i = 0$ , we obtain

$$\dot{x}^i \dot{x}^i = \frac{\lambda^2 h(r)}{1 + \lambda^2}. \quad (4.23)$$

---

<sup>5</sup>Recall that in order to make a world sheet volume invariant under world sheet general coordinate transformation, we have to multiply with  $\sqrt{-g}$ . A repeated index denotes Einstein summation index.

Assume  $\lambda$  is constant, the equations of motion are now simplified to

$$\ddot{x}^i = -\frac{\lambda^2 h(r)}{1 + \lambda^2} x^i. \quad (4.24)$$

The general solution is given by

$$x(t)^i = a^i \sin\left(\lambda \sqrt{\frac{h(r)}{1 + \lambda^2}} t\right) + b^i \cos\left(\lambda \sqrt{\frac{h(r)}{1 + \lambda^2}} t\right), \quad (4.25)$$

where  $a^i$  and  $b^i$  are constants. The constraint requires that these constants obey

$$a^i a^i = b^i b^i = 1, \quad a^i b^i = 0. \quad (4.26)$$

These solutions are the general great circle solutions in the plane spanned by  $\vec{a}$  and  $\vec{b}$ . However, these solutions have an angular velocity which depends on  $r$  and therefore they are not consistent with the ansatz.

There is another solution which is similar to (4.25) where angular velocity  $v$  is a constant but  $\lambda = \lambda(r)$  depends on radial coordinate,

$$x(t)^i = a^i \sin(vt) + b^i \cos(vt). \quad (4.27)$$

From equation (4.23), we find that

$$\lambda(r)^2 = \frac{v^2}{h(r) - v^2}. \quad (4.28)$$

Unfortunately for this solution  $-g$  is not positive definite. This is similar to the non-global case discussed in Herzog et al [35] and we will take as our starting point.

### curved equatorial ansatz

Motivated by equatorial solution (4.13) and general great circle solutions (4.27) previously, we take the ansatz depends on time and radial coordinate as follows:

$$x(t, r)^i = a^i \sin(vt + c(r)) + b^i \cos(vt + c(r)), \quad (4.29)$$

with  $v$  is a constant and  $c(r)$  is a function will be determined later. Using the constraint equation, as we did in radial independent ansatz, the equations of motion now become

$$\sqrt{-g} \frac{\partial}{\partial r} \left( \frac{r^4 h x^i}{\sqrt{-g}} \right) = \left( \frac{\lambda^2}{1 + \lambda^2} - \frac{v^2}{h} \right) x^i, \quad (4.30)$$

where  $-g = \frac{1}{1+\lambda^2}$  and we have  $\lambda = \lambda(r)$ . The  $-g$  can also be written, by substituting the ansatz to (4.30), as

$$-g = 1 + r^4 h(r) c'(r)^2 - \frac{v^2}{h(r)}. \quad (4.31)$$

Comparing this with the equatorial solution we can identify  $c(r) = \eta(r)$  and  $v = \omega$ . One can check, using these two expressions of  $-g$ , that at equatorial we get back the equatorial solution (4.13). Now, the equations of motion reduce to

$$\frac{\partial}{\partial r} \left( \frac{r^4 h c'(r)}{\sqrt{-g}} \right) = 0 \quad (4.32)$$

which is the same equation for  $\eta(r)$  as in the equatorial case. Furthermore one can also find the expression for  $\lambda$  which is given by

$$\lambda(r)^2 = \frac{v^2 r^4 - r_{Sch}^4}{r^4 h(r) - v^2}, \quad (4.33)$$

where  $r_{Sch}$  is defined as  $h(r_{Sch}) = v^2$ . This guarantees that  $\lambda(r)$  is a positive definite function.

Adding the constraint into the original Nambu-Goto action, we have manifest rotation symmetry  $SO(3)$  in  $x, y, z$  coordinates. In this case the drag force is related to angular momentum currents in  $r$  direction or torques of the world sheet

$$J_r^i = \frac{dL^i}{dt} = -\frac{r^4}{2\pi\alpha'\sqrt{-g}} \left( \dot{x}^j x'^j \varepsilon_{imn} x^m \dot{x}^n - (\dot{x}^j \dot{x}^j - h(r)) \varepsilon_{imn} x^m x'^n \right), \quad (4.34)$$

where  $\varepsilon_{imn}$  is a totally antisymmetric tensor, with  $\varepsilon_{123} = 1$ . The angular momentum currents or torques, after substituting the ansatz and the constraint, are

$$J_r^i = \frac{dL^i}{dt} = -\frac{r^4 h(r) \varepsilon_{ijk} x^j x'^k}{2\pi\alpha' \sqrt{-g}} = -\frac{r^4 h(r) c'(r)}{2\pi\alpha' \sqrt{-g}} \varepsilon_{ijk} b^j a^k = -\frac{r^4 h(r) c'(r)}{2\pi\alpha' \sqrt{-g}} n^i \quad (4.35)$$

where  $n^i \equiv (n_x, n_y, n_z)$  is the normal vector of great circle with the norm unity. The equations of motion imply that these angular momentum currents or torques are constants. The norm of total angular momentum current or total torque equals to the norm of drag force (4.18),  $J_r^2 \equiv J_r^i J_r^i = \frac{dL^i}{dt} \frac{dL^i}{dt} = \left( \frac{dp_\phi}{dt} \right)^2$ . This shows that the total drag force is the same as before.

The drag force of string moving in the background of a four dimensions AdS-Schwarzschild is thus a constant related to momentum of a particle represented by the end of a string at the boundary. We can derive the full motion

of the particle, e.g. the friction as it moves in the plasma with a constant angular velocity  $\omega$ , with the boundary metric

$$ds_B^2 = -dt^2 + \frac{1}{l^2} (d\theta^2 + \sin^2 \theta d\phi^2). \quad (4.36)$$

To illustrate the relativistic angular velocity of this particle at the boundary is  $u^\mu = \gamma(1, 0, \omega)$ , in terms of coordinates  $(t, \theta, \phi)$ , with  $\gamma = (1 - \omega^2/l^2)^{-1/2}$  and  $\theta = \pi/2$ . Taking non-relativistic limit,  $\omega \ll l$ , we obtain  $P^\mu \equiv m(1, 0, \omega) \left(1 + \frac{1}{2} \frac{\omega^2}{l^2} + \dots\right)$  with  $m$  is the mass of particle. In this limit, the drag force becomes

$$\frac{dp_\phi}{dt} = -\frac{1}{2\pi\alpha'} \frac{p_\phi}{m} r_H^2 + O(\omega) \quad (4.37)$$

and thus the friction coefficient is

$$\mu_\phi = \frac{r_H^2}{2m\pi\alpha'} + O(\omega). \quad (4.38)$$

Recall that  $r_H = r_{Sch}(\omega = 0)$ .

### 4.3 Anisotropic drag on a string in 4D Kerr-AdS black hole

As has been explained before in the introduction, we are looking for a background metric as a solution to Einstein equation with negative cosmological constant that naturally has anisotropy at the boundary. One such solution is Kerr-AdS black holes. We shall use Kerr-AdS in Boyer-Lindquist coordinates which has less mixing terms than the other coordinates representation and it manifestly reduces to the non-rotating solution of previous section when the rotation parameter  $a$  vanishes. A disadvantage is that this coordinates representation does not have manifest  $SO(3)$  symmetry at the boundary  $r \rightarrow \infty$  even though it is restored there, as can be seen by a transformations to another coordinates. The metric of four dimensions Kerr-AdS black hole in Boyer-Lindquist coordinates is explicitly written as [110]

$$ds^2 = -\frac{\Delta_r}{\rho^2} \left(dt - \frac{a}{\Xi} \sin^2 \theta d\phi\right)^2 + \frac{\rho^2}{\Delta_r} dr^2 + \frac{\rho^2}{\Delta_\theta} d\theta^2 + \frac{\Delta_\theta \sin^2 \theta}{\rho^2} \left(adt - \frac{r^2 + a^2}{\Xi} d\phi\right)^2, \quad (4.39)$$

where

$$\begin{aligned}
 \rho^2 &= r^2 + a^2 \cos^2 \theta \\
 \Delta_r &= (r^2 + a^2)(1 + l^2 r^2) - 2Mr \\
 \Delta_\theta &= 1 - l^2 a^2 \cos^2 \theta \\
 \Xi &= 1 - l^2 a^2,
 \end{aligned} \tag{4.40}$$

with  $a$  is the rotation parameter constrained to  $1 > a^2 l^2$  in order to have a finite positive value of the horizon area. The event horizon or outer horizon is located at  $r = r_{KH}$  which is the largest root of  $\Delta_r$ . The Hawking temperature is given by

$$T_H = r_{KH} \frac{3l^2 r_{KH}^2 + 1 + a^2 l^2 - a^2 / r_{KH}}{4\pi(r_{KH}^2 + a^2)}. \tag{4.41}$$

The Nambu-Goto action for the metric above is

$$\begin{aligned}
 S_{NG} &= -\frac{1}{2\pi\alpha'} \int d\sigma^2 \sqrt{-g}, \\
 -g &= \left( (a\Delta_r - a(r^2 + a^2)\Delta_\theta) \frac{\sin^2 \theta}{\Xi \rho^2} \dot{\phi}' + \frac{\rho^2}{\Delta_\theta} \dot{\theta} \theta' \right. \\
 &\quad \left. + (\Delta_\theta (r^2 + a^2)^2 - a^2 \Delta_r \sin^2 \theta) \frac{\sin^2 \theta}{\Xi^2 \rho^2} \dot{\phi} \phi' \right)^2 \\
 &\quad - \left( \frac{\rho^2}{\Delta_r} + \frac{\rho^2}{\Delta_\theta} \theta'^2 + (\Delta_\theta (r^2 + a^2)^2 - a^2 \Delta_r \sin^2 \theta) \frac{\sin^2 \theta}{\Xi^2 \rho^2} \phi'^2 \right) \times \\
 &\quad \times \left( (a^2 \Delta_\theta \sin^2 \theta - \Delta_r) \frac{1}{\rho^2} + (a\Delta_r - a(r^2 + a^2)\Delta_\theta) \frac{2 \sin^2 \theta}{\Xi \rho^2} \dot{\phi} \right. \\
 &\quad \left. (\Delta_\theta (r^2 + a^2)^2 - a^2 \Delta_r \sin^2 \theta) \frac{\sin^2 \theta}{\Xi^2 \rho^2} \dot{\phi}^2 + \frac{\rho^2}{\Delta_\theta} \dot{\theta}^2 \right).
 \end{aligned} \tag{4.42}$$

Let us consider the equatorial solution for  $\theta = \pi/2$  and take the ansatz (4.13) such that the equation of motion now becomes

$$\begin{aligned}
 \eta'(r) &= \frac{\pi_\phi^r (1 - a^2 l^2)}{\Delta_r} \sqrt{\frac{(1 - a^2 l^2 - a\omega)^2 \Delta_r - f(r)}{\Delta_r - (1 - a^2 l^2)^2 (\pi_\phi^r)^2}}, \\
 f(r) &= (a - a^3 l^2 - a^2 \omega - \omega r^2)^2,
 \end{aligned} \tag{4.43}$$

requiring real solution everywhere demands

$$\frac{(1 - a^2 l^2)^2 (1 - a^2 l^2 - a\omega)^2 \pi_\phi^2 - f(r)}{(1 - a^2 l^2 - a\omega)^2 \Delta_r - f(r)} \leq 1. \tag{4.44}$$

Again, lets first look at  $r \rightarrow \infty$ , then we obtain<sup>6</sup>

$$l^2 \geq \frac{\omega^2}{(1 - a^2 l^2 - a\omega)^2}. \quad (4.45)$$

Limiting the calculation for real positive  $r$ , in order to satisfy the inequality (4.44) we need to know the profile of both numerator and denominator on the left hand side of the inequality (4.44) at least in the region  $r_{KH} \leq r < \infty$ . Unfortunately this is not an easy task unlike in the case of AdS-Schwarzschild. Here we assume that for some values of parameter  $l, \omega, M$ , and  $a$  the numerator and denominator behave like in the case of AdS-Schwarzschild where at some radius  $r = r_K$ , which is the largest positive root of  $(1 - a^2 l^2 - a\omega)^2 \Delta_r - f(r)$ , the numerator and denominator change their sign as we move from the boundary at  $r \rightarrow \infty$  down to the horizon  $r = r_{KH}$  with

$$(\pi_\phi^r)^2 = \frac{(a - a^3 l^2 - a^2 \omega - r_K^2 \omega)^2}{(1 - a^2 l^2)^2 (1 - a^2 l^2 - a\omega)^2}. \quad (4.46)$$

Then we can compute the drag force as follows

$$\begin{aligned} \frac{dp_\phi}{dt} &= -\frac{\sqrt{f(r_K)}}{2\pi\alpha'(1 - a^2 l^2 - a\omega)(1 - a^2 l^2)}. \\ &= -\frac{\pi_\phi^r}{2\pi\alpha'}. \end{aligned} \quad (4.47)$$

The drag force actually can be easily computed using the fact that the equation of motion for  $\phi$  is the conservation current in radial  $r$  direction, i.e.  $\partial_r J_\phi^r = 0$ . This is true since we are considering the dynamical field in  $\phi$  to depend on the radial direction  $r$ . So, the conserved current in radial direction  $r$  for  $\phi$  is actually the conjugate momentum of  $\phi$  in radial direction  $r$  such that  $J_\phi^r = \frac{\partial \mathcal{L}}{\partial \dot{\phi}^r}$  which is just the constant  $\pi_\phi^r$ . What we have to do then is to determine the values of  $\pi_\phi^r$  that give physical solution.

The exact expression for  $r_K$ , as solution to  $f(r_K) = (1 - a^2 l^2 - a\omega)^2 \Delta_r(r_K)$ , in this case is very long and complicated. In the small limit  $a \ll 1$ , we can write  $r_K = r_0 + a r_1 + O(a^2)$ , with  $r_0 = r_{Sch}$  and

$$r_1 = \frac{\omega l^2 r_0^4 - 2\omega M r_0}{2(l^2 - \omega^2)r_0^3 + r_0 - M}. \quad (4.48)$$

Then we can write  $\pi_\phi^r$  as expansion of  $a$  up to first order as follows

$$\pi_\phi^r \approx \omega r_0^2 - (1 - \omega r_0 (\omega r_0 + 2r_1)) a + O(a^2). \quad (4.49)$$

---

<sup>6</sup>This condition is related to light and time-like region of the spacetime at the boundary where the light-like is given by  $\frac{\omega^2}{l^2} = (1 - a^2 l^2 - a\omega)^2$ .



Thus the drag force can be written as

$$\frac{dp_\phi}{dt} = -\frac{1}{2\pi\alpha'} [\omega r_0^2 - (1 - \omega r_0 (\omega r_0 + 2r_1)) a + O(a^2)]. \quad (4.50)$$

The first term is the drag force of the 4D non-rotating black hole (4.18) and the second term can be considered as correction in the presence of small angular momentum  $a$ . Explicitly for small  $a$ , the drag force is written as

$$\begin{aligned} \frac{dp_\phi}{dt} &= -\frac{1}{2\pi\alpha'} [\pi_\phi^0 - a + C \pi_\phi^0 a + O(a^2)], \\ C &= \omega \left[ \frac{2(2l^2 - \omega^2)r_0^3 + r_0 - 5M}{2(l^2 - \omega^2)r_0^3 + r_0 - M} \right], \end{aligned} \quad (4.51)$$

with  $\pi_\phi^0$  is the drag force of non-rotating AdS-Schwarzschild black hole. The first linear term in  $a$  is simply due to a change of frame, but the term with coefficient  $C$  exhibits a nonlinear-enhancement of the drag force in the presence of angular momentum.

### 4.3.1 Static solution

Generalization of the arbitrary great circle solutions (4.29) to Kerr-AdS black holes is very difficult because of the complexity of the equations of motion. However, we can still solve these equations for a particular solution where we consider the string to be static. We will define shortly what we mean by static. This kind of solution can already capture the drag force effect of a rotating plasma. In the equatorial plane, the effect should be the same as considering a moving string in a non-rotating black hole by switching observers. For motion that is not equatorial, we will find a new force due to the anisotropy breaking by the angular momentum. We expect it to be centripetal force-like and drive the motion back to equatorial orbits. Specifically this means that this force will not depend on the direction of the angular momentum, but only on its magnitude. To lowest order in  $a$  therefore, this contribution goes as  $a^2$ . Here we will compute this lowest order consequence of anisotropy by expanding and solving the static equations of motion to order  $a^2$ . This will establish the lowest order contribution of anisotropic effects to the drag force. In the rotating black hole case, the static solution is not the time-independent solution with  $\theta = \theta(r)$  and  $\phi = \phi(r)$ .

There is a subtle aspect of the Kerr-AdS metric in Boyer-Lindquist coordinates. It is actually not manifest asymptotically AdS metric at the boundary. We need to do the following coordinate transformation to obtain this.

$$\begin{aligned} T &= t, & \Phi &= \phi - al^2t, \\ y \cos \Theta &= r \cos \theta, & y^2 &= \frac{1}{\Xi} (r^2 \Delta_\theta + a^2 \sin^2 \theta). \end{aligned} \quad (4.52)$$

The full expression for the Kerr-AdS metric in coordinates  $T, y, \Theta, \Phi$  is very complicated. For  $M = 0$ , however it is the regular AdS metric

$$ds^2 = -(1 + l^2 y^2) dT^2 + \frac{1}{1 + l^2 y^2} dy^2 + y^2 (d\Theta^2 + \sin^2 \Theta d\Phi^2). \quad (4.53)$$

In this metric the static straight string, with  $\Theta = C_\Theta$  and  $\Phi = C_\Phi$  constants, is a solution of the equation of motion. This then corresponds to a “time-dependent” solution in Boyer-Lindquist coordinates

$$\phi = C_\Phi + a l^2 t, \quad (4.54)$$

$$\theta = \arccos\left(\frac{y}{r} \cos C_\Theta\right), \quad (4.55)$$

with

$$y^2 = \frac{r^2(r^2 + a^2)}{(1 - a^2 l^2 \sin^2 C_\Theta) r^2 + a^2 \cos^2 C_\Theta}. \quad (4.56)$$

That is nevertheless describing a static string. For finite  $M$ , we expect these constants to be function of  $r$  in Boyer-Lindquist coordinates. Thus the “static” ansatz as an expansion in small  $a$  is taken to be

$$\theta(r) = \theta_0(r) + a^2 \theta_1(r) + O(a^4), \quad (4.57)$$

$$\phi(t, r) = \phi_0(r) + a l^2 t \phi_t(r) + a \phi_1(r) + O(a^2). \quad (4.58)$$

Let’s consider  $\phi_0(r) = P_0$ ,  $\theta_0(r) = \Theta_0$ , and  $\phi_t(r) = P_t$  constants. From the mapping of coordinates above, immediately  $P_t$  can be set to 1. Solving the equations of motion order by order in power of  $a$ , we obtain

$$\phi_1(r) = - \int dr \frac{P_1}{r^4 h(r)}, \quad (4.59)$$

with  $P_1$  a constant. The solution for  $\theta_1$  is quite complicated, but for our purpose we will just need the near boundary solution which can be computed using Mathematica. Substituting the solutions, we find that the world sheet conjugate momenta in radial direction as an expansion of small  $a$  near the boundary are given by

$$\pi_\theta^r \approx \left( -3l^2 r + \frac{2T_2}{\sin(2\Theta_0)} + (1 - P_1^2) \frac{\log(r)}{M} - \frac{3}{r} + \dots \right) \frac{a^2}{2} \sin(2\Theta_0) + O(a^4), \quad (4.60)$$

$$\pi_\phi^r \approx P_1 \sin(\Theta_0)^2 a + O(a^2), \quad (4.61)$$

with  $T_2$  a constant.  $P_1$  can be fixed by comparing the result at  $P_t = 0$  with the equatorial solution (4.49) at zero angular velocity which gives us  $P_1 = -1$ .

Interestingly, this also fixes  $T_2 = 0$ . The conjugate momentum  $\pi_\theta^r$  has a singularity at  $r \rightarrow \infty$  which goes linearly in  $r$ . This singularity at  $r \rightarrow \infty$  corresponds to infinite mass of the quark [35]. In order to have a more realistic picture, we consider a finite large mass of quark by introducing a cut-off in the geometry near the boundary at  $r = r_c$  which in the bulk can be interpreted as the location of a probe D-brane where the string can end. Following [35], the static thermal rest mass of quark can be computed at leading order in  $a$  by setting  $P_t = 0$ ,

$$m_{rest} = \frac{1}{2\pi\alpha'} \left( r_c - \frac{1}{3l^2} \left( 2\pi T + \sqrt{4\pi^2 T^2 - 3l^2} \right) \right), \quad (4.62)$$

with  $T$  is the temperature of plasma written as (4.41). Then by evaluating conjugate momenta above at  $r = r_c$  we obtain the leading contribution of the conjugate momenta

$$\pi_\theta^r \approx - \left( 6\pi\alpha' l^2 m_{rest} + 2\pi T + \sqrt{4\pi^2 T^2 - 3l^2} \right) \frac{a^2}{2} \sin(2\Theta_0), \quad (4.63)$$

$$\pi_\phi^r \approx - \sin(\Theta_0)^2 a, \quad (4.64)$$

### 4.3.2 Drag force

Having the solution in the  $a$  expansion, now we are ready to compute the drag forces to leading order in double expansions of small  $a$  and  $\omega$ :

$$\frac{dp_\theta}{dt} \approx \pi_\theta^r(a \neq 0 \ll 1, \omega = 0)_{r \rightarrow \infty} + \pi_\theta^r(a = 0, \omega \neq 0 \ll 1)_{r \rightarrow \infty}, \quad (4.65)$$

$$\frac{dp_\phi}{dt} \approx \pi_\phi^r(a \neq 0 \ll 1, \omega = 0)_{r \rightarrow \infty} + \pi_\phi^r(a = 0, \omega \neq 0 \ll 1)_{r \rightarrow \infty}. \quad (4.66)$$

The  $(a = 0, \omega = 0)$  term is just a constant which can be set to zero. We have included in this expression the lowest order  $(a = 0, \omega \neq 0)$  solution, which is valid as long as both  $a$  and  $\omega$  are small. The leading contribution to  $\pi_\theta^r(a = 0)$  and  $\pi_\phi^r(a = 0)$  is simply  $\pi_\theta^r(a = 0) \approx \omega_\theta$  and  $\pi_\phi^r(a = 0) \approx \omega_\phi$ , with  $\omega_\theta$  and  $\omega_\phi$  are small. So, we obtain the leading contribution to the drag forces

$$\frac{dp_\theta}{dt} \approx \left( 3l^2 m_{rest} + \frac{1}{2\pi\alpha'} \left( 2\pi T + \sqrt{4\pi^2 T^2 - 3l^2} \right) \right) \frac{a^2}{2} \sin(2\Theta_0) - \frac{\omega_\theta}{2\pi\alpha'}, \quad (4.67)$$

$$\frac{dp_\phi}{dt} \approx - \frac{1}{2\pi\alpha'} (\omega_\phi - \sin(\Theta_0)^2 a). \quad (4.68)$$

Here we can see that at the poles, defined at  $\Theta_0 = 0$  and  $\Theta_0 = \pi$ , there is no additional drag forces to the static quark, with  $\omega_\theta = \omega_\phi = 0$ . These are unstable points for a generic value of  $\Theta_0$  that the drag force in  $\theta$  direction tends to drag the static quark to the equator,  $\Theta_0 = \pi/2$ . The general situation at instantaneous time is illustrated in figures 4.1, 4.2, 4.3, and 4.4. The figures describe

motion of quarks at different positions on the boundary with an uniform velocity (blue arrow), in Cartesian coordinates, or with

$$\begin{aligned}\omega_\theta &= \frac{1}{10}(\cos \phi - \sin \phi), \\ \omega_\phi &= -\frac{1}{10\theta}(\cos \phi + \sin \phi),\end{aligned}\tag{4.69}$$

in Polar coordinates, being seen from the north pole of  $S^2$  projected into a plane. The circle, with bold line, denotes the equator of  $S^2$ . The circular brown arrow is the direction of angular momentum of the black hole. The red arrows show direction of the drag force effect of the plasma with its length proportional to the strength how much the drag force needed to drive the quarks to the equatorial. We have drawn the figures for different values of  $a$  and  $M_T = (3l^2 m_{rest} + 2\pi T + \sqrt{4\pi^2 T^2 - 3l^2})/2$ , with  $1/\alpha' = 2\pi$ .

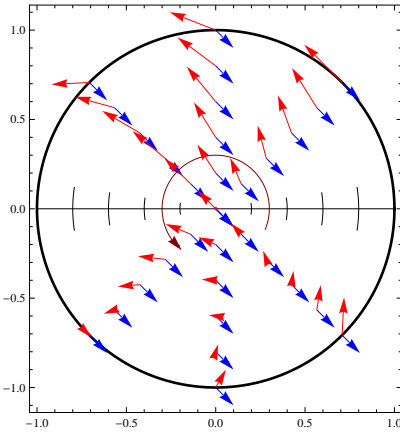


Figure 4.1:  $a = 0.1, M_T = 10$

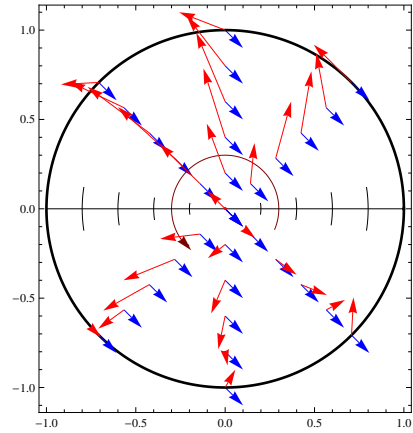
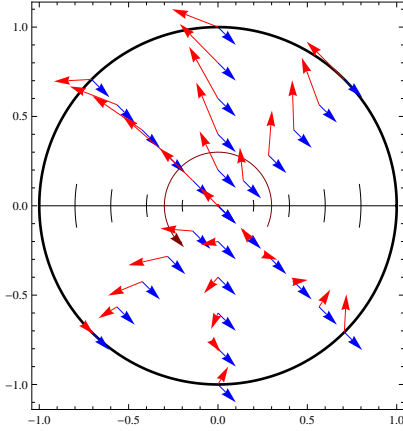
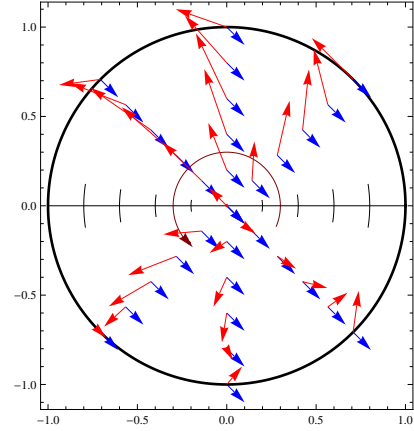


Figure 4.2:  $a = 0.1, M_T = 30$

Figure 4.3:  $a = 0.1, M_T = 20$ Figure 4.4:  $a = 0.118, M_T = 20$ 

## 4.4 Discussion and conclusion

In a non-rotating 4D global AdS-Schwarzschild black hole, the moving curved string solution (4.13), or in general (4.29), corresponds to a heavy quark moving in relativistic plasma living on a sphere  $S^2$ . The motion of this quark follows the geodesic of  $S^2$  namely a great circle. A novel physical consistency condition of this solution is that the string velocity  $\omega$  must be smaller than curvature radius of the black hole  $l$ . In this setting, we obtained the drag force as a function of the velocity  $\omega$  times the square of critical radius  $r_{Sch}$  defined by the largest positive root of  $h(r) = \omega^2$ . In the non-relativistic limit,  $\omega \rightarrow 0$ , this friction coefficient is simply the square of horizon  $r_H$  as in the flat case [35, 39]. Unlike the flat case, the friction coefficient has non-linear dependence on the temperature. Furthermore, the temperature of plasma in this background is bounded from below limited by the Hawking-Page transition to Euclidean AdS [9].

Our main result is to take a first step towards the study of anisotropic effects on drag force. For this, we considered the background metric of the rotating 4D Kerr-AdS black hole. For equatorial motion, the drag force is simply solved in the same way as the non-rotating case. The velocity  $\omega$  is now bounded non-trivially by the angular momentum  $a$  and curvature radius  $l$  (4.45). Also unlike the previous non-rotating case, at zero velocity,  $\omega = 0$ , the drag force does not vanish but is proportional to the angular momentum of the black hole  $a$ . This can be understood at the boundary as the drag force effect of dropping a static quark into a rotating plasma where the rotating plasma forces the quark to move accordingly with the plasma. In order to get a vanishing drag force,

the quark must move at a critical velocity

$$\omega_C = a \left( \frac{1 - a^2 l^2}{a^2 + r_{KH}^2} \right). \quad (4.70)$$

The drag force changes its direction when the quark's velocity crosses this critical velocity.

The generalization to arbitrary great circle motion is rather difficult. Taking a “static” solution in Boyer-Lindquist coordinates, corresponding to a static quark in a rotating plasma, we were able to compute the leading contribution to the drag force. Based on parity this drag force in the  $\theta$ -direction should be an even function of the angular momentum  $a$  whereas the drag force in the  $\phi$ -direction to linear order in  $a$  should be a generalization of the equatorial motion. As illustrated in figures 4.1 to 4.4, we conclude that the resulting drag force in a rotating strongly coupled plasma tends to drive the quark back to the equatorial plane and the amount of force is proportional to the static thermal rest mass of the quark  $m_{rest}$  and temperature of the plasma  $T$  in an analytic expression (4.67).



---

## BIBLIOGRAPHY

---

- [1] M. B. Green, J. H. Schwarz and E. Witten, "SUPERSTRING THEORY. VOL. 1: INTRODUCTION," Cambridge, Uk: Univ. Pr. ( 1987) 469 P. ( Cambridge Monographs On Mathematical Physics); J. Polchinski, "String theory. Vol. 1: An introduction to the bosonic string," Cambridge, UK: Univ. Pr. (1998) 402 p; K. Becker, M. Becker and J. H. Schwarz, "String theory and M-theory: A modern introduction," Cambridge, UK: Cambridge Univ. Pr. (2007) 739 p.
- [2] J. M. Maldacena, "The large N limit of superconformal field theories and supergravity," Adv. Theor. Math. Phys. **2** (1998) 231 [Int. J. Theor. Phys. **38** (1999) 1113] [arXiv:hep-th/9711200].
- [3] S. S. Gubser, I. R. Klebanov and A. M. Polyakov, "Gauge theory correlators from non-critical string theory," Phys. Lett. B **428**, 105 (1998) [arXiv:hep-th/9802109].
- [4] E. Witten, "Anti-de Sitter space and holography," Adv. Theor. Math. Phys. **2**, 253 (1998) [arXiv:hep-th/9802150].
- [5] S. Caron-Huot, P. Kovtun, G. D. Moore, A. Starinets and L. G. Yaffe, "Photon and dilepton production in supersymmetric Yang-Mills plasma," JHEP **0612**, 015 (2006) [arXiv:hep-th/0607237].
- [6] B. Duplantier, "Brownian Motion, 'Diverse and Undulating'," arXiv:0705.1951v1 [cond-mat.stat-mech].
- [7] G. 't Hooft, "A planar diagram theory for strong interactions," Nucl. Phys. B **72**, 461 (1974).
- [8] F. Karsch, "Lattice simulations of the thermodynamics of strongly interacting elementary particles and the exploration of new phases of matter in relativistic heavy ion collisions," J. Phys. Conf. Ser. **46**, 122 (2006) [arXiv:hep-lat/0608003].
- [9] E. Witten, "Anti-de Sitter space, thermal phase transition, and confinement in gauge theories," Adv. Theor. Math. Phys. **2**, 505 (1998) [arXiv:hep-th/9803131].



- [10] L. Susskind and E. Witten, "The holographic bound in anti-de Sitter space," arXiv:hep-th/9805114.
- [11] G. Policastro, D. T. Son and A. O. Starinets, "From AdS/CFT correspondence to hydrodynamics," JHEP **0209**, 043 (2002) [arXiv:hep-th/0205052].
- [12] J. Erlich, E. Katz, D. T. Son and M. A. Stephanov, "QCD and a holographic model of hadrons," Phys. Rev. Lett. **95**, 261602 (2005) [arXiv:hep-ph/0501128].
- [13] J. de Boer, E. P. Verlinde and H. L. Verlinde, "On the holographic renormalization group," JHEP **0008**, 003 (2000) [arXiv:hep-th/9912012].
- [14] M. A. Shifman, A. I. Vainshtein and V. I. Zakharov, "QCD And Resonance Physics. Sum Rules," Nucl. Phys. B **147**, 385 (1979).
- [15] A. Karch, E. Katz, D. T. Son and M. A. Stephanov, "Linear confinement and AdS/QCD," Phys. Rev. D **74**, 015005 (2006) [arXiv:hep-ph/0602229].
- [16] C. P. Herzog, "A holographic prediction of the deconfinement temperature," Phys. Rev. Lett. **98**, 091601 (2007) [arXiv:hep-th/0608151].
- [17] <http://www.gsi.de/fair/experiments/CBM/Phasendiagram.jpg>.
- [18] <http://gruppo3.ca.infn.it/usai/images/dileptons.jpg>.
- [19] A. Nata Atmaja and K. Schalm, "Photon and Dilepton Production in Soft Wall AdS/QCD," arXiv:0802.1460 [hep-th]. Published in JHEP **1008**:124, 2010.
- [20] A. N. Atmaja, J. de Boer and M. Shigemori, "Holographic Brownian Motion and Time Scales in Strongly Coupled Plasmas," arXiv:1002.2429 [hep-th]. To be published in Nucl. Phys. B.
- [21] A. Nata Atmaja and K. Schalm, "Drag Force in 4D Kerr-AdS Black Hole," work in progress.
- [22] M. Bianchi, D. Z. Freedman and K. Skenderis, "Holographic Renormalization," Nucl. Phys. B **631**, 159 (2002) [arXiv:hep-th/0112119].
- [23] D. Mateos, "String theory and RHIC physics: The fundamental story," String Conference 2007, Madrid, Spain.  
D. Mateos and L. Patiño, "Bright branes for strongly coupled plasmas," JHEP **0711**, 025 (2007) [arXiv:0709.2168 [hep-th]].
- [24] P. Stankus, "Direct photon production in relativistic heavy-ion collisions," Ann. Rev. Nucl. Part. Sci. **55**, 517 (2005).

- [25] M. Le Bellac, “Thermal Field Theory,” Cambridge (1996). Cambridge, UK: Univ. Pr. (1996)
- [26] D. T. Son and A. O. Starinets, “Minkowski-space correlators in AdS/CFT correspondence: Recipe and applications,” JHEP **0209**, 042 (2002) [arXiv:hep-th/0205051].
- [27] S. Scherer and M. R. Schindler, “A chiral perturbation theory primer,” arXiv:hep-ph/0505265.
- [28] P. K. Kovtun and A. O. Starinets, “Quasinormal modes and holography,” Phys. Rev. D **72**, 086009 (2005) [arXiv:hep-th/0506184].
- [29] F. W. J. Olver, “The Asymptotic Solution of Linear Differential Equations of Second Order for Large Values of a Parameter,” Phil. Trans. Roy. Soc. Lon. Series A. Mathematical and Physical Sciences, **930** 247, (1954); F. W. J. Olver, “Asymptotics and Special Functions,” A K Peters, Wellesley (1997).
- [30] P. Kovtun, D. T. Son and A. O. Starinets, “Holography and hydrodynamics: Diffusion on stretched horizons,” JHEP **0310**, 064 (2003) [arXiv:hep-th/0309213].
- [31] D. Mateos, R. C. Myers and R. M. Thomson, “Holographic viscosity of fundamental matter,” Phys. Rev. Lett. **98**, 101601 (2007) [arXiv:hep-th/0610184].
- [32] R. Brown, “A brief account of microscopical observations made in the months of June, July and August, 1827, on the particles contained in the pollen of plants; and on the general existence of active molecules in organic and inorganic bodies,” Philos. Mag. **4**, 161 (1828); reprinted in Edinburgh New Philos. J. **5**, 358 (1928).
- [33] G. E. Uhlenbeck and L. S. Ornstein, “On The Theory Of The Brownian Motion,” Phys. Rev. **36**, 823 (1930); S. Chandrasekhar, “Stochastic problems in physics and astronomy,” Rev. Mod. Phys. **15**, 1 (1943); M. C. Wang and G. E. Uhlenbeck, “On the Theory of the Brownian Motion II,” Rev. Mod. Phys. **17**, 323 (1945).
- [34] P. Kovtun, D. T. Son and A. O. Starinets, “Viscosity in strongly interacting quantum field theories from black hole physics,” Phys. Rev. Lett. **94**, 111601 (2005) [arXiv:hep-th/0405231].
- [35] C. P. Herzog, A. Karch, P. Kovtun, C. Kozcaz and L. G. Yaffe, “Energy loss of a heavy quark moving through  $N = 4$  supersymmetric Yang-Mills plasma,” JHEP **0607**, 013 (2006) [arXiv:hep-th/0605158].
- [36] A. Karch and E. Katz, “Adding flavor to AdS/CFT,” JHEP **0206**, 043 (2002) [arXiv:hep-th/0205236].

- [37] J. Erdmenger, N. Evans, I. Kirsch and E. Threlfall, "Mesons in Gauge/Gravity Duals - A Review," *Eur. Phys. J. A* **35**, 81 (2008) [arXiv:0711.4467 [hep-th]].
- [38] H. Liu, K. Rajagopal and U. A. Wiedemann, "Calculating the jet quenching parameter from AdS/CFT," *Phys. Rev. Lett.* **97**, 182301 (2006) [arXiv:hep-ph/0605178].
- [39] S. S. Gubser, "Drag force in AdS/CFT," *Phys. Rev. D* **74**, 126005 (2006) [arXiv:hep-th/0605182].
- [40] C. P. Herzog, "Energy loss of heavy quarks from asymptotically AdS geometries," *JHEP* **0609**, 032 (2006) [arXiv:hep-th/0605191].
- [41] J. Casalderrey-Solana and D. Teaney, "Heavy quark diffusion in strongly coupled  $N = 4$  Yang Mills," *Phys. Rev. D* **74**, 085012 (2006) [arXiv:hep-ph/0605199].
- [42] C. P. Herzog and D. T. Son, "Schwinger-Keldysh propagators from AdS/CFT correspondence," *JHEP* **0303**, 046 (2003) [arXiv:hep-th/0212072].
- [43] J. Polchinski, "Dirichlet-Branes and Ramond-Ramond Charges," *Phys. Rev. Lett.* **75**, 4724 (1995) [arXiv:hep-th/9510017].
- [44] O. Aharony, S. S. Gubser, J. M. Maldacena, H. Ooguri and Y. Oz, "Large  $N$  field theories, string theory and gravity," *Phys. Rept.* **323**, 183 (2000) [arXiv:hep-th/9905111].
- [45] A. J. Niemi and G. W. Semenoff, "Finite Temperature Quantum Field Theory In Minkowski Space," *Annals Phys.* **152**, 105 (1984).
- [46] V. Balasubramanian, P. Kraus, A. E. Lawrence and S. P. Trivedi, "Holographic probes of anti-de Sitter space-times," *Phys. Rev. D* **59**, 104021 (1999) [arXiv:hep-th/9808017].
- [47] V. Balasubramanian, S. B. Giddings and A. E. Lawrence, "What do CFTs tell us about anti-de Sitter spacetimes?," *JHEP* **9903**, 001 (1999) [arXiv:hep-th/9902052].
- [48] V. Balasubramanian, P. Kraus and A. E. Lawrence, "Bulk vs. boundary dynamics in anti-de Sitter spacetime," *Phys. Rev. D* **59**, 046003 (1999) [arXiv:hep-th/9805171].
- [49] J. B. Hartle and S. W. Hawking, "Path Integral Derivation Of Black Hole Radiance," *Phys. Rev. D* **13**, 2188 (1976).
- [50] W. G. Unruh, "Notes on black hole evaporation," *Phys. Rev. D* **14**, 870 (1976).

- [51] W. Israel, "Thermo field dynamics of black holes," *Phys. Lett. A* **57**, 107 (1976).
- [52] E. Barnes, D. Vaman, C. Wu and P. Arnold, "Real-time finite-temperature correlators from AdS/CFT," arXiv:1004.1179 [hep-th].
- [53] S. S. Gubser, "Momentum fluctuations of heavy quarks in the gauge-string duality," *Nucl. Phys. B* **790**, 175 (2008) [arXiv:hep-th/0612143].
- [54] H. Liu, K. Rajagopal and U. A. Wiedemann, "Wilson loops in heavy ion collisions and their calculation in AdS/CFT," *JHEP* **0703**, 066 (2007) [arXiv:hep-ph/0612168].
- [55] J. Casalderrey-Solana and D. Teaney, "Transverse momentum broadening of a fast quark in a  $N = 4$  Yang Mills plasma," *JHEP* **0704**, 039 (2007) [arXiv:hep-th/0701123].
- [56] S. Bhattacharyya, V. E. Hubeny, S. Minwalla and M. Rangamani, "Nonlinear Fluid Dynamics from Gravity," *JHEP* **0802**, 045 (2008) [arXiv:0712.2456 [hep-th]].
- [57] S. Bhattacharyya *et al.*, "Local Fluid Dynamical Entropy from Gravity," *JHEP* **0806**, 055 (2008) [arXiv:0803.2526 [hep-th]].
- [58] P. M. Chesler and L. G. Yaffe, "Horizon formation and far-from-equilibrium isotropization in supersymmetric Yang-Mills plasma," *Phys. Rev. Lett.* **102**, 211601 (2009) [arXiv:0812.2053 [hep-th]].
- [59] P. M. Chesler and L. G. Yaffe, "The wake of a quark moving through a strongly-coupled  $\mathcal{N} = 4$  supersymmetric Yang-Mills plasma," *Phys. Rev. Lett.* **99**, 152001 (2007) [arXiv:0706.0368 [hep-th]].
- [60] P. M. Chesler and L. G. Yaffe, "The stress-energy tensor of a quark moving through a strongly-coupled  $N=4$  supersymmetric Yang-Mills plasma: comparing hydrodynamics and AdS/CFT," *Phys. Rev. D* **78**, 045013 (2008) [arXiv:0712.0050 [hep-th]].
- [61] F. Becattini, F. Piccinini and J. Rizzo, "Angular momentum conservation in heavy ion collisions at very high energy," *Phys. Rev. C* **77**, 024906 (2008) [arXiv:0711.1253 [nucl-th]].
- [62] N. Armesto *et al.*, "Heavy Ion Collisions at the LHC - Last Call for Predictions," *J. Phys. G* **35**, 054001 (2008) [arXiv:0711.0974 [hep-ph]].
- [63] D. T. Son and A. O. Starinets, "Viscosity, Black Holes, and Quantum Field Theory," *Ann. Rev. Nucl. Part. Sci.* **57**, 95 (2007) [arXiv:0704.0240 [hep-th]].
- [64] A. E. Lawrence and E. J. Martinec, "Black Hole Evaporation Along Macroscopic Strings," *Phys. Rev. D* **50**, 2680 (1994) [arXiv:hep-th/9312127].

- [65] S. J. Rey and J. T. Yee, “Macroscopic strings as heavy quarks in large N gauge theory and anti-de Sitter supergravity,” *Eur. Phys. J. C* **22**, 379 (2001) [arXiv:hep-th/9803001].
- [66] R. C. Myers, A. O. Starinets and R. M. Thomson, “Holographic spectral functions and diffusion constants for fundamental matter,” *JHEP* **0711**, 091 (2007) [arXiv:0706.0162 [hep-th]].
- [67] J. de Boer, V. E. Hubeny, M. Rangamani and M. Shigemori, “Brownian motion in AdS/CFT,” *JHEP* **0907**, 094 (2009) [arXiv:0812.5112 [hep-th]].
- [68] D. T. Son and D. Teaney, “Thermal Noise and Stochastic Strings in AdS/CFT,” *JHEP* **0907**, 021 (2009) [arXiv:0901.2338 [hep-th]].
- [69] G. C. Giecold, E. Iancu and A. H. Mueller, “Stochastic trailing string and Langevin dynamics from AdS/CFT,” *JHEP* **0907**, 033 (2009) [arXiv:0903.1840 [hep-th]].
- [70] G. C. Giecold, “Heavy quark in an expanding plasma in AdS/CFT,” *JHEP* **0906**, 002 (2009) [arXiv:0904.1874 [hep-th]].
- [71] J. Casalderrey-Solana, K. Y. Kim and D. Teaney, “Stochastic String Motion Above and Below the World Sheet Horizon,” *JHEP* **0912**, 066 (2009) [arXiv:0908.1470 [hep-th]].
- [72] K. Skenderis, “Lecture notes on holographic renormalization,” *Class. Quant. Grav.* **19**, 5849 (2002) [arXiv:hep-th/0209067].
- [73] K. Skenderis and B. C. van Rees, “Real-time gauge/gravity duality: Prescription, Renormalization and Examples,” *JHEP* **0905**, 085 (2009) [arXiv:0812.2909 [hep-th]].
- [74] B. C. van Rees, “Real-time gauge/gravity duality and ingoing boundary conditions,” arXiv:0902.4010 [hep-th].
- [75] R. Kubo, “The fluctuation-dissipation theorem,” *Rep. Prog. Phys.* **29**, 255-284 (1966).
- [76] H. Mori, “Transport, collective motion, and Brownian motion,” *Prog. Theor. Phys.* **33**, 423 (1965).
- [77] R. Kubo, M. Toda, and N. Hashitsume, “Statistical Physics II – Nonequilibrium Statistical Mechanics,” Springer-Verlag.
- [78] M. Chernicoff, J. A. Garcia and A. Guijosa, “A Tail of a Quark in N=4 SYM,” *JHEP* **0909**, 080 (2009) [arXiv:0906.1592 [hep-th]].
- [79] N. D. Birrell and P. C. W. Davies, “Quantum Fields In Curved Space,” Cambridge, UK: Univ. Pr. (1982) 340p

- [80] K. Behrndt, M. Cvetič and W. A. Sabra, “Non-extreme black holes of five dimensional  $N = 2$  AdS supergravity,” Nucl. Phys. B **553**, 317 (1999) [arXiv:hep-th/9810227].
- [81] M. Cvetič *et al.*, “Embedding AdS black holes in ten and eleven dimensions,” Nucl. Phys. B **558**, 96 (1999) [arXiv:hep-th/9903214].
- [82] P. Kraus, F. Larsen and S. P. Trivedi, “The Coulomb branch of gauge theory from rotating branes,” JHEP **9903**, 003 (1999) [arXiv:hep-th/9811120].
- [83] J. G. Russo and K. Sfetsos, “Rotating D3 branes and QCD in three dimensions,” Adv. Theor. Math. Phys. **3**, 131 (1999) [arXiv:hep-th/9901056].
- [84] E. Caceres and A. Guijosa, “Drag force in charged  $N = 4$  SYM plasma,” JHEP **0611**, 077 (2006) [arXiv:hep-th/0605235].
- [85] C. P. Herzog and A. Vuorinen, “Spinning Dragging Strings,” JHEP **0710**, 087 (2007) [arXiv:0708.0609 [hep-th]].
- [86] T. Harmark, J. Natario and R. Schiappa, “Greybody Factors for d-Dimensional Black Holes,” arXiv:0708.0017 [hep-th].
- [87] J. Dunkel and P. Hänggi, “Relativistic Brownian Motion,” arXiv:0812.1996 [cond-mat].
- [88] P. Hänggi, P. Talkner and M. Borkovec, “Reaction-rate theory: fifty years after Kramers,” Rev. Mod. Phys. **62**, 251 (1990).
- [89] A.A. Dubkov, P. Hänggi, and I. Goychuk, “Non-linear Brownian motion: the problem of obtaining the thermal Langevin equation for a non-Gaussian bath,” J. Stat. Mech. P01034 (2009).
- [90] G. F. Efremov “A Fluctuation Dissipation Theorem for Nonlinear Media,” Sov. Phys. JETP **28**, 1232 (1969); M. S. Gupta, “Thermal fluctuations in driven nonlinear resistive systems,” Phys. Rev. A **18**, 2725 (1978); M. G. Gupta, “Thermal Noise in Nonlinear Resistive Devices and Its Circuit Representation,” Proc. IEEE **70**, 788 (1982); G. N. Bochkov, Yu. E. Kuzovlev, “Nonlinear fluctuation-dissipation relations and stochastic models in nonequilibrium thermodynamics : I. Generalized fluctuation-dissipation theorem,” Physica A **106**, 443 (1981); E. Wang and U. Heinz, “Generalized fluctuation-dissipation theorem for nonlinear response functions,” Phys. Rev. D **66**, 025008 (2002)
- [91] S. D. Avramis and K. Sfetsos, “Supergravity and the jet quenching parameter in the presence of R-charge densities,” JHEP **0701**, 065 (2007) [arXiv:hep-th/0606190].

- [92] S. D. Avramis, K. Sfetsos and D. Zoakos, “On the velocity and chemical-potential dependence of the heavy-quark interaction in  $N = 4$  SYM plasmas,” *Phys. Rev. D* **75**, 025009 (2007) [arXiv:hep-th/0609079].
- [93] N. Armesto, J. D. Edelstein and J. Mas, “Jet quenching at finite ’t Hooft coupling and chemical potential from AdS/CFT,” *JHEP* **0609**, 039 (2006) [arXiv:hep-ph/0606245].
- [94] F. L. Lin and T. Matsuo, “Jet quenching parameter in medium with chemical potential from AdS/CFT,” *Phys. Lett. B* **641**, 45 (2006) [arXiv:hep-th/0606136].
- [95] J. Mas, “Shear viscosity from R-charged AdS black holes,” *JHEP* **0603**, 016 (2006) [arXiv:hep-th/0601144].
- [96] M. Cvetič and S. S. Gubser, “Thermodynamic Stability and Phases of General Spinning Branes,” *JHEP* **9907**, 010 (1999) [arXiv:hep-th/9903132].
- [97] S. Bhattacharyya, S. Lahiri, R. Loganayagam and S. Minwalla, “Large rotating AdS black holes from fluid mechanics,” *JHEP* **0809**, 054 (2008) [arXiv:0708.1770 [hep-th]].
- [98] P. Hayden and J. Preskill, “Black holes as mirrors: quantum information in random subsystems,” *JHEP* **0709**, 120 (2007) [arXiv:0708.4025 [hep-th]].
- [99] Y. Sekino and L. Susskind, “Fast Scramblers,” *JHEP* **0810**, 065 (2008) [arXiv:0808.2096 [hep-th]].
- [100] P. Arnold and L. G. Yaffe, “Effective theories for real-time correlations in hot plasmas,” *Phys. Rev. D* **57**, 1178 (1998) [arXiv:hep-ph/9709449].
- [101] N. Iqbal and H. Liu, “Universality of the hydrodynamic limit in AdS/CFT and the membrane paradigm,” arXiv:0809.3808 [hep-th].
- [102] L. Fidkowski, V. Hubeny, M. Kleban and S. Shenker, “The black hole singularity in AdS/CFT,” *JHEP* **0402**, 014 (2004) [arXiv:hep-th/0306170].
- [103] E. V. Shuryak, “Strongly coupled quark-gluon plasma: The status report,” arXiv:hep-ph/0608177.
- [104] P. F. Kolb, J. Sollfrank and U. W. Heinz, “Anisotropic transverse flow and the quark-hadron phase transition,” *Phys. Rev. C* **62**, 054909 (2000) [arXiv:hep-ph/0006129].
- [105] P. F. Kolb, P. Huovinen, U. W. Heinz and H. Heiselberg, “Elliptic flow at SPS and RHIC: From kinetic transport to hydrodynamics,” *Phys. Lett. B* **500**, 232 (2001) [arXiv:hep-ph/0012137].

- 
- [106] P. F. Kolb and U. W. Heinz, "Hydrodynamic description of ultrarelativistic heavy-ion collisions," arXiv:nucl-th/0305084.
- [107] J. M. Maldacena, "Wilson loops in large N field theories," Phys. Rev. Lett. **80**, 4859 (1998) [arXiv:hep-th/9803002].
- [108] S. J. Rey, S. Theisen and J. T. Yee, "Wilson-Polyakov loop at finite temperature in large N gauge theory and anti-de Sitter supergravity," Nucl. Phys. B **527**, 171 (1998) [arXiv:hep-th/9803135].
- [109] S. Hemming and L. Thorlacius, "Thermodynamics of Large AdS Black Holes," JHEP **0711**, 086 (2007) [arXiv:0709.3738 [hep-th]].
- [110] S. W. Hawking, C. J. Hunter and M. Taylor, "Rotation and the AdS/CFT correspondence," Phys. Rev. D **59**, 064005 (1999) [arXiv:hep-th/9811056].
- [111] G. W. Gibbons, M. J. Perry and C. N. Pope, "The first law of thermodynamics for Kerr - anti-de Sitter black holes," Class. Quant. Grav. **22**, 1503 (2005) [arXiv:hep-th/0408217].





---

# SUMMARY

---

QGP is one of the phases in QCD where quarks are deconfined and form a fluid with gluons. It could exist in an environment with strong or weak coupling. However, there are many indications that the QGPs created at RHIC are strongly coupled. Hence, we need a tool that goes beyond perturbation theory. AdS/CFT (or in general gauge/gravity) correspondence is one of the tools which we discussed briefly in chapter 1. In this thesis, we used AdS/CFT correspondence to compute some of observables of QGP such as photon and dilepton production rates, mean-free path time of the plasma constituents, and anisotropic drag force effect to the elliptic flow.

There is still no a complete description of gauge/gravity correspondence where the dual theory is QCD. Nevertheless, there are models constructed to mimic some of phenomenological properties of QCD such as linear confinement, lowest mesons spectrum, and etc. One of these models is soft-wall AdS/QCD which is an interesting model particularly because the critical temperature is found to be relatively close to the current lattice computation. This model has non-trivial dilaton background in addition to the gravity background. We used this model to compute photon and dilepton production rates in chapter 2.

The observable that we computed in photon and dilepton production rates is the spectral density function  $\chi(K)$  given as the imaginary part of the retarded electromagnetic current-current correlation function. For this purpose, we only considered the quadratic terms of the  $U(1)$  gauge field in softwall AdS/QCD action. Using Minkowski prescription by Son and Starinets, we computed the results analytically at low and high frequency and then confirmed them with numerical result.

At low frequency, the result depended on the IR-cutoff parameter  $c$ , with  $c \geq 0$ . Unfortunately, for some higher values of  $c$  we found no peaks in the spectrum which meant no signal of confinement. This may be due to the fact that softwall AdS/QCD does not take into account the backreaction from dilaton field to the geometry. Softwall AdS/QCD is somehow much cruder description of QCD in the unstable regime  $c > 0.419035$ . We showed this by comparing with the computation from  $\mathcal{N} = 2$  SQCD theory, where the peaks appear in the spectrum. Although softwall AdS/QCD does not capture the confinement in

the unstable regime, it still describes the IR-consequences of a mass gap from the confinement phase remarkably well in the stable regime  $0 \leq c \leq 0.419035$ . We also computed the electrical conductivity  $\sigma$  and found that the IR-cutoff parameter  $c$  gives a damping effect.

The mean-free path time of the plasma can be computed by studying the Brownian motion of an external quark in the plasma. The Brownian motion is described by the generalized Langevin equation which basically consists of two terms: friction and random force terms. We showed in chapter 3 that for a simple model, the mean-free path time can be extracted from two- and four-point functions of random force  $R$  at low frequency limit  $\omega \rightarrow 0$ .

In the bulk, this Brownian motion is represented by the motion of a fundamental string  $X$  at the boundary where the action is given by Nambu-Goto action under some black hole backgrounds. We computed the two- and four-point functions using holographic prescription to the small fluctuation around static strings configuration. Holographically, the boundary value of the string  $x = X(r \rightarrow \infty)$  couples to the total force  $F$  on an external quark. In the large mass limit,  $m \rightarrow \infty$ , the total force is equal to random force. We also used Minkowski prescription by Skenderis and van Rees to compute the real-time propagators and holographic renormalization to remove the UV divergence that appear at the boundary. However, there was also an IR divergence near the horizon. We argued that this IR divergence can be removed by introducing an IR cut-off to the geometry.

An explicit computation of the mean-free path time was done for the case of non-rotating BTZ black hole, which corresponds to a neutral plasma. We generalized the computation for various black hole backgrounds and obtained a general formula of the mean-free path time. This generalized formula was used to compute the mean-free path time of STU black holes, which corresponds to charged plasma. The results showed that the mean-free path time is proportional to the inverse of  $\log \eta$ , with  $\eta$  is a function of Hawking temperature  $T_H$  and charge  $\kappa$ . When  $\kappa$  increases, the plot 3.4 showed that  $\eta$  decreases for 1- and 2-charge cases and increases for 3-charge case. These results are in accordance with our intuition as for the black holes with a fixed mass the mean free path-time increases when  $\kappa$  increases in all of the charge cases. We also computed friction coefficient of STU black holes and found that the result at low frequency limit,  $\omega \rightarrow 0$ , is similar to the drag force computation at non-relativistic limit.

The non-central collisions at the RHIC experiments show an anisotropic particle distribution of QGP. The signal of this anisotropic distribution can be seen in some of observables e.g. jet-quenching or drag force. In gauge/gravity correspondence's language, the anisotropic distribution can be related to the anisotropic of black hole backgrounds. One way to realize this is by considering the rotating black holes. This is the main focus of chapter 4.

At first, we considered the non-rotating 4D AdS-Schwarzschild black hole. The drag force in gravity side is interpreted as a world sheet conjugate momen-

tum in radial direction of the Nambu-Goto action evaluated at the boundary. With a linear ansatz, we obtained that the total drag force of arbitrary great circle is proportional to the angular velocity of the string  $\omega$  and the square of critical radius  $r_{Sch}$ , which is similar to the flat case [35, 39]. Unfortunately, we found that the friction coefficient is not a linear function of the plasma temperature  $T$ .

We then continued the study of the drag force to the 4D Kerr-AdS black hole. A simple computation was done for equatorial case. Unlike the case of 4D AdS-Schwarzschild black hole, the drag force does not vanish if we take the angular velocity of the string to be zero,  $\omega = 0$ , but instead it is proportional to the angular momentum of the black hole  $a$ . For more general case, we considered a particular “static” solution in Boyer-Lindquist coordinates. This solution contributes to the leading order of drag forces at small angular momentum  $a$  with vanishing velocities  $\omega = 0$ . We plotted the drag forces for different values of angular momentum  $a$  and parameter  $M_T$ . We found that the drag force in  $\theta$ -direction tends to drive the quark back to the equatorial plane and the amount of force is proportional to the static thermal rest mass of the quark  $m_{rest}$  and temperature of the plasma  $T$ .



---

# SAMENVATTING

---

Quark-gluonplasma (QGP) is een van de fasen van quantumchromodynamica (QCD), de theorie die de sterke kracht beschrijft. In deze fase zijn quarks niet gebonden in mesonen en hadronen (confined) maar vormen daarentegen een vloeistof met gluonen (deconfined). Deze fase kan bestaan in een omgeving met zowel sterke als zwakke effectieve koppelingsconstante. In de QGPs gemaakt bij botsingen in de RHIC-versneller zijn er sterke aanwijzingen dat deze QGPs gekenmerkt worden door een sterke effectieve koppelingsconstante. Daarom hebben we een methode nodig die verder gaat dan storingsrekening. Anti-de Sitter/conforme veldentheorie-dualiteit (AdS/CFT-dualiteit of, in het algemeen, ijk/zwaartekrachtsdualiteit) is een van deze methoden. Deze methode is kort beschreven in hoofdstuk 1. In dit proefschrift hebben we de AdS/CFT-dualiteit gebruikt om sommige observabelen van een QGP te berekenen. Voorbeelden van deze observabelen zijn de productiefrequenties van fotonen en dileptonen, de gemiddelde tijd tussen botsingen van de elementen van het plasma en anisotrope weerstand als gevolg van een elliptische stroming.

Er is nog steeds geen complete beschrijving van de ijk/zwaartekrachts dualiteit waarbij de duale theorie QCD is. Desondanks zijn er modellen die fenomenen van QCD zoals lineaire opsluiting en lichtste mesonenspectra nabootsen. Een van deze modellen is de zachte muur-AdS/QCD, wat een interessant model is omdat de kritische temperatuur relatief dicht bij de kritische temperatuur van roosterberekeningen ligt. Dit model heeft, naast de zwaartekracht-achtergrond, een niet-triviale dilaton-achtergrond. In 2 hebben we dit model gebruikt om productiefrequenties van fotonen en dileptonen te berekenen.

De observabele voor de productiefrequenties van fotonen en dileptonen die we berekend hebben is de spectrale dichtheidsfunctie  $\chi(K)$ , het imaginaire gedeelte van de geretardeerde elektromagnetische stroom-stroom-correlatiefunctie. Voor dit doel hebben we alleen de kwadratische termen van het  $U(1)$  ijkveld in de zachte muur AdS/QCD beschouwd. Met behulp van de Minkowski-methode van Son en Starinets hebben we de analytische resultaten voor lage en hoge frequentie berekend en vergeleken met numerieke resultaten.

Bij lage frequentie bleek het resultaat af te hangen van de IR-cutoff parameter  $c$ , met  $c \geq 0$ . Helaas vonden we voor sommige hogere waarden van  $c$  geen pieken in het spectrum wat betekent dat er geen confinement optreedt. Dit kan komen doordat de zachte muur-AdS/QCD de terugkoppeling van het dilatonveld op de geometrie niet meeneemt. Zachte muur-AdS/QCD is een onnauwkeurige beschrijving van QCD in het onstabiele domein  $c > 0.419035$ . We hebben dit laten zien door zachte muur-AdS/QCD te vergelijken met berekeningen van de  $\mathcal{N} = 2$  SQCD-theorie, waar pieken in het spectrum optreden. Hoewel zachte muur-AdS/QCD geen confinement in het onstabiele regime heeft beschrijft het de IR-gevolgen van een massasplitsing van de confined fase opvallend goed in het stabiele domein  $0 \leq c \leq 0.419035$ . We hebben ook de elektrische geleiding  $\sigma$  berekend en vonden dat de IR-cutoff parameter  $c$  een dempend effect heeft.

De gemiddelde tijd tussen botsingen van het plasma kan berekend worden door het bestuderen van Brownse beweging van een extern quark in het plasma. De Brownse beweging wordt beschreven door de veralgemeniseerde Langevinvergelijking, welke bestaat uit twee termen: frictietermen en termen die een kracht ten gevolge van willekeurige botsingen beschrijven. We hebben in 3 laten zien dat voor een eenvoudig model de gemiddelde tijd tussen botsingen berekend kan worden met behulp van de twee- en vierpuntsfuncties van de kracht ten gevolge van willekeurige botsingen  $R$  in de lage frequentielimiet  $\omega \rightarrow 0$ .

In de bulk wordt deze Brownse beweging gerepresenteerd door de beweging van een fundamentele snaar  $X$  aan de rand, waarbij de actie gegeven is door de Nambu-Gotoactie in een zwart gat-achtergrond. Gebruik makend van de holografische beschrijving van een kleine fluctuatie rond statische snaarconfiguraties hebben we de twee- en vierpuntsfuncties berekend. Vanuit holografisch perspectief koppelt een fundamentele snaar aan de rand  $x = X(r \rightarrow \infty)$  aan de totale kracht  $F$  op een externe quark. In de hoge massalimiet  $m \rightarrow \infty$  is de totale kracht gelijk aan de kracht ten gevolge van willekeurige botsingen. We hebben ook de Minkowskibeschrijving van Skenderis en van Rees gebruikt om de reële tijdpropagatoren en de holografische renormalisatie van de UV-divergentie die aan de rand optreedt te berekenen. Er trad echter ook een IR divergentie op nabij de horizon. We hebben beargumenteerd dat deze divergentie verwijderd kan worden door een IR cutoff in de geometrie te implementeren.

We hebben een expliciete berekening van de gemiddelde tijd tussen botsingen gedaan voor het geval van een niet roterend BTZ zwart gat, wat correspondeert met een neutraal plasma. We hebben deze berekening veralgemeniseerd naar verscheidene zwart gat-achtergronden en hebben een algemene formule van de gemiddelde tijd tussen botsingen verkregen. Vervolgens hebben we deze algemene formule gebruikt om de gemiddelde tijd tussen botsingen van STU zwarte gaten, overeenkomend met een geladen plasma, te berekenen. De resultaten tonen dat de gemiddelde tijd tussen botsingen proportioneel is

met de inverse van  $\log \eta$ , met  $\eta$  een functie van de Hawkingtemperatuur  $T_H$  en lading  $\kappa$ . Wanneer  $\kappa$  toeneemt blijkt uit de grafiek 3.4 dat  $\eta$  afneemt voor de één- en tweeladinggevallen en toeneemt voor het drieladinggeval. Deze resultaten zijn in overeenstemming met onze intuïtie dat voor een zwart gat met een vaste massa de gemiddelde tijd tussen botsingen toeneemt wanneer  $\kappa$  toeneemt in alle gevallen met lading. We hebben eveneens de weerstandscoefficient van een STU zwart gat berekend en gevonden dat het resultaat in de lage frequentielimiet,  $\omega \rightarrow 0$ , vergelijkbaar is met de weerstandsberekening in de niet-relativistische limiet.

De niet-centrale botsingen bij de RHIC experimenten tonen een anisotrope deeltjesverdeling van het QGP. Het signaal van deze anisotrope verdeling is terug te vinden in sommige observabelen, zoals jet-quenching en wrijving. In de taal van ijk/zwaartekrachtsdualiteit is de anisotrope verdeling gerelateerd aan het anisotrope gedeelte van een zwart gatachtergrond. Een manier om dit te realiseren is door een roterend zwart gat te beschouwen. Dit is de kern van 4.

Om te beginnen hebben we een vierdimensionaal AdS-Schwarzschild zwart gat beschouwd. De weerstand aan de zwaartekrachtskant van de dualiteit wordt geïnterpreteerd als een kanonische impuls van het wereldoppervlak in de radiële richting van de Nambu-Gotoactie geëvalueerd aan de rand. Met een lineaire benadering hebben we gevonden dat de wrijving van een quark bewegend langs een willekeurig grote cirkel proportioneel is met de hoeksnelheid van een snaar  $\omega$  en het kwadraat van de kritieke straal  $r_{Sch}$ . Dit is vergelijkbaar met het vlakke geval [35, 39]. Helaas hebben we ook gevonden dat de frictiecoëfficiënt geen lineaire functie is van de temperatuur  $T$ .

Vervolgens hebben we weerstand veroorzaakt door een vierdimensionaal Kerr-zwart gat bestudeerd. We hebben een simpele berekening gedaan voor het equatoriale geval. De wrijving niet verdwijnt, in tegenstelling tot bij het vierdimensionale AdS-Schwarzschild zwarte gat, wanneer we de hoeksnelheid van de snaar nul nemen,  $\omega = 0$ , maar is proportioneel met het impulsmoment van het zwarte gat  $a$ . Voor een meer algemeen geval hebben we een speciaal “statisch” geval in Boyer-Lindquistcoördinaten beschouwd. Deze oplossing draagt bij aan de leidende om van de weerstand bij kleine impulsmomenten  $a$  en verwaarloosbare snelheden  $\omega = 0$ . We hebben de weerstand voor verschillende waarden van het impulsmoment  $a$  en de parameter  $M_T$  weergegeven. Hiermee hebben we gevonden dat de weerstand in de  $\theta$ -richting een quark dichter bij het equatoriale vlak wil brengen. Dit gebeurt met een kracht die proportioneel is met de massa van de quark en de temperatuur van het plasma.





---

# ACKNOWLEDGEMENT

---

Al-hamdu lillahi rabbil 'alamin.

This thesis is based on works done at Lorentz Institute, Leiden University, and Institute for Theoretical Physics, Amsterdam University. During the work of this thesis, I had invaluable discussions with people from both institutes.

I'm in a great debt to my supervisor, Dr. Koenraad Schalm, for his continuous guidance and support in all academic and non-academic matters. I learned a lot from him about physics, coding in Mathematica, and also how to write a good publication from our projects.

I'm also grateful to my collaborators, Prof. Jan de Boer and Masaki Shigemori, during the work of my second project. I really took a lot of benefits from our discussions and had a chance to learn many important things in quite detail which I usually just took for granted.

It's a pleasure to have Xerxes Arsiwalla as an officemate in Amsterdam who helped me reading the chapter 1. My gratitude goes to Johannes Oberreuter and Sjoerd Hardeman for willing to be the paranimfen in my thesis defense; especially Sjoerd Hardeman who did a very good job in translating the summary to Dutch. Joost Hoogeveen has been a good opponent in table tennis and I acknowledge his clear view on geometry which enabled me to understand great circle more. I thank Dr. Marika Taylor for her explanation on Kerr-AdS black holes. I would be lost administratively without assistances from Fran, Marianne, Paula, Lotti, Bianca, and Yocklang. I also would like to thank Ariadi Nugroho for helping me with the printer. My sincere thanks to other people whom I can not write all their names here.

I want to give my deepest thanks to my family for their endless support, understanding, and sacrifice. Especially to both my dearest parents who can not witness what their son has achieved now. For my lovely wife, Elza, thanks for your love and care all these times.



---

# CURRICULUM VITAE

---

I was born on 30th August 1979 in Medan, Indonesia. I spent my junior and senior high school from 1991 to 1997 in Jakarta, Indonesia.

I started my Bachelor program at Informatics Department of College of Technology Telkom (STT Telkom) in 1997 and a year later I entered another Bachelor program at Physics Department of Bandung Institute of Technology (ITB), Indonesia. For my final projects, I worked on parallel computing (STT Telkom) and quantum computer (ITB). I obtained my degrees from STT Telkom in 2002 and from ITB in 2003. I continued my study for a Master program at Physics Department of ITB in 2003 and obtained my degree in 2005. I did my master thesis on magnetic monopole. Later on, I went to The Abdus Salam ICTP in Italy for one year Diploma program at High Energy Physics in 2005. I wrote a thesis in AdS/CFT correspondence under supervision of Prof. K.S. Narain.

In 2006, I came to the Netherlands to start my four years PhD program in theoretical physics under supervision of Dr. Koenraad Schalm. I did my first year at University of Amsterdam and then continued the rest of the years at University of Leiden. My works were mostly about applications of AdS/CFT correspondence to various phenomena in Quark Gluon Plasma.



---

## LIST OF PUBLICATIONS

---

- Atmaja, A. N. and Schalm, K. "Photon and Dilepton Production in Soft Wall AdS/QCD". ITFA-2008-02. arXiv:0802.1460 [hep-th]. Published in JHEP 1008:124, 2010.
- Atmaja, A. N., Boer, J. de , and Shigemori, M. "Holographic Brownian Motion and Time Scales in Strongly Coupled Plasmas". ITFA-2010-06. arXiv:1002.2429 [hep-th]. To be published in Nuc. Phys. B.
- Atmaja, A.N. and Schalm, K. "Drag Force in 4D Kerr-AdS Black Hole". work in progress.

